

# Iterative Least Squares Algorithms for Digital Filter Design

by

Michel Rossi

A thesis submitted to  
the School of Graduate Studies and Research  
in partial fulfillment of  
the requirements for the degree  
Master of Applied Science

Ottawa-Carleton Institute for Electrical Engineering  
Faculty of Engineering  
Department of Electrical Engineering  
University of Ottawa  
Ottawa, Ontario, Canada, K1N 6N5

July 8, 1996

© Michel Rossi, Ottawa, Canada, 1996.



National Library  
of Canada

Acquisitions and  
Bibliographic Services Branch

395 Wellington Street  
Ottawa, Ontario  
K1A 0N4

Bibliothèque nationale  
du Canada

Direction des acquisitions et  
des services bibliographiques

395, rue Wellington  
Ottawa (Ontario)  
K1A 0N4

*Your file* *Votre référence*

*Our file* *Notre référence*

**The author has granted an irrevocable non-exclusive licence allowing the National Library of Canada to reproduce, loan, distribute or sell copies of his/her thesis by any means and in any form or format, making this thesis available to interested persons.**

**L'auteur a accordé une licence irrévocable et non exclusive permettant à la Bibliothèque nationale du Canada de reproduire, prêter, distribuer ou vendre des copies de sa thèse de quelque manière et sous quelque forme que ce soit pour mettre des exemplaires de cette thèse à la disposition des personnes intéressées.**

**The author retains ownership of the copyright in his/her thesis. Neither the thesis nor substantial extracts from it may be printed or otherwise reproduced without his/her permission.**

**L'auteur conserve la propriété du droit d'auteur qui protège sa thèse. Ni la thèse ni des extraits substantiels de celle-ci ne doivent être imprimés ou autrement reproduits sans son autorisation.**

ISBN 0-612-16461-6

**Canada**



UNIVERSITÉ D'OTTAWA  
UNIVERSITY OF OTTAWA

## Abstract

In this thesis, we propose new algorithms to simplify and improve the design of IIR digital filters and M-band cosine modulated filter banks. These algorithms are based on the Iterative Least Squares (ILS) approach.

We first review the various Iterative Reweighted Least Squares (IRLS) methods used to design Chebyshev and  $L_p$  linear phase FIR filters. Then we focus on the ILS design of IIR filters and filter banks.

For the design of Chebyshev IIR filters in the log magnitude sense, we propose a Remez-type IRLS algorithm. This novel approach accelerates significantly Kobayashi's and Lim's IRLS methods and simplifies the traditional rational Remez algorithm.

For the design of M-band cosine modulated filter banks, we propose three new ILS algorithms. These algorithms are specific to the design of Pseudo Quadrature Mirror Filter (QMF) banks, Near Perfect Reconstruction (NPR) Pseudo QMF banks and Perfect Reconstruction (PR) QMF banks. They are fast convergent, simple to implement and flexible compared to traditional nonlinear optimization methods. Short MATLAB programs implementing the proposed algorithms are included.

# Acknowledgments

I would like to thank my supervisor, Dr. Willem Steenaart, and Dr. Jin-Yun Zhang, from Nortel, for their great availability and consistent advices.

I am very thankful to Nortel which has supported part of this research, under the Grant No ROTTW9596WS, and has provided me with powerful computational facilities.

I also acknowledge support for this research under NSERC Grant No 8572.

# Contents

Abstract	iii
Acknowledgments	iv
List of Figures	viii
List of Acronyms	xi
List of Symbols	xii
<b>1 Introduction</b>	<b>1</b>
1.1 Background	1
1.2 Motivation	2
1.3 Contributions	3
1.4 Outline of the thesis	4
<b>2 Iterative Reweighted Least Squares Design of Linear Phase FIR filters</b>	<b>5</b>
2.1 Filter design problem and design criteria	6
2.1.1 The Least Squares criterion	7
2.1.2 The Chebyshev criterion	8
2.1.3 Mixtures of the $L_2$ and the $L_\infty$ criteria	10
2.2 Intuitive introduction to the IRLS methods for the $L_\infty$ and $L_p$ designs	11
2.3 Lawson's algorithm	12
2.4 Rate of Convergence of Lawson's algorithm for the $L_\infty$ approximation	14

2.5	Relation between Lawson's and Remez algorithms . . . . .	15
2.6	Lawson's acceleration schemes for the $L_\infty$ approximation . . . . .	16
2.7	Lim's acceleration scheme for the $L_\infty$ approximation . . . . .	16
2.8	Generalization of Lawson's algorithm for the $L_p$ approximation . . . . .	17
2.9	Kahng's algorithm for the $L_p$ approximation . . . . .	19
2.10	Extensions of the IRLS methods to multiple criteria and gain constrained least squares designs . . . . .	21
2.11	Design examples and comparative tests . . . . .	22
2.12	Conclusions . . . . .	31
<b>3</b>	<b>Iterative Reweighted Least Squares Design of Log-IIR Filters</b>	<b>33</b>
3.1	Log IIR Filter Design Problem . . . . .	34
3.2	Least squares log IIR filter design using Kobayashi's IRLS method . . . . .	35
3.3	Chebyshev log IIR filter design using Kobayashi's IRLS method . . . . .	38
3.4	Chebyshev log IIR filter design using Lim's IRLS method . . . . .	38
3.5	Rational Remez algorithms . . . . .	40
3.6	Proposed Remez-type IRLS algorithm for Chebyshev log IIR filter design . . . . .	42
3.7	Design examples and comparative tests . . . . .	45
3.8	Conclusions . . . . .	56
<b>4</b>	<b>ILS Design of Uniform Cosine Modulated Filter Banks</b>	<b>59</b>
4.1	Filter banks design problem . . . . .	60
4.2	ILS design of Pseudo QMF banks . . . . .	63
4.2.1	Unweighted Pseudo QMF bank ILS design algorithm . . . . .	63
4.2.2	Pseudo QMF bank IRLS design algorithm . . . . .	67
4.2.3	Pseudo QMF bank design examples . . . . .	69
4.2.4	MATLAB program for the ILS design of Pseudo QMF banks . . . . .	73
4.3	ILS design of Near Perfect Reconstruction Pseudo QMF banks . . . . .	75
4.3.1	NPR Pseudo QMF bank ILS design algorithm . . . . .	75
4.3.2	NPR Pseudo QMF bank design examples . . . . .	77

4.3.3	MATLAB program for the ILS design of NPR Pseudo QMF banks . . . . .	80
4.4	ILS design of Perfect Reconstruction filter banks . . . . .	81
4.4.1	PR filter banks ILS design algorithm . . . . .	81
4.4.2	PR filter bank design examples . . . . .	84
4.4.3	MATLAB program for the ILS design of PR Filter banks . . . . .	86
4.5	Conclusions . . . . .	88
<b>5</b>	<b>Conclusions</b>	<b>90</b>
5.1	Thesis summary . . . . .	90
5.2	Suggestions for further research . . . . .	91
	<b>Appendix</b>	<b>91</b>
	<b>A Filter Bank Transfer Function</b>	<b>92</b>
	<b>Bibliography</b>	<b>93</b>

# List of Figures

2.1	typical approximation error envelopes, — magnitude approximation error $ E_i(\omega) $ , — — — $env( E_i(\omega) )$ , - - - - $env_2( E_i(\omega) )$ . . . . .	18
2.2	Example 1, Chebyshev filter frequency response . . . . .	23
2.3	Example 1, $\ E_i(\omega)\ _\infty/\ E_\infty(\omega)\ _\infty - 1$ , - - - Lim, - - - - Kahng, — Lawson . . . . .	24
2.4	Example 1, Lim's weighting function at the iteration $i = 100$ . . . . .	24
2.5	Example 1, weighting function at the iteration $i = 100$ , x Kahng, o Lawson . . . . .	25
2.6	Example 2, magnitude approximation error, — $L_{10}$ design, $\cdots L_\infty$ design	26
2.7	Example 2, $\ E_i(\omega)\ _{10}/\ E_\infty(\omega)\ _{10} - 1$ , — Lawson, — — — Kahng . . . . .	26
2.8	Example 3, approximation error, o extremals, * additional frequencies $f_1 < f_2 < f_3 < f_4$ . . . . .	28
2.9	Example 3, $\ E_i(\omega)\ _\infty/\ E_\infty(\omega)\ _\infty - 1$ , frequency grid: — $\Phi$ , - - - $\Phi \cup \{f_2\}$ , - - - - $\Phi \cup \{f_2, f_1\}$ , $\cdots \Phi \cup \{f_3\}$ and xxx $\Phi \cup \{f_4\}$ . . . . .	28
2.10	Example 4, * $L_p$ design, o gain constrained $L_2$ design . . . . .	30
2.11	Example 4, magnitude approximation error, — $L_2$ with gain constraints design, $\cdots L_{10}$ design . . . . .	30
2.12	Example 5, passband frequency response, — $L_2$ multiple criteria design, $\cdots L_\infty$ design . . . . .	31
2.13	Example 5, stopband frequency response, — $L_2$ multiple criteria design, $\cdots L_\infty$ design . . . . .	32
3.1	Example 6, IIR filter frequency response . . . . .	47

3.2	Example 6, — log magnitude approximation error, o extremal,* extra ripple . . . . .	47
3.3	Example 6, $R(t_i)$ for $1 \leq i \leq 500$ , . . . Kobayashi's method, — . . . — Lim's method, - - - Lim's method with rejection scheme, — proposed Remez-type algorithm . . . . .	48
3.4	Example 6, o zero, x pole . . . . .	48
3.5	Example 6, weighting function $L_{500}(e^{j\omega_n})$ , x Proposed algorithm, o Kobayashi's method . . . . .	49
3.6	Example 6, weighting function $L_{500}(e^{j\omega_n})$ , . . . Lim's method with rejection of extra extremals, — . . . — original Lim's method . . . . .	50
3.7	Example 7, IIR filter frequency response . . . . .	51
3.8	Example 7, — log magnitude approximation error, o extremal,* extra ripple . . . . .	52
3.9	Example 7, $R(t_i)$ for $1 \leq i \leq 500$ , . . . Kobayashi's method, — . . . — Lim's method, - - - Lim's method with rejection scheme, — proposed Remez-type algorithm . . . . .	52
3.10	Example 7, o zero, x pole . . . . .	53
3.11	Example 8, —log magnitude approximation error, o extremal,* extra ripple . . . . .	54
3.12	Example 8, $R(t_i)$ for $1 \leq i \leq 500$ , . . . Kobayashi's method, — . . . — Lim's method, - - - Lim's method with rejection scheme, — proposed Remez-type algorithm . . . . .	54
3.13	Example 8, o zero, x pole . . . . .	55
3.14	Example 9, IIR filter frequency response . . . . .	56
3.15	Example 9, —log magnitude approximation error, o extremal,* extra ripple . . . . .	57
3.16	Example 9, $R(t_i)$ , . . . Kobayashi's method, — . . . — Lim's method, - - - Lim's method with rejection scheme, — proposed Remez-type algorithm	57
3.17	Example 9, o zero, x pole . . . . .	58

4.1	Uniform M-band filter bank . . . . .	60
4.2	Example 11, 8-band Pseudo QMF analysis filter bank . . . . .	71
4.3	Example 11, filter bank magnitude transfer function, $ A_0(e^{j\omega}) $ . . . . .	71
4.4	Example 11, aliasing transfer functions, $ A_r(e^{j\omega}) $ for $r = 1, \dots, 7$ . . . . .	72
4.5	Example 11, 8-band Pseudo QMF prototype filter with a gain constrained least squares stopband . . . . .	72
4.6	Example 12, 4-band Pseudo QMF bank magnitude transfer function, $ A_0(e^{j\omega}) $ , - - - - least squares design, — equiripple design . . . . .	73
4.7	Example 13, 16-band NPR Pseudo QMF analysis filter bank . . . . .	78
4.8	Example 13, filter bank magnitude transfer function, $ A_0(e^{j\omega}) $ . . . . .	78
4.9	Example 14, equiripple prototype filter of a 16-band NPR Pseudo QMF bank . . . . .	79
4.10	Example 15, gain constrained least squares prototype filter of a 16-band NPR Pseudo QMF bank . . . . .	80
4.11	Example 16, 8-band analysis filter bank . . . . .	84
4.12	Example 16, filter bank magnitude transfer function, $ A_0(e^{j\omega}) $ . . . . .	85
4.13	Example 16, aliasing transfer functions, $ A_r(e^{j\omega}) $ for $r = 1, \dots, 7$ . . . . .	85
4.14	Example 17, 8-band PR analysis filter bank . . . . .	86
4.15	Example 17, filter bank magnitude transfer function, $ A_0(e^{j\omega}) $ . . . . .	87
4.16	Example 17, aliasing transfer functions, $ A_r(e^{j\omega}) $ for $r = 1, \dots, 7$ . . . . .	87

# List of Acronyms

Acronym	Definition
dB	Decibel
FIR	Finite Impulse Response
IIR	Infinite Impulse Response
ILS	Iterative Least Squares
IRLS	Iterative Reweighted Least Squares
Log-IIR	IIR filters optimized in the log magnitude sense
$L_2$	Least squares norm
$L_\infty$	Chebyshev or minimax norm
NPR Pseudo QMF	Near Perfect Reconstruction Pseudo QMF
PR	Perfect Reconstruction
Pseudo QMF	QMF extension to $M > 2$ bands
QMF	Quadrature Mirror Filter

# List of Symbols

Symbol	Definition
$Card(\Phi)$	Number of elements of a set $\Phi$
$\omega$	Angular frequency ( $\omega = \pi$ is the Nyquist frequency)
$f$	Frequency ( $\omega = 2\pi f$ )
$H(z)$	Z-transform of the sequence $h(n)$
$h(n) * g(n)$	Convolution $y(n) = h(n) * g(n) = \sum_{k=-\infty}^{+\infty} h(n-k)g(k)$
$j$	$\sqrt{-1}$
$z^*$	Complex conjugate of $z$
$M^t$	Transpose of a matrix $M$
$M^{-1}$	Inverse of a square matrix $M$
$\delta(n)$	Kronecker symbol, i.e. $\delta(0) = 1$ and $\delta(n) = 0$ for $n \neq 0$
$\ E(e^{j\omega})\ _p$	$L_p$ norm, $(\frac{1}{2\pi} \int_{-\pi}^{\pi}  E(e^{j\omega}) ^2 d\omega)^{1/p}$
$\ E(e^{j\omega})\ _{\infty}$	$L_{\infty}$ norm, $\max_{\omega \in [0, \pi]} ( E(e^{j\omega}) )$
$k \leftarrow f(k)$	Update the value of $k$ with $f(k)$

# Chapter 1

## Introduction

### 1.1 Background

In the past thirty years digital signal processing has been a dynamic and rapidly growing field with a wide range of applications including communications, acoustics, image processing, remote sensing and many others. Digital filters play a key role in digital signal processing systems. The design of digital filters consists of approximating a desired magnitude and/or phase (or delay) response according to a given criterion.

There exists a number of efficient noniterative methods to design FIR and IIR filters [1]-[8]. These direct design methods were derived from the analog signal processing theory in the seventies [1]-[4]. They are the windowing method for the design of linear phase FIR filters, and the closed form analytical formulas for chebyshev, butterworth and elliptic IIR digital filters. These methods along with the efficient Remez algorithm for the design of Chebyshev linear phase FIR filters are available in any commercial filter design packages [9]-[10]. They are used to design 1-D linear phase FIR filters and lowpass (bandpass or highpass) IIR filters. However in many applications, more sophisticated filters are required such as IIR filters with arbitrary magnitude function, allpass IIR filters with arbitrary phase, M-band filter banks and 2-D filters. In the absence of efficient noniterative design techniques, iterative

nonlinear optimization methods are generally used. This results in computationally intensive designs requiring significant human intervention [11]-[12],[61]-[73].

To simplify, improve and speed up the design of digital filters, alternatives to nonlinear optimization methods need to be found. One alternative is the Iterative Least Squares approach. This method consists of minimizing nonlinear objective functions by successive least squares approximations. It was first applied to the design of 2-D minimax FIR filters in 1986 [13]. Since then, the ILS approach has led to a number of filter design algorithms: log IIR filters design [15], filter banks design [16]-[19], Chebyshev FIR and IIR filters design [20]-[21],  $L_p$  approximation FIR filters design [22], allpass IIR equalizers design [23]-[24], complex chebyshev FIR filters design [25]-[28]. These ILS methods are dedicated to specific designs and are closely related to the objective functions considered. Hence they generally yield better, more reliable and faster convergences than general purpose nonlinear optimizations.

## 1.2 Motivation

Recently the research on digital filter design has been mainly focused on the design of FIR filters. Many methods to design FIR filters with prescribed magnitude and/or phase in 1D or 2D have been developed. Several of these methods were based on ILS algorithms [13]-[28]. The design of IIR digital filters and filter banks is less advanced and is generally based on nonlinear optimizations. A few articles deal with the design of IIR filters [15],[20] and filter banks [16]-[19] using the ILS approach.

The design of IIR filters and filters banks is more complicated than the design of FIR filters. The instability of IIR filters and the cancelation of the filter bank distortions generally lead to complicated design algorithms. IIR filters and filters banks present many features that make them very attractive for modern digital signal processing systems. IIR filters are often preferred over FIR filters, when the phase is not required to be linear, because they generally meet magnitude specifications with lower delays and complexity. Filter banks are used in many applications such

as speech and image encoding [54], transmultiplexing [55], adaptive filtering [56]-[57] and estimation [58]. Hence it is important to find simple and efficient algorithms to design them.

The scope of this thesis is to improve and simplify the design of IIR filters and filter banks by developing appropriate ILS algorithms. To understand the ILS approach, we review and compare the Iterative Reweighted Least Squares (IRLS) algorithms used to design of  $L_p$  and Chebyshev linear phase FIR filters.

### 1.3 Contributions

In this thesis, we unify and compare the various IRLS algorithms, for the design of  $L_p$  and Chebyshev linear phase FIR filters, that have been previously reported in the literature [13]-[21]. Design examples and comparative tests are provided.

We propose an IRLS algorithm to design Chebyshev IIR filters [75] in the log magnitude sense based on a Remez-type method. This novel approach improves significantly the convergence speed and the computational efficiency of Kobayashi's and Lim's ILS design methods [15], [20]. In addition it is simpler and more flexible than the traditional rational Remez algorithm [48]-[53]. Design examples and comparative tests are included.

We propose three ILS algorithms for the design of M-band Pseudo Quadrature Mirror Filter (QMF) banks [76], M-band Near Perfect Reconstruction (NPR) Pseudo QMF banks [77] and M-band Perfect Reconstruction (PR) QMF banks [78]. These methods are simple, fast convergent and flexible alternatives to the traditional non-linear optimization methods. Design examples and the MATLAB programs implementing the proposed ILS algorithms are included.

## 1.4 Outline of the thesis

In chapter 2, we present an overview of the IRLS methods used to design  $L_p$  and Chebyshev linear phase FIR filters. Comparison tests are presented and explained.

In chapter 3, we review Kobayashi's and Lim's IRLS methods to design Chebyshev IIR filters in the log magnitude sense [15], [20]. We review the rational Remez algorithms [48]-[53]. To speed up Kobayashi's and Lim's methods and to simplify the traditional rational Remez algorithm, we propose a new Remez-type IRLS algorithm. Design examples and comparative tests are presented.

In chapter 4, we review the theory of uniform cosine modulated filter banks [59]. To simplify and improve the design of M-band filter banks, we present three new ILS algorithms. These algorithms are simple, efficient and flexible. The MATLAB programs implementing these algorithms and design examples are provided.

The thesis summary and suggestions for further research are given in chapter 5.

## Chapter 2

# Iterative Reweighted Least Squares Design of Linear Phase FIR filters

In this chapter we examine and compare the various IRLS methods to design Chebyshev and  $L_p$  linear phase filters that have been recently reported in the literature. These IRLS algorithms are all extensions of Lawson's algorithm [35]-[38]. This algorithm was developed in 1961 to perform the  $L_p$  and the Chebyshev approximation by successive weighted  $L_2$  approximations. Its convergence is proven and has been studied extensively [35]-[38]. Lawson's algorithm was first applied to the design of digital filters in 1986 by Algazi [13]. Since then, many IRLS filter design algorithms have been developed: log IIR filter design [15],  $L_p$  FIR filter design [22], complex Chebyshev FIR filter design [25]-[28]. The success of the IRLS methods comes from their generality and flexibility. As opposed to the Parks McClellan Remez algorithm [32]-[34], which is only applicable to the design of linear phase FIR filters, IRLS methods are more general and can be used in two dimensional and/or in the complex domain.

In section 2.1, we review the filter design problem and the corresponding optimization criteria, i.e. the least square, the Chebyshev criteria and new ones based

on mixtures of these two. Lawson's algorithm and its rate of convergence are presented in section 2.3 and 2.4. The relations between Lawson's algorithm and Remez exchange algorithm are presented in section 2.5. Then accelerating methods for the design of Chebyshev and  $L_p$  filters [20]-[22] are reviewed in section 2.6 2.7, 2.8 and 2.9. Extensions to the design of gain constrained least squares filters or multiple criteria filters [22] are presented in section 2.10. Design examples and comparative tests are presented in section 2.11. The conclusions of this chapter are given in section 2.12.

## 2.1 Filter design problem and design criteria

The problem of designing digital filters consists of approximating a desired magnitude function and/or phase function, according to a given criterion. The least squares and minimax criteria are most commonly used. The motivations behind these two design criteria and the corresponding design methods are reviewed in section 2.1.1 and 2.1.2. Then we present design criteria based on mixtures between the  $L_2$  and  $L_\infty$  criteria in section 2.1.3.

Let us consider the design of a linear phase FIR filter  $H(z)$ . For the sake of convenience, we can ignore the linear phase term and express its frequency response as follows

$$H(\omega) = \sum_{n=1}^M a_n \text{trig}(\omega, n) \quad (2.1)$$

where  $\text{trig}(\omega, n)$  is an appropriate cosine function [8], the coefficients  $a_n$  are related to the impulse response of the filter and  $M$  is a function of the filter length. Let  $D(\omega)$  be the desired real valued frequency response. The approximation error is the following one

$$E(\omega) = H(\omega) - D(\omega)$$

### 2.1.1 The Least Squares criterion

The least squares design consists of minimizing the  $L_2$  norm of the approximation error defined as follows

$$\|E(\omega)\|_2 = \sqrt{\frac{1}{2\pi} \int_{-\pi}^{\pi} |D(\omega) - H(\omega)|^2 d\omega} \quad (2.2)$$

The design of least squares FIR filters is straight forward and consists of truncating the Fourier series of the desired frequency response  $D(\omega)$ . This design can be perceived as the multiplication of the Fourier series by a rectangular window. The resulting filters are characterized by the Gibbs phenomenon, i.e. large peak values of the approximation error at the frequencies where  $D(\omega)$  shows discontinuities. These large peak values can be reduced using non-rectangular windows such as the Kaiser, Bartlett, Blackmann, Hamming or the Hanning windows [1]-[8].

As pointed out in [29], a least squares filter minimizes the point wise value of the worst case error signal. Let us consider an input signal,  $\{x(n)\}$ , with unit energy, i.e.  $\|X(\omega)\|_2 = 1$ . Using the inverse Fourier transform, the error signal can be expressed as

$$y(n) = (h(n) - d(n)) * x(n) = \frac{1}{2\pi} \int_{-\pi}^{\pi} E(\omega) X(\omega) e^{jn\omega} d\omega \quad (2.3)$$

Using the Gauss inequality and the identity  $\|X(\omega)\|_2 = 1$  we obtain

$$y(n)^2 \leq \frac{1}{2\pi} \int_{-\pi}^{\pi} |E(\omega)|^2 d\omega \frac{1}{2\pi} \int_{-\pi}^{\pi} |X(\omega)|^2 d\omega = \|E(\omega)\|_2^2 \quad (2.4)$$

When  $X(\omega) = e^{-jn\omega} E(\omega) / \|E(\omega)\|_2$ , the upper bound of  $y(n)^2$  is reached. Hence we can write

$$\max_{\{X(\omega) \mid \|X(\omega)\|_2=1\}} |y(n)| = \|E(\omega)\|_2 \quad (2.5)$$

This means that the point wise characteristics of the signal are best preserved when the least squares criterion is used.

To shape the error curve and reduce the Gibbs phenomenon, the weighted least squares design can be used. It consists of minimizing the integrated squared weighted error defined as follows

$$\|w(\omega)E(\omega)\|_2 = \sqrt{\frac{1}{\pi} \int_0^{\pi} |w(\omega)(D(\omega) - H(\omega))|^2 d\omega} \quad (2.6)$$

where  $w(\omega)$  is a weighting function defined on  $[0, \pi]$ . The integration (2.6) can be discretized on a  $L$ -point dense and uniform frequency grid  $\Omega = \{\omega_0, \dots, \omega_{L-1}\}$  of  $[0, \pi]$ , with  $L \gg M$ , leading to the following matrix form

$$\|w(\omega)E(\omega)\|_2^2 \approx \frac{1}{L}(d - Ca)^t W^t W (d - Ca) \quad (2.7)$$

where  $d = [D(e^{j\omega_0}), \dots, D(e^{j\omega_{L-1}})]^t$ ,  $a = [a_1, \dots, a_M]^t$  and  $C$  is a  $L$  by  $M$  matrix whose coefficients are  $c_{i,j} = \text{trig}(\omega_{i-1}, j)$  and where  $W$  is the diagonal matrix  $\text{diag}([w(\omega_0), \dots, w(\omega_{L-1})])$ . The weighted least squares filter can be obtained by solving the following overdetermined system of linear equations in the least squares sense

$$WCa = Wd \quad (2.8)$$

The solution can be obtained using the pseudo-inverse of the matrix  $WC$  as follows

$$a = (C^t W^t W C)^{-1} C^t W^t W d \quad (2.9)$$

Equivalently, the solution can be obtained by applying the QR least squares algorithm directly to the overdetermined system (2.8). This algorithm avoids the explicit calculation of the pseudo inverse matrix and prevents ill conditioned situations. A robust implementation of the QR least squares algorithm is provided by the MATLAB package [9].

### 2.1.2 The Chebyshev criterion

The Chebyshev, minimax or  $L_\infty$  criterion corresponds to the minimization of the maximum approximation error value, i.e.

$$\|E(\omega)\|_\infty = \max_{\omega \in [-\pi, \pi]} |D(\omega) - H(\omega)| \quad (2.10)$$

There is no direct method to design Chebyshev filters. However in the case of linear phase 1-D FIR filters, the Remez exchange algorithm provides an efficient iterative design technique. This algorithm is based on the alternation theorem that characterizes the best Chebyshev approximation of linear phase FIR filters.

### Alternation Theorem

A linear phase filter,  $H(\omega)$ , is the best  $L_\infty$  approximation to  $D(\omega)$  on compact subset  $F$  of  $[0 \ \pi]$  if and only if the approximation error,  $E(\omega)$ , exhibits at least  $M + 1$  alternations on  $F$ , i.e.  $M + 1$  frequencies which verify  $\omega_0 < \omega_1 < \dots < \omega_M$ , and for  $i = 0, \dots, M$

$$E(\omega_i) = -E(\omega_{i-1})$$

and

$$|E(\omega_i)| = \|E(\omega)\|_\infty$$

The Remez algorithm can be summarized as follows

1. **Initialization**, initialize the reference set with  $M + 2$  frequency points,
2. **Interpolate**, find the approximation having alternated errors on the reference set,
3. **Update**, update the reference set with the largest  $M + 2$  ripples of the approximation error, go to step 2.

Parks and McClellan [32] proposed an efficient method for the interpolation step which requires only the inversion of a size  $M + 2$  matrix. In general, less than two transition bands are specified and the approximation has exactly  $M + 2$  ripples. Hence the update of the reference set is straight forward and the Remez algorithm converges typically in 6 iterations.

However, as noted in [33], when the number of transition bands is larger than 2, there are potential extra ripples which need to be rejected from the reference set. Although there exist more sophisticated update procedures, they are globally unefficient when the number of transition band is relatively large and the resulting Remez algorithm often fails to converge towards optimal solutions.

As shown in [29], a minimax filter minimizes the energy of the worst case error signal. In fact, by considering an input signal,  $\{x(n)\}$ , with unit energy, the energy

of the error signal can be expressed as

$$\|Y(\omega)\|_2 = \sqrt{\frac{1}{2\pi} \int_{-\pi}^{\pi} |E(\omega)|^2 |X(\omega)|^2 d\omega} \quad (2.11)$$

which leads to

$$\|Y(\omega)\|_2 \leq \max_{\omega \in [-\pi, \pi]} |E(\omega)| \quad (2.12)$$

The upper bound of  $\|Y(\omega)\|_2$  is reached when the input signal is a sine wave at a frequency  $\omega_t$  such that  $\max(|E(\omega)|) = |E(\omega_t)|$ . Thus we have

$$\max_{\{X(\omega) \mid \|X(\omega)\|_{\infty}=1\}} \|Y(\omega)\|_2 = \max_{\omega \in [-\pi, \pi]} |E(\omega)| \quad (2.13)$$

Hence the  $L_{\infty}$  criterion is optimal when the minimization of the energy of the error signal is required. This is particularly suitable filter stopbands when the unwanted signal is unknown and possibly highly correlated.

### 2.1.3 Mixtures of the $L_2$ and the $L_{\infty}$ criteria

There are many situations where a better performance would be obtained with a mixture of the  $L_2$  and  $L_{\infty}$  error measures. For instance the pure  $L_2$  criterion is rarely used to design digital filters, and the popular windowing method is a way of obtaining a trade-off between the  $L_2$  and  $L_{\infty}$  criteria. Thanks to its simplicity, the windowing method is widely used. However it leads to sub-optimal design criteria where it is difficult to minimize meaningful error measures.

In [30] and [31], a meaningful design criterion is introduced to reduce the Gibbs phenomenon while keeping the  $L_2$  criterion. This new criterion is the gain constrained least squares criterion. It is shown that for an optimum  $L_2$  filter, considerable reduction of the Chebyshev error can be obtained by allowing a small increase in the squared error. For the Chebyshev the opposite is true, a considerable reduction of the squared error can be obtained by allowing a small increase in the Chebyshev error.

In some cases, filters with  $L_2$  and  $L_{\infty}$  design criterion in two different bands might also perform better than pure  $L_2$  or  $L_{\infty}$  filters. Let us consider the case of a lowpass filter used to separate an useful lowpass signal in the frequency band  $[0, \omega_p]$  from an

unwanted single frequency in  $[\omega_s, \pi]$  with  $\omega_s < \omega_c$ . If the purpose of the filtering is to minimize the energy of the unwanted signal while preserving the point wise properties of the useful signal in the time domain, then an optimal design criterion consists of a  $L_2$  criterion in the passband and a  $L_\infty$  criterion in the stopband.

The  $L_p$  criterion can also be considered as a trade-off between the  $L_2$  and  $L_\infty$  criteria. The squared error of a  $L_p$  approximation is smaller than with the  $L_2$  approximation. Moreover the  $L_\infty$  design can be obtained when  $p$  tends toward  $+\infty$ . Remember that the  $L_p$  approximation consists of minimizing the  $L_p$  norm of the approximation error, i.e.

$$\|E(\omega)\|_p = \left( \frac{1}{2\pi} \int_{-\pi}^{\pi} |D(\omega) - H(\omega)|^p d\omega \right)^{1/p} \quad (2.14)$$

The flexible IRLS design methods presented in the next section allows the design of filters with such design criteria.

## 2.2 Intuitive introduction to the IRLS methods for the $L_\infty$ and $L_p$ designs

The approximation error of a weighted least squares filter is directly related to the weighting function. Increasing the weight at a given frequency results in the reduction of the corresponding approximation error. Hence the large peak values of least squares filters can be reduced by using relatively large weights near the discontinuities of  $D(\omega)$ . To achieve the equiripple approximation, one can imagine an iterative process that determines the appropriate weighting function, adaptively, according to the approximation error at each iteration.

When the  $L_p$  approximation is desired, one can think of using a weighting function equal to  $|D(\omega) - H(\omega)|^{\frac{p-2}{2}}$ . In fact, with such a weighting function, the minimization of (2.6) minimizes the  $p^{\text{th}}$  power of  $|D(\omega) - H(\omega)|$ . However this cannot be done in one step because we need the solution to find the weights. An iterative algorithm can then be considered, where the weights are iteratively set to the approximation error,

of the previous iteration, to the power of  $\frac{p-2}{2}$ .

These iterative methods to perform the Chebyshev and  $L_p$  approximations exists and are presented in the next sections.

## 2.3 Lawson's algorithm

The idea of using a iterative reweighted least squares algorithm to achieve a  $L_\infty$  approximation was first developed by Lawson [35] in 1961 and extended to the  $L_p$  ( $p > 2$ ) approximation by Rice and Usow [36]-[37] in 1968. Lawson's algorithm starts with arbitrary weights  $w_0(\omega_n)$ . Then at each iteration  $i \geq 1$ , the weighted least squares design is performed and the weights are updated according to the approximation error obtained,  $E_i(\omega) = D(\omega) - H_i(\omega)$ , as follows

- for the  $L_p$  design,  $p > 2$

$$w_{i+1}(\omega) = (w_i(\omega) \sqrt{|E_i(\omega)|})^{\frac{p-2}{p-1}} \quad (2.15)$$

- for the  $L_\infty$  design

$$w_{i+1}(\omega) = w_i(\omega) \sqrt{|E_i(\omega)|} \quad (2.16)$$

To maintain a reasonable dynamic range, the weights are normalized after each update as follows

$$w_{i+1}(\omega_n) \leftarrow \frac{w_{i+1}(\omega_n)}{\sqrt{\sum_k w_{i+1}(\omega_k)^2}} \quad (2.17)$$

Lawson's algorithm can be summarized into the following steps

- *Step 1*,  $i \leftarrow 0$ , initialize  $\{w_0(\omega_n)\}$  arbitrarily,
- *Step 2*, solve the weighted  $L_2$  approximation using (2.9),
- *Step 3*, update and normalize the weights using (2.16) or (2.16) and (2.17),
- *Step 4*,  $i \leftarrow i + 1$  go to step 2.

Lawson, Rice and Usow [35]-[37] state that

- The filter  $H_i(\omega)$  converges to  $H_\infty(\omega)$  which is the best  $L_p$  (respectively  $L_\infty$ ) approximation to  $D(\omega)$  over a subset  $\hat{\Omega}$  of  $\Omega$  defined as follows

$$\hat{\Omega} = \{\omega_n | \exists \epsilon > 0 \quad w_k(\omega_n) \geq \epsilon \quad \forall k\} \cup \{\omega_n | \lim_{k \rightarrow \infty} w_k(\omega_n) = 0, \forall k \quad w_k(\omega_n) > 0\} \quad (2.18)$$

- The sequence of integrated weighted  $L_2$  error  $\sigma_i$  increases monotonically with  $i$  to  $\tau_\infty$  where

$$\sigma_i = \sqrt{\frac{1}{2\pi} \int_{-\pi}^{\pi} |w(\omega)(D(\omega) - H_i(\omega))|^2 d\omega} \quad (2.19)$$

and

$$\tau_\infty = \max_{\omega_n \in \hat{\Omega}} |D(e^{j\omega_k}) - H_\infty(e^{j\omega_k})| \quad (2.20)$$

- if  $\hat{\Omega}$  is a proper subset of  $\Omega$ , the algorithm may be restarted at any iteration  $i$  with the following weights

$$\hat{w}_i(\omega_n) = (1 - \lambda) \lim_{k \rightarrow \infty} w_k(\omega_n) + \lambda u(\omega_n) \quad 0 \leq \lambda < 1 \quad (2.21)$$

where  $u(\omega_n) = 1$  if  $\omega_n \in \Omega - \hat{\Omega}$  and  $u(\omega_n) = 0$  if  $\omega_n \in \hat{\Omega}$ . For  $\lambda$  sufficiently small, we have  $\|\hat{w}_i(\omega)E(\omega)\|_2 > \|w_i(\omega)E(\omega)\|_2$  and after a finite number of restarts we obtain the best  $L_p$  (respectively  $L_\infty$ ) approximation to  $D(\omega)$  on the entire set  $\Omega$

The restart procedure is useful when an "accidental" zero occurs in the iterative process to guarantee the optimality of approximation on the entire set  $\Omega$ . In fact when the approximation is equal to zero at some iteration, the corresponding weights become and remain equal to zero regardless of the value of the error in the following iterations. This "accidental" zero may prevent the solution to be the best approximation on  $\Omega$ . However as noted in [13], it occurs rather infrequently in the design of 1-D FIR filters.

## 2.4 Rate of Convergence of Lawson's algorithm for the $L_\infty$ approximation

Cline [38] has studied in detail the convergence of Lawson's algorithm for the Chebyshev approximation. He has proven that Lawson's algorithm has a linear convergence, and has identified the convergence factor.

In the weight update formula (2.16), the weights are multiplied by the error values at each iteration. Hence the algorithm tends to drive the weights toward zero everywhere but at the extremal frequencies,  $\Phi$ , of the Chebyshev filter,  $H_\infty(\omega)$ . More precisely, as shown in [38]

$$\frac{w_{i+1}(\omega_n)}{w_i(\omega_n)} \rightarrow \frac{|D(e^{j\omega_n}) - H_\infty(e^{j\omega_n})|}{\tau_\infty} = \rho(\omega_n) < 1 \quad (2.22)$$

From this expression, we can see that the weights at the frequencies close to the extremal frequencies tend toward zero very slowly since the corresponding approximation error values are almost equal to  $\tau_\infty$ .

Cline proved that the convergence of Lawson's algorithm is linear and that the factor of convergence is at most  $\rho$ , where

$$\rho = \max_{\omega_n \in \Omega - \Phi} (\rho(\omega_n)) \quad (2.23)$$

This means that

$$\forall \lambda > \rho \exists M > 0 \forall i \max_{n=1, \dots, M} |h_i(n) - h_\infty(n)| \leq M\lambda^i. \quad (2.24)$$

This proves the following experimental observations made by Lawson

$$\frac{\tau_\infty - \sigma_{i+1}}{\tau_\infty - \sigma_i} \rightarrow \rho \quad (2.25)$$

$$\frac{\tau_\infty - \tau_{i+1}}{\tau_\infty - \tau_i} \rightarrow \rho \quad (2.26)$$

where

$$\tau_i = \max_{\omega_n \in \Omega} |D(e^{j\omega_n}) - H_i(e^{j\omega_n})| \quad (2.27)$$

Note that the denser the frequency grid is, the closer  $\rho$  is to 1 and the slower the resulting convergence is. Design examples, presented in section 2.11, illustrate the effect of the frequency grid on the convergence speed of Lawson's algorithm.

## 2.5 Relation between Lawson's and Remez algorithms

Lawson's and the Remez algorithms, which are both used perform the minimax approximation, have several similarities.

First the Lawson's algorithm, as the Remez algorithm, determines iteratively the location of the extremals of the optimum equiripple filter. In fact the extremals are determined by the value of the corresponding weight. At convergence the extremal frequencies are the only frequencies whose weights are not equal to zero. The frequencies that are unlikely to be extremal frequencies, i.e. where  $\rho(\omega_n) \ll 1$ , are identified fairly rapidly. On the contrary, the determination of the extremal frequencies among the critical points, where  $\rho(\omega_n) \approx 1$ , requires a lot more iterations.

In addition, with Lawson's algorithm as with the Remez algorithm the knowledge of the extremals location is used to find the optimal equiripple filter. The Parks McClellan Remez method interpolates the frequency response among the current set of  $M + 1$  extremals. Lawson's algorithm uses the least squares approximation instead. Note that when the number of non zero weights is exactly  $M + 1$ , Lawson's algorithm converges immediately to the same solution as with the Parks McClellan interpolation method.

The Parks McClellan Remez algorithm is an efficient and fast method for the design of one dimensional linear phase FIR filters. Lawson's algorithm has a relatively slow convergence. However, it is more general and flexible and has been used successfully to design 2-D minimax FIR filters [13]-[14], gain constrained least squares FIR filters [22], minimax nonlinear phase FIR filters [27] and minimax log IIR filters [15].

To speed up the convergence of Lawson's algorithm, several methods have been proposed [35]-[39], [20]-[22]. These acceleration schemes are presented in the next sections.

## 2.6 Lawson's acceleration schemes for the $L_\infty$ approximation

Lawson's methods for accelerating the convergence of his algorithm consists of making the weights converge towards zero as fast as possible except at the extremals frequencies by modifying the weight update formula as follows

$$w_{i+1}(\omega) = w_i(\omega)|E_i(\omega)| \quad (2.28)$$

or

$$w_{i+1}(\omega) = w_i(\omega)^2 \sqrt{|E_i(\omega)|} \quad (2.29)$$

these modifications make  $w_k(\omega_n)$  tend toward zero like  $\rho^{2k}$  and  $\rho^{2^k}$ , respectively and increase the convergence provided that the resulting algorithm converges. However the convergence of the resulting algorithms is not guaranteed and less reliable.

Lawson has noted that the algorithm distinguishes rather quickly the critical frequencies and proposed to do a few steps of the algorithm and then set  $w(\omega_n) = 0$  except at the points likely to be critical. By doing so, computational saving can be achieved at each weighted least square approximation. However the convergence rate,  $\rho$ , remains unchanged unless the weights are set to zero at the frequencies where  $\rho(\omega_n) \approx 1$ . This is extremely difficult since it implies the a priori knowledge of the extremal frequencies.

## 2.7 Lim's acceleration scheme for the $L_\infty$ approximation

The most successful acceleration scheme for the  $L_\infty$  approximation was proposed by Lim [20] in 1992. As opposed to the accelerating methods previously described, Lim's method does not aim to make the weights tend toward zero faster. His method consists of replacing the approximation error in the weight update formula by the

envelope of the approximation error to the power of  $\theta > .5$ . The resulting weight update formula is the following

$$w_{i+1}(\omega) = w_i(\omega) \text{env}(|E_i(\omega)|)^{\frac{\theta}{2}} \quad (2.30)$$

where the envelope considered,  $\text{env}(|E_i(\omega)|)$ , is the function which connects the magnitude error local maxima with straight lines. Sunder proposed in 1994 a similar method [21]. It uses a different kind of envelope,  $\text{env}_2$ . Typical envelopes,  $\text{env}(|E_i(\omega)|)$  and  $\text{env}_2(|E_i(\omega)|)$ , are shown in Fig. 2.1.

The convergence of Lim's IRLS method is not guaranteed. However it was shown [20] to be robust and to converge several time faster than Lawson's algorithm. Comparative tests are presented in section 2.11.

We believe that Lim's method converges relatively fast because the limit of its weighting function is continuous and easier to tend to than the limit of Lawson's weighting function. Lawson's and Lim's algorithms offer fast initial convergences. It takes a few iterations for the envelope  $\text{env}(|E_i(\omega)|)$  to become almost flat. Then, whereas Lawson's weighting function is multiplied by the square root of the approximation error and need many iterations to make the weights tend toward zero, especially those close to the extremals, Lim's weighting function is multiplied by an almost flat function, and is affected by minor changes. Hence Lim's weights converge faster towards their limits, resulting in the fast convergence of the overall algorithm.

The robustness and the convergence speed of Lim's method depend of  $\theta$ . As shown in [20], the optimum value of  $\theta$  is statistically around .75.

## 2.8 Generalization of Lawson's algorithm for the $L_p$ approximation

As proposed by Rice and Usow [36], Lawson's algorithm for the  $L_p$  approximation can be generalized thanks to a proper parametrization. Let us consider the following

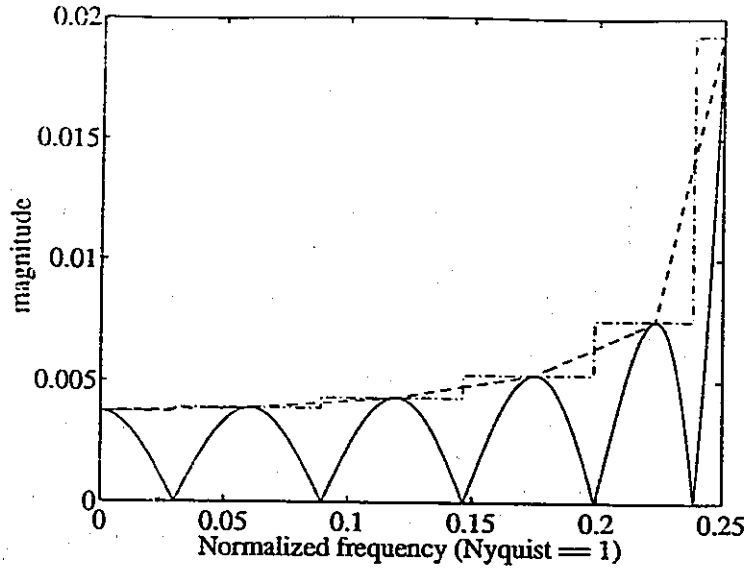


Figure 2.1: typical approximation error envelopes, — magnitude approximation error  $|E_i(\omega)|$ , - - -  $env(|E_i(\omega)|)$ , - . - . -  $env_2(|E_i(\omega)|)$

weight update formula

$$w_{i+1}(\omega) = w_i(\omega)^\alpha |E_i(\omega)|^\beta \quad (2.31)$$

If the algorithm converges, the filter obtained is the best  $L_p$  approximation if the limit of the weighting function satisfies

$$w_\infty(\omega) = |E_i(\omega)|^{\frac{p-2}{2}} \quad (2.32)$$

Equating (2.31) and (2.32) gives

$$|E_i(\omega)|^{\frac{p-2}{2}} = |E_i(\omega)|^{\frac{\alpha(p-2)}{2}} |E_i(\omega)|^\beta \quad (2.33)$$

which leads to the following condition on  $\alpha$ ,  $\beta$  and  $p$

$$\alpha(p-2) + 2\beta = p-2 \quad (2.34)$$

As proposed [36], the following parametrization can be introduced

$$\gamma = \frac{\alpha}{2\beta} \quad (2.35)$$

Given  $p$  and the relation (2.34), the weight update formula is entirely determined by the parameter  $\gamma$ . The importance of the past iterations in the calculation of the weighting function depends on  $\gamma$ . When  $\gamma > 1$ , the algorithm is conservative, i.e. the weight used in the previous iteration represents a major part of the updated weight. In this case the convergence of the algorithm is slow but very reliable. On the contrary, when  $\gamma < 1$  the weighting function depends more on the actual approximation error and can adapt faster to its variations. Hence the resulting algorithm converge fast, however its convergence is less reliable.

- $\gamma = 0 \implies w_{i+1}(\omega) = |E_i(\omega)|^{\frac{p-2}{2}}$
- $\gamma = 1/2 \implies w_{i+1}(\omega) = (w_i(\omega)|E_i(\omega)|)^{\frac{p-2}{p}}$ , modified Lawson's algorithm
- $\gamma = 1 \implies w_{i+1}(\omega) = (w_i(\omega)\sqrt{|E_i(\omega)|})^{\frac{p-2}{p-1}}$ , Lawson's algorithm
- $\gamma = \infty \implies w_{i+1}(\omega) = w_i(\omega)$ , no iteration algorithm

As pointed out in [22], Lawson's and Lim's methods can not achieve quadratic convergence as long as a multiplicative weight updating formula is used. Note that with the above parametrization, the weight update formula is nonmultiplicative in only two case, i.e.  $\gamma = 0$  and  $\gamma = \infty$ . The case  $\gamma = \infty$  present no interest since the weights remain unchanged from iteration to iteration. The case  $\gamma = 0$  is addressed in the next section, it offers indeed a significant acceleration to the traditional Lawson's algorithm.

## 2.9 Kahng's algorithm for the $L_p$ approximation

Kahng [39] proposed in 1972 an IRLS algorithm to perform the  $L_p$  approximation for  $p > 2$ . Kahng's method has first been applied to the design of FIR filters by Burrus in [22] in 1994. At each iteration the filters coefficients are updated using the Newton's method. Thanks to Newton's method the convergence of Kahng's algorithm is quadratic.

The algorithm starts by solving the  $L_2$  approximation. At each iteration  $i$ , the weighted least squares approximation is performed with the following weighting function which corresponds to  $\gamma = 0$

$$w_{i+1}(\omega) = |E_i(\omega)|^{\frac{p-2}{2}} \quad (2.36)$$

The time domain coefficients of the weighted least squares filter obtained,  $\{g_i(n)\}$ , are used to update the filter's coefficients as follows

$$h_i(n) = \frac{p-2}{p-1} h_{i-1}(n) + \frac{1}{p-1} g_i(n) \text{ for } n = 0, \dots, N \quad (2.37)$$

The above update formula corresponds to Newton's method. It is obtained by setting to zero, with respect to the coefficients  $\{h_{i-1}(n)\}$ , the derivative of the following quantity

$$\|E_{i-1}(\omega)\|_p^p = \int_{-\pi}^{\pi} \frac{1}{2\pi} |D(\omega) - H_{i-1}(\omega)|^p d\omega \quad (2.38)$$

Thanks to the Newton's method, the convergence is quadratic, i.e.

$$\exists \lambda, M > 0 \forall i \max_{n=1, \dots, M} |h_i(n) - h_{\infty}(n)| \leq M\lambda^2$$

As noted by Kahng, when the starting point, i.e. the  $L_2$  approximation, is not sufficiently close to the best  $L_p$  approximation filter  $H_{\infty}(\omega)$ , the initial convergence is relatively slow. As  $p$  increases, more iterations are needed to achieve results of the same accuracy. Kahng proposed an accelerating method consisting in a variable  $p$ . At each iteration  $i$ , the value of  $p_i$  is increased progressively from the value 2 to its final value as follows

$$p_0 = 2, \forall i \geq 1 \ p_i = \min(Kp_{i-1}, p) \quad (2.39)$$

A small value of  $K$  gives very reliable convergence because the approximation is achieved at each iteration but requires a large number of iterations for  $p_i$  to reach its final value.

Kahng's algorithms can be summarized as follows

- Step 1.  $i \leftarrow 0, w_0(\omega_n) = 1$  for any  $n$  and  $p_0 = 2$ .

- *Step 2.* solve the weighted  $L_2$  problem using (2.9), the solution is denoted as  $\{g_i(n)\}$ .
- *Step 3.* update the filter coefficients using (2.37).
- *Step 4.* update the weights using (2.36).
- *Step 5.*  $i \leftarrow i + 1$ ,  $p_i = \min(p, K p_{i-1})$  go to step 2.

## 2.10 Extensions of the IRLS methods to multiple criteria and gain constrained least squares designs

Lawson's, Lim's and Kahng's algorithms can all be extended to the design of filters with different criteria in different bands and gain constrained least squares filters.

The multiple criteria design is obtained by making the error power a function of the frequency,  $p(\omega)$ , allowing a  $L_2$  measure in the passband and a  $L_p$  measure in the stopband. For Lawson's algorithm this modification is straightforward, whereas for Kahng's algorithm it is recommended to update the filters in the frequency domain as follows

$$H_i(\omega) = \frac{p(\omega) - 2}{p(\omega) - 1} H_{i-1}(\omega) + \frac{1}{p(\omega) - 1} G_i(\omega) \quad (2.40)$$

The multiple criteria design can be extended to the gain constrained least squares approximation. It consists of a least squares approximation with the constraint that the magnitude approximation error be less than a prescribed maximum gain  $g_{max}(\omega)$ , i.e.

$$\min \int_{-\pi}^{\pi} |E(\omega)|^2 d\omega \text{ subject to } |E(\omega)| < g_{max}(\omega)$$

This can be obtained by using, at each iteration  $i$ , a minimax weight update formula only at those frequencies  $\omega_n \in \hat{\Omega}_i$  where the approximation error is larger than the prescribed gain and keeping the same weights elsewhere. When Lim's method is used, the gain constrained algorithm can be summarized as follows

- *Step 1*,  $i \leftarrow 0$  and  $w_0(\omega_n) = 1$  for any  $n$ ,
- *Step 2*, solve the weighted  $L_2$  problem using (2.9),
- *Step 3*, determine  $\hat{\Omega}_i = \{\omega_n \in \Omega \mid |E_i(\omega_n)| > g_{max}(\omega_n)\}$ ,
- *Step 4*, for  $\omega_n \in \hat{\Omega}_i$  do  $w_{i+1}(\omega_n) = w_i(\omega_n) \text{env}(|E_i(\omega_n)|/g_{max})^{\frac{6}{2}}$
- *Step 5*,  $i \leftarrow i + 1$ , go to step 2.

Design examples illustrating these design criteria, and comparison tests between the IRLS algorithms are presented in the next section.

## 2.11 Design examples and comparative tests

The design examples presented here have been performed with MATLAB on a SPARC-10 workstation.

### Example 1: Chebyshev design, comparative test

A 30<sup>th</sup> order equiripple lowpass filter has been designed using Lawson's, Lim's and Kahng's algorithms. The passband and stopband frequency edges are  $\omega_p = .4\pi$  and  $\omega_s = .44\pi$ . The frequency grid used has 1000 points uniformly distributed on  $[0 \ \omega_p] \cup [\omega_s \ \pi]$ . The frequency response of the filter obtained is plotted in Fig. 2.2. At convergence the maximum value of the approximation error is  $\|E_\infty(\omega)\|_\infty = 0.130956481411$ .

The convergences of the three algorithms in terms of  $\|E_i(\omega)\|_\infty / \|E_\infty(\omega)\|_\infty - 1$  are plotted in Fig. 2.3. Lim's method has been used with  $\theta = 1.4$  and Kahng's algorithm has been used with  $K = 1.4$ . These values have been found experimentally to maximize the convergence speed of the corresponding algorithm. We can see that the convergence is linear for the three methods. Kahng's algorithm does not have a quadratic convergence in this case because  $p$  is not fixed and increases from iteration to iteration ( $p_{100} = 5E^{14}$ ). Lim's Kahng's and Lawson's weighting functions at the

iteration  $i = 100$  are plotted in Fig. 2.4 and Fig. 2.5. We can see that Lawson's and Kahng's algorithm tend toward the same weighting function, with all weights equal to zero except at the extremal frequencies. Lim's algorithm tend toward a different weighting function which is continuous on  $[0, \omega_p] \cup [\omega_s, \pi]$ .

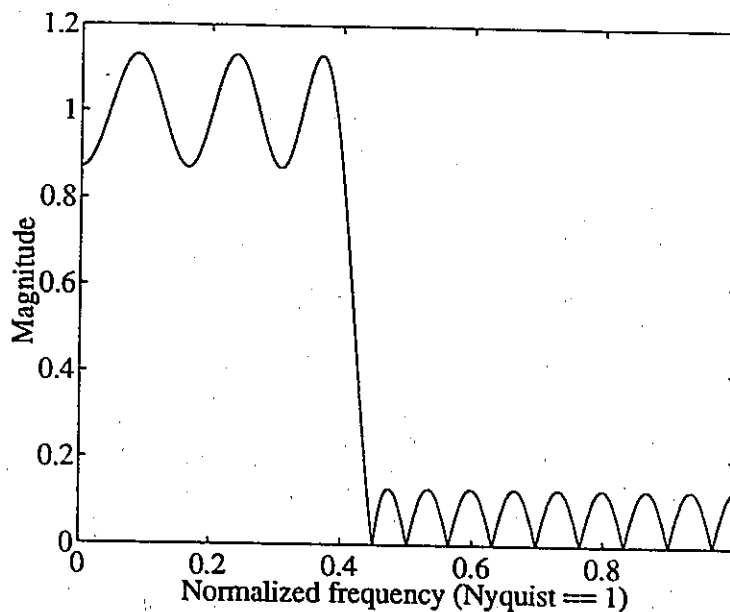


Figure 2.2: Example 1, Chebyshev filter frequency response

### Example 2: $L_{10}$ design, comparative test

A 30<sup>th</sup> order  $L_{10}$  lowpass filter with the same specifications as in example 1 has been designed using Lawson's and Kahng's algorithms. The magnitude approximation error obtained is plotted in Fig. 2.6. We can see that, compared to the Chebyshev design, the  $L_{10}$  approximation results in a smaller approximation error everywhere but near the frequency edges. At convergence  $\|E_{\infty}(\omega)\|_{10} = 0.09263$ , and  $\|E_{\infty}(\omega)\|_{\infty} = 0.156359$ . The convergences of the two algorithms in terms of  $\|E_i(\omega)\|_{10} / \|E_{\infty}\|_{10} - 1$  are plotted in Fig. 2.7. Kahng's algorithm has been used with  $K = 1.4$ . We can see that the final convergence of Kahng's algorithm is quadratic and extremely fast compared to Lawson's algorithm.

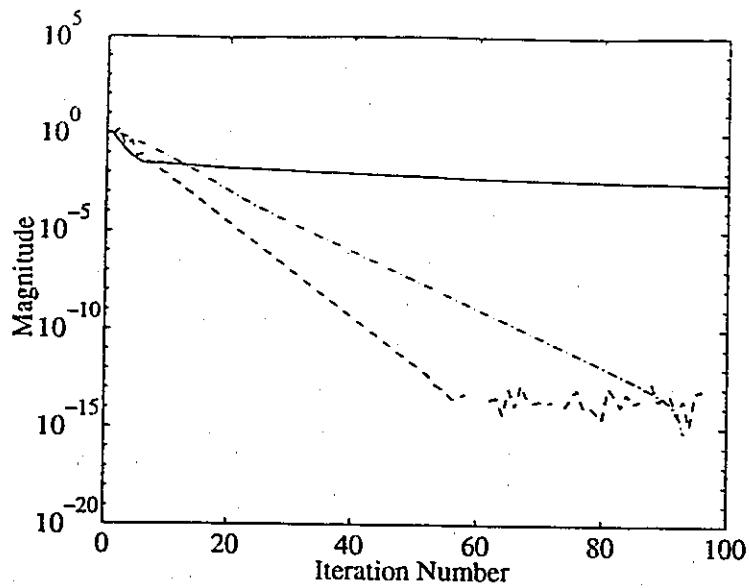


Figure 2.3: Example 1,  $\|E_i(\omega)\|_\infty / \|E_\infty(\omega)\|_\infty - 1$ , --- Lim, -·-·- Kahng, — Lawson

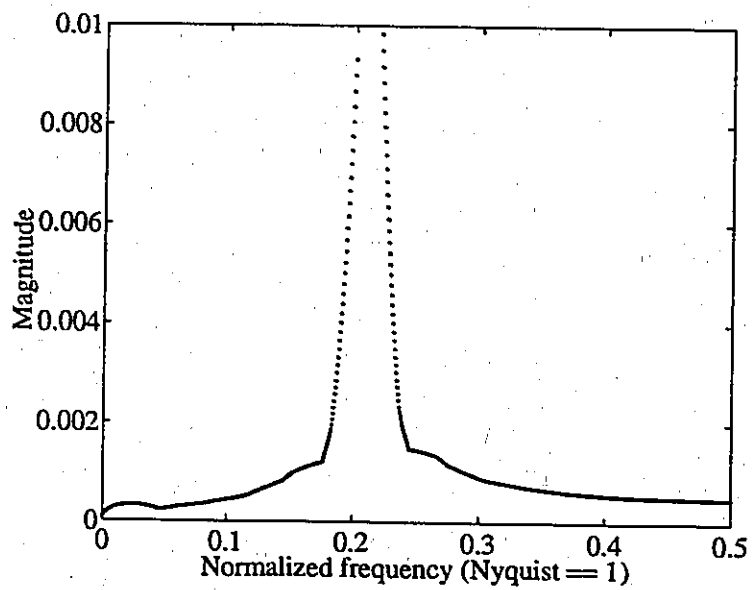


Figure 2.4: Example 1, Lim's weighting function at the iteration  $i = 100$

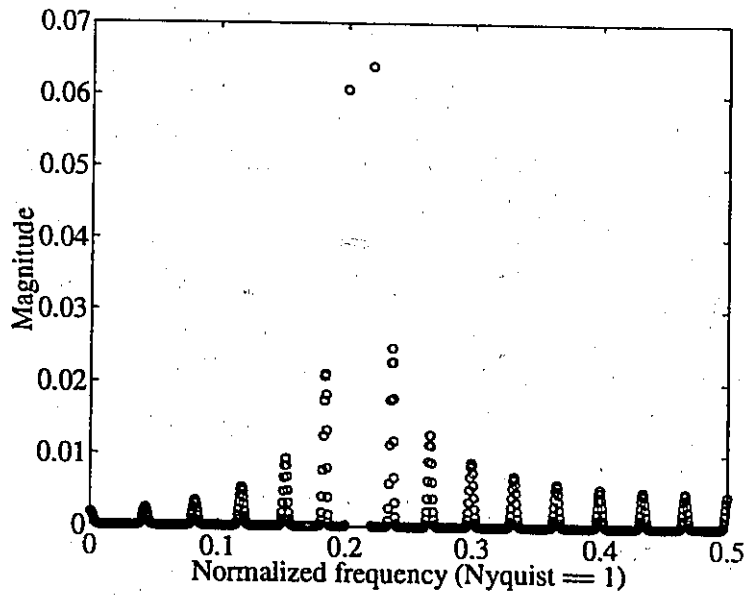
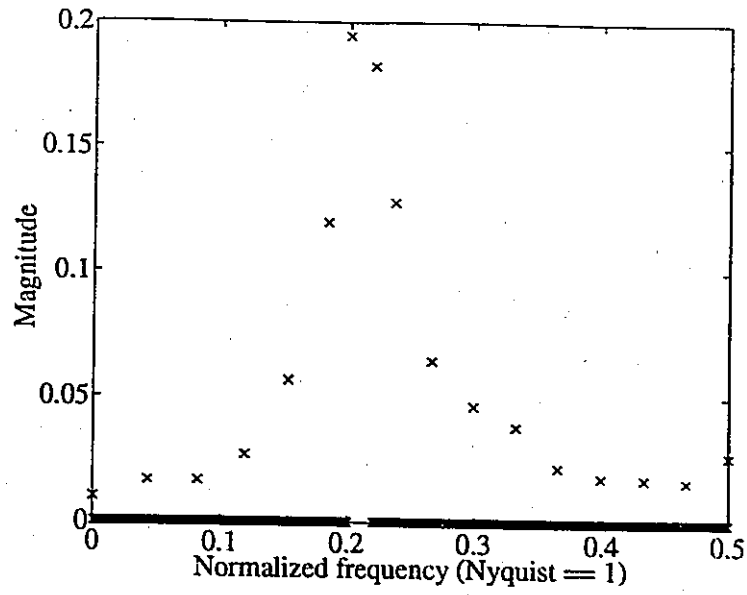


Figure 2.5: Example 1, weighting function at the iteration  $i = 100$ , x Kahng, o Lawson

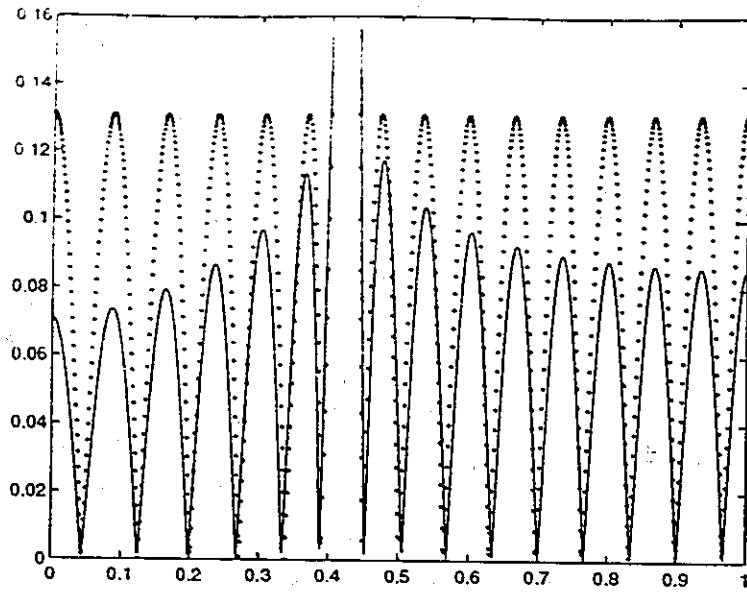


Figure 2.6: Example 2, magnitude approximation error, —  $L_{10}$  design,  $\cdots$   $L_{\infty}$  design

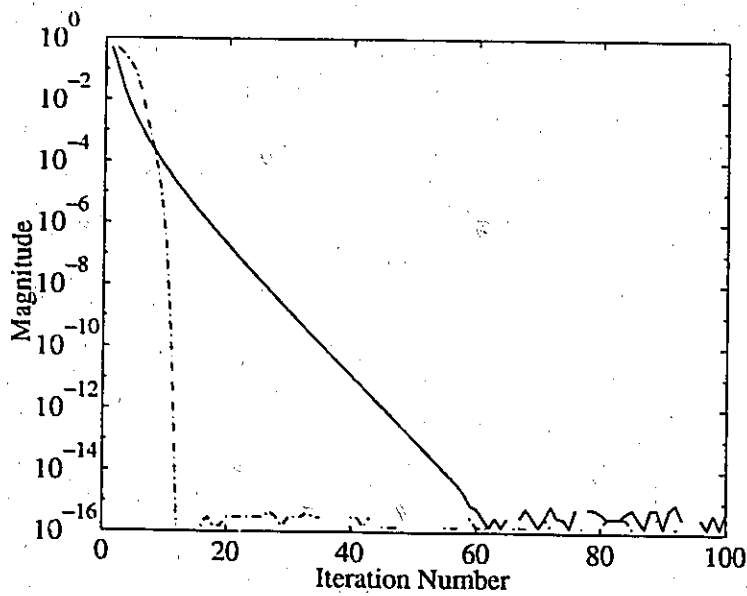


Figure 2.7: Example 2,  $\|E_i(\omega)\|_{10}/\|E_{\infty}(\omega)\|_{10} - 1$ , — Lawson, - - - Kahng

### Example 3: Lawson's convergence parameter

A 30<sup>th</sup> order Chebyshev lowpass filter with the same specifications as in example 1 has been designed using Lawson's algorithm with different convergence factor  $\rho$ . The Remez algorithm has been used to determined the extremals of the Chebyshev filter denoted  $\Phi$ . Then Lawson's algorithm has been used with different frequency grid  $\Phi \cup \{f_2\}$ ,  $\Phi \cup \{f_2, f_1\}$ ,  $\Phi \cup \{f_3\}$  and  $\Phi \cup \{f_4\}$  where

$$\begin{cases} f_1 = .97\pi \\ f_2 = .980\pi \\ f_3 = .985\pi \\ f_4 = .990\pi \end{cases} \quad (2.41)$$

The location of the frequencies  $\{f_i\}$  and the corresponding approximation error of the Chebyshev filter are shown in Fig. 2.8.

The convergences in terms of  $\|E_i(\omega)\|_\infty / \|E_\infty(\omega)\|_\infty - 1$  for the different frequency grids are plotted in Fig. 2.9. We can see that when the frequency grid is  $\Phi$  the convergence of Lawson's algorithm is immediate. When additional frequencies are used, the convergence is relatively slow and linear. As shown in section 2.4 the convergence speed depends on the value of the convergence factor  $\rho$ , i.e. on how close the additional frequency(s)  $\{f_i\}$  is/are to the extremals frequencies  $\phi$ . We have calculated an approximation of the convergence factor,  $\rho_e$ , for each case by calculating the mean of  $(\|E_i(\omega)\|_\infty - \|E_\infty(\omega)\|_\infty) / (\|E_{i-1}(\omega)\|_\infty - \|E_\infty(\omega)\|_\infty)$  for  $i = 20, \dots, 50$ . The values of  $\rho$  and  $\rho_e$  are presented on table 2.1. We can see that the experimental convergence factor  $\rho_e$  is very close to the theoretical  $\rho$ . Note that the cases  $\Phi \cup \{f_2\}$  and  $\Phi \cup \{f_2, f_1\}$  have the same convergence factor  $\rho$  but the number of iteration to achieve the same accuracy is greater for the case  $\Phi \cup \{f_2, f_1\}$ .

### Example 4: gain constrained least squares and $L_p$ designs

Several 30<sup>th</sup> order lowpass filter with the same specifications as in example 1 have been designed using the  $L_p$  criterion for  $p = 1, \dots, 80$  and the gain constrained least

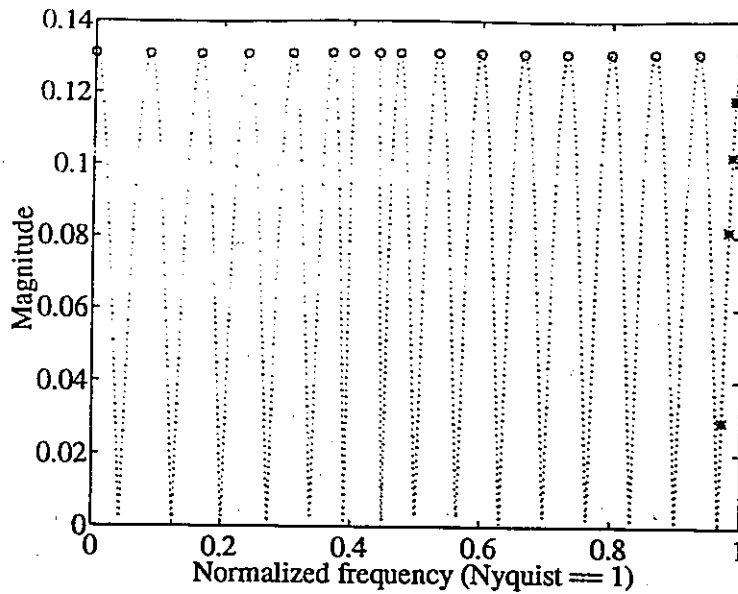


Figure 2.8: Example 3, approximation error, o extremals, \* additional frequencies  $f_1 < f_2 < f_3 < f_4$

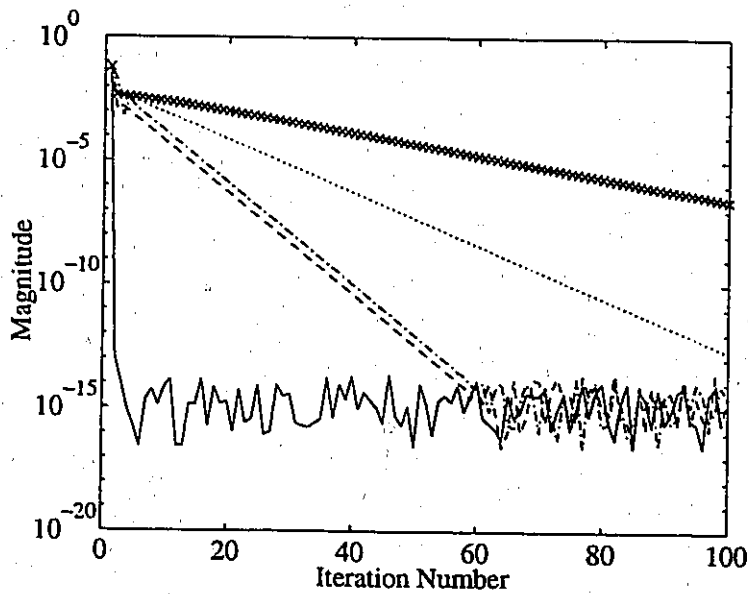


Figure 2.9: Example 3,  $\|E_i(\omega)\|_\infty / \|E_\infty(\omega)\|_\infty - 1$ , frequency grid: —  $\Phi$ , ---  $\Phi \cup \{f_2\}$ , - · - · -  $\Phi \cup \{f_2, f_1\}$ , · · ·  $\Phi \cup \{f_3\}$  and xxxx  $\Phi \cup \{f_4\}$

Table 2.1: Example 3. Experimental and theoretical convergence factor

	$\Phi \cup \{f_2\}$	$\Phi \cup \{f_2, f_1\}$	$\Phi \cup \{f_3\}$	$\Phi \cup \{f_4\}$
$\rho$	.62	.62	.78	.90
$ \rho - \rho_c $	$9E^{-5}$	$3E^{-5}$	$7E^{-5}$	$2E^{-6}$

squares criterion for 30 prescribed maximal gain uniformly distributed between the  $L_\infty$  norm of the best Chebyshev approximation  $\|E_\infty(\omega)\|_\infty = 0.13$  and the  $L_\infty$  norm of the best  $L_2$  approximation  $\|\tilde{E}_\infty(\omega)\|_\infty = 0.24$ . The points obtained in terms of the  $L_\infty$  error versus the  $L_2$  error are plotted in Fig. 2.10. As explained in section 2.1, the Chebyshev error can be reduced by a slight increase of the  $L_2$  error, and the opposite is true. For the same  $L_\infty$  error the gain constrained least squares method offers a smaller squared error. A gain constrained least squares filter with the same Chebyshev error as the  $L_{10}$  approximation filter has been designed and is plotted in Fig. 2.11. The approximation errors for the two designs have the same maximum value at the frequency edges  $\omega_p$  and  $\omega_s$ . We can see that the gain constrained design least squares approximation results in a smaller approximation error except near the frequency edges.

#### Example 5: least squares passband and Chebyshev stopband design

To illustrate the usefulness of the design with multiple criteria we have design a 30<sup>th</sup> order lowpass filter with the same specifications as in example 1 and with a least squares approximation in the passband and a Chebyshev approximation in the stopband. The passband and the stopband of the filter obtained and the corresponding minimax filter are plotted in Fig. 2.12 and Fig. 2.13. The passband of the multiple criteria design has been appropriately weighted such that the  $L_2$  norm of the approximation error in the passband is the same for the two filters, i.e.  $\|E_\infty(\omega)\|_2 = 0.092$ . The point wise maximal error value is the same. However the signal corresponding to the point-wise maximal error,  $X(e^{j\omega}) = e^{-j\omega} E_\infty(\omega) / \|E_\infty(\omega)\|_2$ , is not the same for

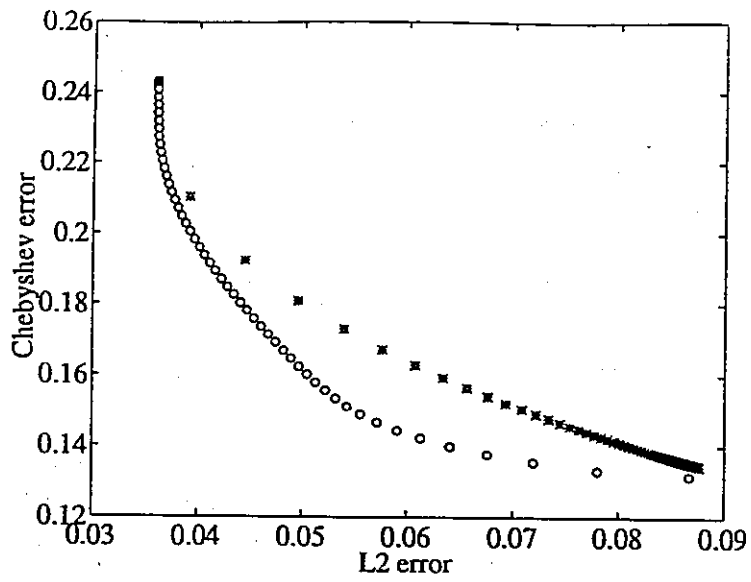


Figure 2.10: Example 4, \*  $L_p$  design, o gain constrained  $L_2$  design

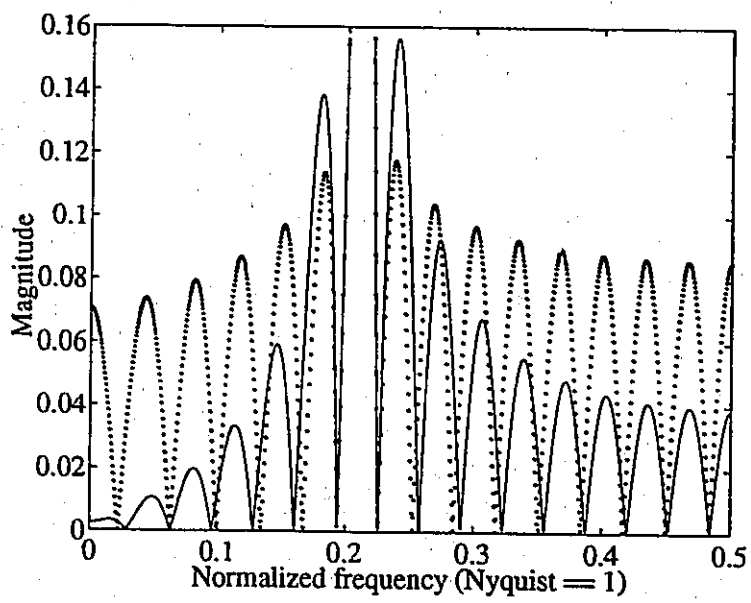


Figure 2.11: Example 4, magnitude approximation error, —  $L_2$  with gain constraints design, ...  $L_{10}$  design

the two filters. If the signal to process has its energy concentrated in the low frequencies, the maximal pointwise error occurs less frequently with the  $L_2$  approximation than with the  $L_\infty$  approximation. In the stopband the multiple criteria filter achieve  $10dB$  more attenuation than the  $L_\infty$  filter. Hence the energy of the output residual stopband noise signal is significantly less than with the pure Chebyshev design.

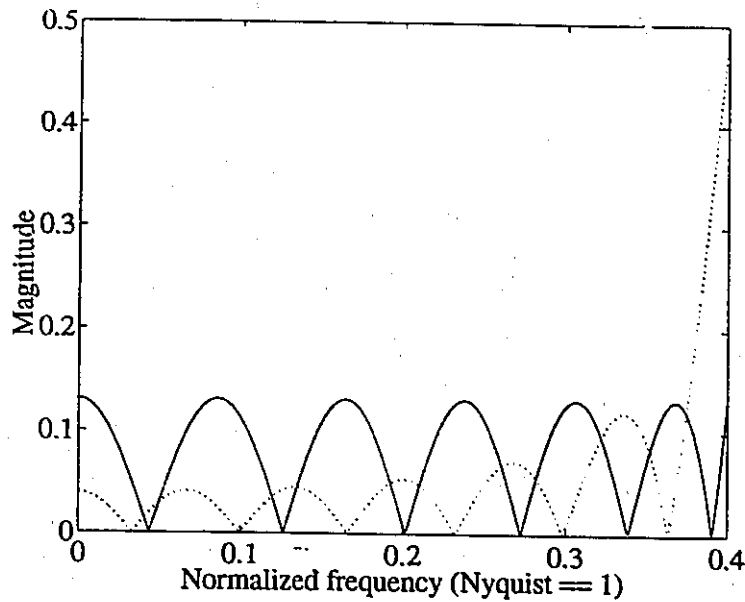


Figure 2.12: Example 5, passband frequency response, —  $L_2$  multiple criteria design, ...  $L_\infty$  design

## 2.12 Conclusions

In this chapter we have examined the various IRLS methods to design Chebyshev and  $L_p$  linear phase FIR filters. We reviewed the design criteria used in filter design. The optimality of these criteria has been discussed. Lawson's algorithm along with the mathematical results on its convergence rate has been reported. We have shown the relations between Lawson's, Lim's, Kahng's and Remez algorithms. Design examples have been presented to compare the convergences of the IRLS methods and illustrate the  $L_p$  and the gain constrained least squares criteria.

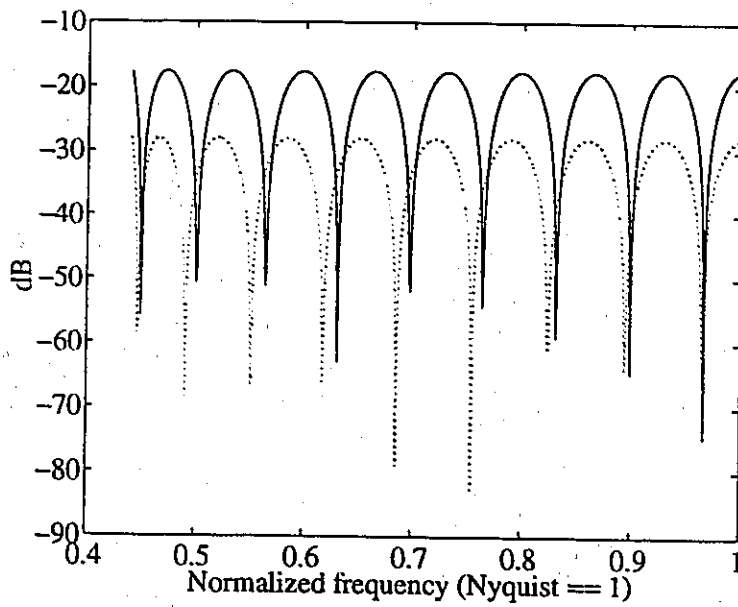


Figure 2.13: Example 5, stopband frequency response, —  $L_2$  multiple criteria design,  
 ...  $L_\infty$  design

## Chapter 3

# Iterative Reweighted Least Squares Design of Log-IIR Filters

In this chapter, we consider the design of IIR digital filter with arbitrary magnitude response. A number of methods have been proposed [43]-[53],[15] to design IIR filters with arbitrary magnitude functions. Most of them [46], [48]-[53] are complicated, computationally intensive and nonrobust because of the nonlinearity of IIR filter design problem and the possible instability of IIR filters. The noniterative methods [43] and [45] are computationally simple, however the resulting approximation is not optimal in any sense.

The most successful approach was proposed in 1990 by Kobayashi [15]. It consists of an IRLS method for the design of least squares IIR filters in the log magnitude sense (Log IIR). This method is conceptually simple, fast convergent and robust. Kobayashi has extended his method to the minimax design using Lawson's algorithm. However as noted [15], the resulting algorithm is slow to converge. To speed up the design, Lim [20] proposed to apply his envelope-based IRLS method. However as explained in this chapter the extra ripples and the possible degeneracy of the IIR approximation prevents Lim's method from accelerating the design in most cases.

To improve the design of minimax log IIR filter we propose a Remez-type IRLS method where the interpolation step is performed by Lawson's algorithm. This novel

approach improves significantly the convergence speed and the computational efficiency of Kobayashi's and Lim's IRLS methods. Moreover it is simpler and more flexible than the traditional rational Remez algorithm [48]-[53].

In section 3.1 we present the log IIR filter design problem. In section 3.2 we review Kobayashi's method for the design of least squares log IIR filters. In section 3.3 and 3.4 we present Kobayashi's and Lim's IRLS methods for minimax log IIR design. In section 3.5 the rational Remez exchange algorithms are presented. The proposed Remez-type IRLS algorithm is presented in section 3.6. Design examples are presented in section 3.7. The conclusions of this chapter are given in section 3.8.

### 3.1 Log IIR Filter Design Problem

In the design of digital filters, such as equalization filters for data communication systems or speech synthesis filters for cepstral vocoders, it is required to realize arbitrary magnitude functions. Moreover for such applications, the log magnitude error is more significant than the magnitude or magnitude squared error to measure how closely the frequency response of the designed filter matches the prescribed specifications. The least squares and Chebyshev criteria in the log magnitude sense are often used to design log IIR filters.

Let us consider the design of a log IIR filter, with  $M$  zeros and  $N$  poles, denoted as follows

$$\frac{B(z)}{A(z)} = \frac{b(0) + b(1)z^{-1} + \dots + b(M)z^{-M}}{1 + a(1)z^{-1} + \dots + a(N)z^{-N}} \quad (3.1)$$

and let  $\ln |D(\omega)|$  be the desired log magnitude function.

The least squares design in the log magnitude sense consists of optimizing the coefficients  $\{b(0), \dots, b(M), a(1), \dots, a(N)\}$  such that the averaged squared log magnitude error defined as follows is minimized

$$\epsilon = \frac{1}{2\pi} \int_{-\pi}^{\pi} (\ln |D(\omega)| - \ln |\frac{B(e^{j\omega})}{A(e^{j\omega})}|)^2 d\omega \quad (3.2)$$

The minimization of (3.2) is not straightforward. The objective function is nonlinear and the resulting filter is unstable when its poles are not within the unit circle.

The minimax or Chebyshev approximation consists of minimizing the maximum value of the log magnitude approximation error defined as follows

$$\xi = \max_{\omega \in [p, \pi]} \left| \ln |D(\omega)| - \ln \left| \frac{B(e^{j\omega})}{A(e^{j\omega})} \right| \right| \quad (3.3)$$

As for the design of FIR filters, there exists a rational remez algorithm. Its implementation is generally complicated and nonrobust because of the interpolation of a rational function is a complicated nonlinear problem.

### 3.2 Least squares log IIR filter design using Kobayashi's IRLS method

In 1990, Kobayashi [15] proposed an efficient IRLS method to simplify the design of log IIR filters [43]-[53]. The complicated nonlinear minimization of (3.2) is performed by a simple Iterative Reweighted Least Squares (IRLS) method. At each iteration  $i$ , the following averaged weighted squared error is minimized

$$\epsilon_i = \frac{1}{2\pi} \int_{-\pi}^{\pi} |w_i(e^{j\omega})(D(e^{j\omega})A_i(e^{j\omega}) - B_i(e^{j\omega}))|^2 d\omega \quad (3.4)$$

and the weights are updated according to the IIR filter obtained, such that the weighted squared error tend towards the log magnitude error, as follows

$$w_{i+1}(e^{j\omega}) = \frac{\ln |D(\omega)| - \ln \left| \frac{B_i(e^{j\omega})}{A_i(e^{j\omega})} \right|}{D(e^{j\omega})A_i(e^{j\omega}) - B_i(e^{j\omega})} \quad (3.5)$$

The minimization of (3.4) is relatively simple since the objective function is a quadratic function of the coefficients  $\{b_i(0), \dots, b_i(M), a_i(1), \dots, a_i(N)\}$ . As shown in [15] the quantity (3.4) can be expressed into the following quadratic matrix expression

$$\epsilon_i = [a_i^t \ b_i^t] \begin{bmatrix} R_i & -Q_i \\ -Q_i^t & P_i \end{bmatrix} \begin{bmatrix} a_i \\ b_i \end{bmatrix} \quad (3.6)$$

where  $a_i = [1 \ a_i(1) \ \dots \ a_i(N)]^t$ ,  $b_i = [b_i(0) \ b_i(1) \ \dots \ b_i(M)]^t$  and

$$R_i = \begin{bmatrix} r_i(0) & r_i(1) & \dots & r_i(N) \\ r_i(1) & r_i(0) & \dots & \vdots \\ \vdots & \dots & \dots & r_i(1) \\ r_i(N) & \dots & r_i(1) & r_i(0) \end{bmatrix} \quad (3.7)$$

$$P_i = \begin{bmatrix} p_i(0) & p_i(1) & \dots & p(M) \\ p_i(1) & p_i(0) & \dots & \vdots \\ \vdots & \dots & \dots & p_i(1) \\ p_i(M) & \dots & p_i(1) & p_i(0) \end{bmatrix} \quad (3.8)$$

$$Q_i = \begin{bmatrix} q_i(0) & q_i(1) & \dots & q_i(M) \\ q_i(-1) & q_i(0) & \dots & q_i(M-1) \\ \vdots & \vdots & \vdots & \vdots \\ q_{-N} & q_{1-N} & \dots & q_i(M-N) \end{bmatrix} \quad (3.9)$$

where

$$r_i(k) = \frac{1}{2\pi} \int_{-\pi}^{\pi} |w_i(e^{j\omega})|^2 |D(e^{j\omega})|^2 e^{jk\omega} d\omega \quad (3.10)$$

$$p_i(k) = \frac{1}{2\pi} \int_{-\pi}^{\pi} |w_i(e^{j\omega})|^2 e^{jk\omega} d\omega \quad (3.11)$$

$$q_i(k) = \frac{1}{2\pi} \int_{-\pi}^{\pi} |w_i(e^{j\omega})|^2 D(e^{j\omega}) e^{jk\omega} d\omega \quad (3.12)$$

Hence the minimization of (3.4) with respect to  $a_i$  and  $b_i$  yields the following set of linear equations with  $M + N + 2$  unknowns

$$\begin{bmatrix} R_i & -Q_i \\ -Q_i^t & P_i \end{bmatrix} \begin{bmatrix} a_i \\ b_i \end{bmatrix} = \begin{bmatrix} \zeta \\ 0 \\ \vdots \\ 0 \end{bmatrix} \quad (3.13)$$

where  $\zeta$  is the minimum value of (3.4). At each iteration  $i$ , the weighted least squares optimization of  $a_i$  and  $b_i$  requires only the calculation of  $3M + N$  independent coefficients  $r_i(k)$ ,  $p_i(k)$  and  $q_i(k)$  and the inversion of a size  $M + N + 2$  matrix.

The IRLS algorithm performs the weighted least squares approximation in the complex domain. Hence both magnitude and phase of the desired frequency response,  $D(e^{j\omega})$ , are necessary. For a minimum phase system without any zero on the unit circle, the Hilbert transform relationship [6] may be used to derive the phase information from the magnitude information and vice versa. Let  $\{\omega_0, \dots, \omega_{2L-1}\}$  be a uniform frequency grid of the interval  $[0, 2\pi]$  with  $\omega_r = \pi r/L$ . the phase information of  $D(e^{j\omega_r})$  for  $r = 0, \dots, 2L - 1$  is obtained as follows

$$\begin{aligned} \ln D(e^{j\omega_r}) &= \ln |D(e^{j\omega_r})| + j \arg |D(e^{j\omega_r})| \\ &= d(0) + 2 \sum_{n=1}^{L-1} d_n e^{jn\omega_r} + d_L e^{jn\omega_r} \end{aligned} \quad (3.14)$$

where for  $n = 0, \dots, 2L - 1$

$$d_n = \sum_{p=0}^{2L-1} \ln |D(e^{j\omega_p})| e^{jn\omega_p} \quad (3.15)$$

The convergence of Kobayashi's algorithm is not proven. However the experimentation shows that it is robust and fast convergent. The algorithm typically converges in 5 iterations. Note that there is no design constraints to insure the stability of the IIR filter. The calculation of the phase information corresponding to a stable minimum phase system is sufficient to obtain stable IIR filter. Moreover, we have observed that the IIR filters obtained are minimum phase too. The least squares design method can be summarized into the following algorithmic steps

- *Step 1*,  $i \leftarrow 0$ , given  $\ln |D(\omega)|$  find the minimum phase frequency response  $D(e^{j\omega_r})$  using (3.14)-(3.15). Set the weights  $w_0(\omega_n) = 1$  for  $n = 0, \dots, L - 1$ ,
- *Step 2*, find the weighted least squares approximation  $B_i(z)/A_i(z)$  using (3.13),
- *Step 3*,  $i \leftarrow i + 1$ , update the weights as in (3.5),
- *Step 4*, go to step 2 unless the convergence is reached.

Several termination criterion can be considered: it can consist of a tolerance on the variation of the weighted least squares error or a tolerance on the maximum variation of the filter coefficients.

### 3.3 Chebyshev log IIR filter design using Kobayashi's IRLS method

As proposed by Kobayashi [15], the IRLS design of least squares log IIR filters can be extended to the minimax design by simply introducing an extra weight factor corresponding to Lawson's algorithm.

The weight update formula for the Chebyshev design is performed on a frequency grid  $\Omega = \{\omega_0, \dots, \omega_{L-1}\}$  as follows

$$w_{i+1}(e^{j\omega_n}) = L_{i+1}(e^{j\omega_n}) \frac{\ln |D(\omega_n)| - \ln \left| \frac{B_i(e^{j\omega_n})}{A_i(e^{j\omega_n})} \right|}{D(e^{j\omega_n})A_i(e^{j\omega_n}) - B_i(e^{j\omega_n})} \quad (3.16)$$

where  $L_{i+1}(e^{j\omega_n})$  corresponds to Lawson's algorithm as follows

$$L_{i+1}(e^{j\omega_n}) = \frac{L_i(e^{j\omega_n}) \sqrt{|\ln |D(\omega_n)| - \ln \left| \frac{B_i(e^{j\omega_n})}{A_i(e^{j\omega_n})} \right|}}{\sqrt{\sum_{n=0}^{L-1} L_{k-i}(e^{j\omega_n})^2 |\ln |D(\omega_n)| - \ln \left| \frac{B_i(e^{j\omega_n})}{A_i(e^{j\omega_n})} \right|}} \quad (3.17)$$

The weights  $L_0(e^{j\omega_n})$  are initialized with the value 1 and are updated after the least squares design has converged. As pointed out in [15], the resulting algorithm is less robust and very slow to converge compared to the least squares design. The slow convergence is due to the slow convergence of Lawson's algorithm explained in chapter 1. In the next section we examine the use of Lim's method to speed up the design of minimax log IIR filters.

### 3.4 Chebyshev log IIR filter design using Lim's IRLS method

Lim [20] proposed to use his envelope-based method instead of Lawson's algorithm to speed up Kobayashi-Lawson's algorithm. In this section we show that Lim's method is in general not faster than Kobayashi-Lawson's method.

Lim's method consists of using the envelope of the approximation error as follows

$$L_{i+1}(e^{j\omega_n}) = \frac{L_i(e^{j\omega_n}) \sqrt{\text{env}(|\ln |D(\omega_n)| - \ln |\frac{B_i(e^{j\omega_n})}{A_i(e^{j\omega_n})}|)|)}^{\theta}}{\sqrt{\sum_{n=0}^{L-1} L_i(e^{j\omega_n})^2 \text{env}(|\ln |D(\omega_n)| - \ln |\frac{B_i(e^{j\omega_n})}{A_i(e^{j\omega_n})}|)|)}^{\theta}} \quad (3.18)$$

where  $\theta$  is a number in [1 2].

As shown in chapter 2, when Lim's method is applied to the design of linear phase FIR filters, the envelope of the approximation error becomes very close to the unit function after a few iterations. Hence the weighting function converges very fast towards its limit, resulting in a fast convergence of the overall algorithm. The envelope of the approximation error is flat when the approximation filter is equiripple and has no extra ripples, i.e. ripples with non maximum approximation error. This is guaranteed for FIR design by the alternation theorem when there is less than two transition bands [33].

However with IIR filters, the Chebyshev approximation have generally extra ripples. This causes the envelope of the approximation error not to tend toward the unit function and results in a relatively slow convergence of the overall algorithm. As shown in example 6 presented in section 3.7, the convergence speed of Lim's algorithm is comparable to that of Lawson's algorithm when there are extra ripples.

To obtain a fast convergence with Lim's method, one can think of computing the envelope of the approximation error by considering only the ripples that are likely to become extremals of the optimum filter. The best Chebyshev approximation has generally  $M+N+2$  extremals. Hence we can consider a simple rejection scheme where only the  $M+N+2$  largest extremals are used to build the envelope at each iteration. As shown in example 6, this method results in a relatively fast convergence in some cases. However, when extra ripples with relatively large amplitudes are present, as in example 8 and 9, the method fails to identify the proper set extremals and the convergence of the algorithm is slow and biased. Moreover, the optimum Chebyshev approximation filter may have less than  $M+N+2$  extremals as shown in example 7. In such a situation this method does not reject all extra ripples and the algorithm is slow to converge.

For the design of equiripple linear phase FIR filters, the Remez algorithm is the most efficient method. In the next section we review the design of IIR filters using the rational Remez algorithm, and the alternation theorem that characterizes the minimax approximation of IIR filters.

### 3.5 Rational Remez algorithms

The Remez algorithm is well known for the design of linear phase FIR filters [32]–[34]. Its convergence towards the best equiripple FIR filter is guaranteed and quadratic [40]–[42]. Moreover, the implementation proposed by Parks and McClellan [32] is computationally efficient.

The Remez algorithm is also used to design IIR filters [48]–[53]. This approach offers many advantages, compared to the elliptic and chebyshev closed form solutions. For instance, it allows the design of filters with any arbitrary magnitude specifications, with unequal number of poles and zeros and with weighted Chebyshev approximations.

The rational Remez algorithm is done in the real domain by considering the magnitude squared of the filter frequency response defined as follows

$$H(\omega) = \left| \frac{B(e^{j\omega})}{A(e^{j\omega})} \right|^2 = \frac{\alpha(0) + \alpha(1) \cos(\omega) + \dots + \alpha(M) \cos(\omega)}{\beta(0) + \beta(1) \cos(\omega) + \dots + \beta(N) \cos(\omega)} \quad (3.19)$$

Once  $H(\omega)$  is optimized under the constraint  $H(\omega) > 0$ , a minimum phase IIR filter is obtain by picking the finite nonzeros roots of the nominator and denominator that lie within the unit circle.

Recall that the best Chebyshev approximation of FIR filters is uniquely characterized by an alternation property. For IIR filters, the alternation condition is only sufficient [40]–[42].

#### Alternation Theorem for Rational approximation

Let  $S$  be a union of intervals included in  $[0 \pi]$  and  $\{\phi_1, \dots, \phi_{M+N+2}\}$  be a sequence of frequency points of  $S$  in ascending order called the reference set. Let  $D(\omega)$  be a

continuous function on  $S$ . Let  $B(z)$  and  $A(z)$  be polynomials with orders  $M$  and  $N$  respectively. If for  $k = 2, \dots, M + N + 2$  the following equality holds

$$H(\phi_k) - D(\phi_k) = -(H(\phi_{k-1}) - D(\phi_{k-1})) \quad (3.20)$$

and  $|H(\phi_k) - D(\phi_k)| = \max_{\omega \in S} (|H(\omega) - D(\omega)|)$  then  $B(e^{j\omega})/A(e^{j\omega})$  is the best Chebyshev approximation to  $D(e^{j\omega})$ .

Therefore, if we obtain a rational function with the alternation property over a sufficient number of extremals frequencies, we are assured that it is optimal. However, this alternation is not necessary, and the size of the reference set of the best approximation may be less than  $M + N + 2$ . In this case, the best approximation is called degenerate. Degeneracy occurs when the leading cosine coefficients of the best approximation  $\alpha(N)$  and  $\beta(M)$  are both zero, i.e. when there is a pole-zero cancellation in the best Chebyshev approximation. The example 7, presented in section 3.7, illustrates an almost degenerate design.

For IIR filter design, the Remez algorithm follows the same strategy as for FIR filter design:

1. **Initialization**, select a reference set of  $M + N + 2$  points.
2. **Interpolation**, find the approximation satisfying the alternation property on the reference set under the constraint  $H(\omega_n) > 0$ .
3. **Update**, update the reference set with the  $M + N + 2$  largest ripples of the approximation error, go to step 2.

The interpolation step is a complicated constrained nonlinear approximation problem. Several interpolation methods have been proposed in the past: the Newton-Raphson nonlinear optimization method [51], the linearization of the approximation problem [50] and a generalized eigenvalue decomposition [53]. It has been shown [40]-[42] that the interpolation of a rational function is not unisolvent, i.e. it has more than one solution. In some cases, none of the solution to the interpolation problem correspond to a stable filter [53], and the rational Remez algorithm fails to converge.

The rational Remez algorithm also fails to converge when degeneracy occurs, since the solution has less than  $M + N + 2$  alternated extremals. The update of the reference set is not straight forward since IIR filters have generally extra ripples which need to be rejected. Hence the implementations of the rational Remez algorithm for IIR design [32]–[34] are generally complicated, computationally intensive and nonrobust.

In the next section we propose a Remez-type IRLS algorithm to design Chebyshev log IIR filters. This algorithm is conceptually simpler and more flexible than the traditional rational Remez algorithm and converge faster than Kobayashi's and Lim's IRLS methods.

### 3.6 Proposed Remez-type IRLS algorithm for Chebyshev log IIR filter design

The traditional rational Remez algorithm can be applied to the design of minimax log IIR filters. An appropriate weighting function can be used such that the weighted Chebyshev approximation results in the Chebyshev approximation in the log magnitude sense. However as shown in the previous section, these methods are complicated, computationally intensive and nonrobust.

To simplify and speed up the design of Chebyshev Log IIR filters, we propose a Remez-type method where the interpolation step is performed by Lawson's algorithm.

As shown in chapter 2, the weights of Lawson's algorithm tend toward zero except at the extremal frequencies of the best Chebyshev approximation, denoted as  $\Phi$ . We have seen that if all weights are initialized to zero except on  $\Phi$ , the convergence of Lawson's algorithm toward the optimum minimax approximation is immediate. Moreover the convergence speed of Lawson's algorithm is determined by the convergence factor  $\rho$  defined in (2.23). The value of  $\rho$  can be reduced and Lawson's algorithm significantly accelerated if the weights at the frequencies close to  $\Phi$ , where the approximation error is nearly maximum, are initialized to zeros. This is not di-

rectly possible in practice, since it requires the exact location of the extremal. The method that we propose here is to determine the reference set by successive guess like in the Remez algorithm. For each reference set  $\hat{\Phi}$ , Lawson's algorithm is used to perform the interpolation step by initializing the weights to zero everywhere except on  $\hat{\Phi}$ . We have observed that 10 iterations are generally sufficient to identify the new reference set. The use of Lawson's algorithm to perform the interpolation step offers many advantages. First, no complicated procedure is necessary to reject extra ripples and select only  $M + N + 2$  extremals. In fact if extra ripples are selected, they are rejected by Lawson's algorithm which make their weights tend toward zero relatively fast depending on their amplitudes. Moreover as illustrated in example 7, Lawson's algorithm does not fail when the best approximation is almost degenerate and has less than  $M + N + 2$  extremals. In fact, the best minimax approximation on the frequency grid  $\hat{\Phi}$  is found regardless of the number of extremals. In addition, the optimization is not performed in the squared magnitude domain, as with the traditional rational Remez algorithm, but directly with the coefficients of the Z-transform. Finally thanks to the phase information of the desired frequency response, no design constraint is necessary to guarantee the stability of the IIR filter.

The proposed algorithm can be summarized in the following steps:

1. **Initialization**,  $k \leftarrow 0$ ,  $i \leftarrow 0$  initialize the reference set with  $K$  uniformly distributed frequency, ( $K \geq M + N + 2$ ).
2. **Interpolation**, Use Lawson's algorithm as follows:
  - (a) if  $k=0$  or the reference set has changed, initialize all weights to 1 on the reference set and to 0 elsewhere, otherwise use the weights of the iteration  $k - 1$ .
  - (b) do 10 iterations of the Kobayashi-Lawson's algorithm, increment  $i$  by one after each weighted least squares approximation,
3. **Update**,  $k \leftarrow k + 1$ , find the new reference set, i.e. select all the ripples of the approximation error, go to step 2.

We have observed that the convergence of the algorithm generally does not depend on the initialization of the reference set at the iteration  $k = 0$ . Moreover the algorithm converges significantly faster than the original IRLS method. The algorithm identifies rather quickly the reference set of the optimal solution, i.e. in typically  $k = 5$  iteration, then it has a linear convergence while refining the weights (3.5). As with the original IRLS methods and with the Remez algorithm, the resulting method fails to converge for some specifications.

Compared to Kobayashi's and Lim's IRLS methods, this method offers two main advantages:

- It is fast convergent thanks to the Remez exchange algorithm,
- It is computationally more efficient, each weighted least squares approximation is done on a frequency grid with  $Card(\hat{\Phi}) \approx M + N + 2 \ll L$  points.

Compared to the traditional rational Remez algorithm, the advantages of the proposed method are:

- It is computationally efficient: nonlinear optimization is not used and no constraint is necessary to insure the stability of the IIR filter,
- It is conceptually simpler: the optimization is done directly on the IIR filter coefficients and not in the squared magnitude domain,
- It is more flexible: the size of  $\hat{\Phi}$  does not have to be strictly equal to  $M+N+2$ ,
- It is more robust: it is able to perform the minimax approximation of degenerated cases.

Experimental tests showing the fast convergence of the proposed Remez-type algorithm compared to Kobayashi's and Lim's IRLS methods are presented in the next section.

### 3.7 Design examples and comparative tests

The examples presented here were performed on a SPARC10 workstation. The frequency grid used has 2048 points uniformly distributed on the interval  $[0, \pi]$ . The convergence of the design algorithms are compared in terms of the factor  $R(t_i)$  defined as follows

$$R(t_i) = \frac{e(t_i)}{e_\infty} - 1 \quad (3.21)$$

where  $e(t_i)$  is the maximum log magnitude error value of the filter obtained after the computation time  $t_i$ , i.e. after  $i$  weighted least squares approximations, and  $e_\infty = \lim_{i \rightarrow +\infty} e(t_i)$ .

#### Example 6: lowpass filter with $M = 10$ zeros and $N = 5$ poles

This example shows the fast convergence of proposed Remez-type algorithm compared to the traditional IRLS methods. In this nondegenerate example, the rejection of the extra ripples, proposed in section 3.4, improves the convergence of Lim's method.

A bandpass IIR filter with  $M = 10$  zeros and  $N = 5$  poles has been designed with the following desired log magnitude frequency response.

$$20 \log |D(\omega)| = \begin{cases} -40dB & 0 \leq \omega \leq 0.2\pi \\ 0dB & 0.3\pi \leq \omega \leq 0.6\pi \\ -30dB & 0.7\pi \leq \omega \leq \pi \end{cases}$$

The filter frequency response and the log magnitude error obtained are plotted in Fig. 3.1 and Fig. 3.2. We can see that the optimal Chebyshev approximation has  $M + N + 2 = 17$  alternated extremals. Hence the solution obtained is the best Chebyshev approximation. The maximum value of the approximation error is  $e_\infty = 0.97567059498dB$ . Let  $\Delta e$  be the difference between the largest and the smallest log magnitude error on the extremal set. At convergence  $\Delta e/e_\infty = 2E^{-4}$ , which proves that the Chebyshev approximation obtained is very accurate.

The factor  $R(t_i)$  is shown in Fig. 3.3 for Kobayashi's, Lim's and the proposed methods respectively. We can see the fast convergence of the proposed method com-

pared to the traditional IRLS methods. The proposed algorithm quickly identifies the proper reference set and then presents a rapid linear convergence. All methods were terminated after 500 weighted least squares approximations, i.e.  $i = 500$ . The weighted least squares approximation on the reference set requires a tenth of the computation time required by the traditional IRLS methods.

In fig. 3.2, we can see that there are two extra ripples at the frequencies  $f = .2$  and  $f = .7$ . Hence the envelope of the approximation error of the best Chebyshev approximation is not flat. This results in a relatively slow convergence of Lim's method. When the extra extremals are rejected and only the largest  $M + N + 2$  ripples are considered to build the envelope, the convergence of Lim's method is significantly accelerated as shown in Fig. 3.3. However as shown in examples 3 and 4, this rejection scheme fails to accelerate the design when degeneracy occurs and when the amplitude of the extra ripples are relatively large.

The poles and zeros of the IIR filter are shown in Fig. 3.4. One can verify that the filter designed is minimum phase.

The weighting function  $L_{500}(\omega_n)$  obtained after 500 weighted least squares approximations is shown in Fig. 3.5 and Fig. 3.6 for Kobayashi's, Lim's and the Remez-type method respectively. We can see that Kobayashi's and the proposed Remez-type method tend toward the same weighting function. The two weighting functions for Lim's method differ around the frequencies  $0.2\pi$  and  $.7\pi$  where the extra ripples make the weights tend to zero when no rejection scheme is used.

**Example 7: bandpass filters  $M = 9$ ,  $N = 5$ , almost degenerate approximation**

This example shows an almost degenerate Chebyshev approximation. The IIR filter designed is a lowpass filter with 9 zeros and 5 poles. The desired log magnitude response is defined as follows

$$20 \log |D(\omega)| = \begin{cases} 0dB & 0 \leq \omega \leq 0.51\pi \\ -50dB & 0.56\pi \leq \omega \leq \pi \end{cases}$$

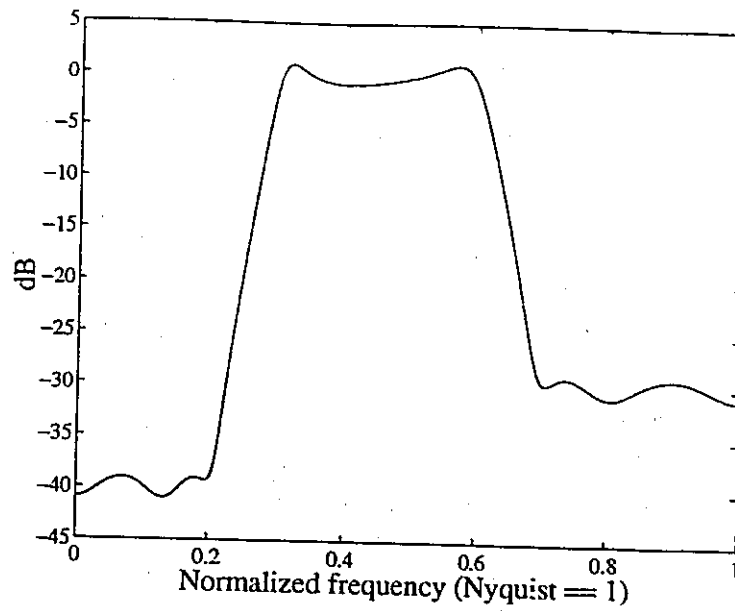


Figure 3.1: Example 6, IIR filter frequency response

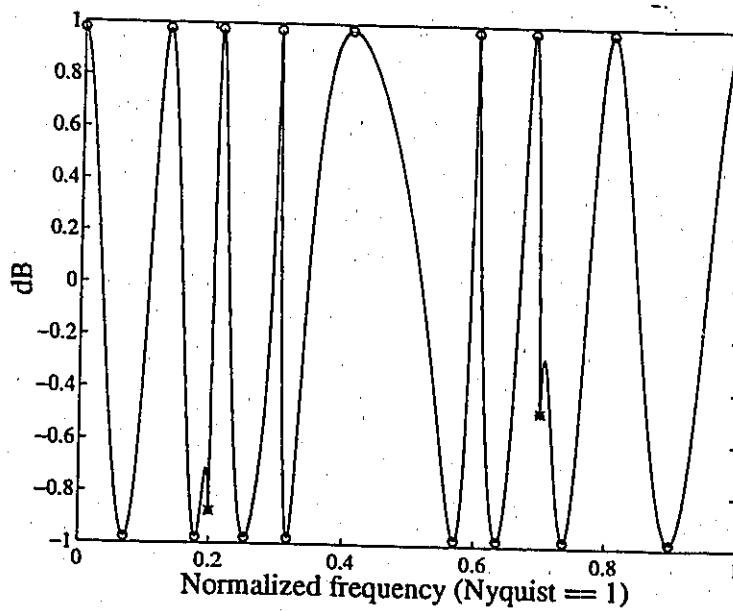


Figure 3.2: Example 6, — log magnitude approximation error, o extremal,\* extra ripple

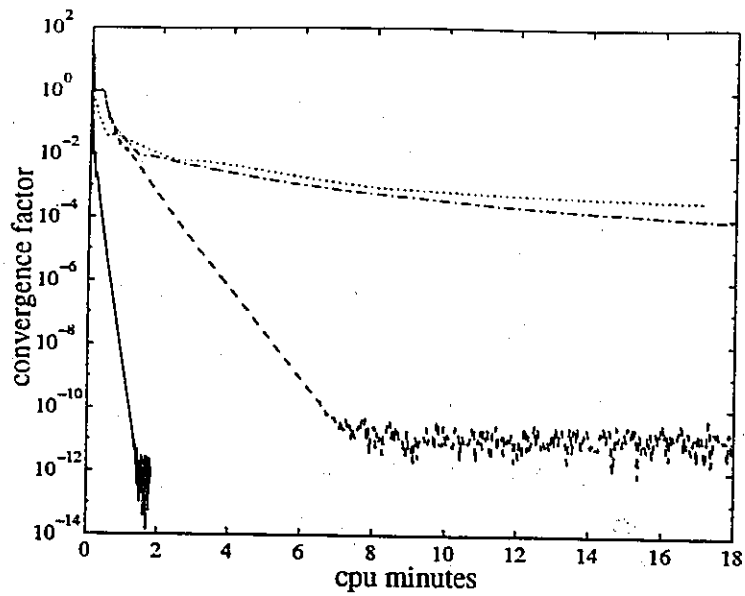


Figure 3.3: Example 6,  $R(t_i)$  for  $1 \leq i \leq 500$ ,  $\cdots$  Kobayashi's method,  $-\cdot-\cdot-$  Lim's method,  $---$  Lim's method with rejection scheme,  $—$  proposed Remez-type algorithm

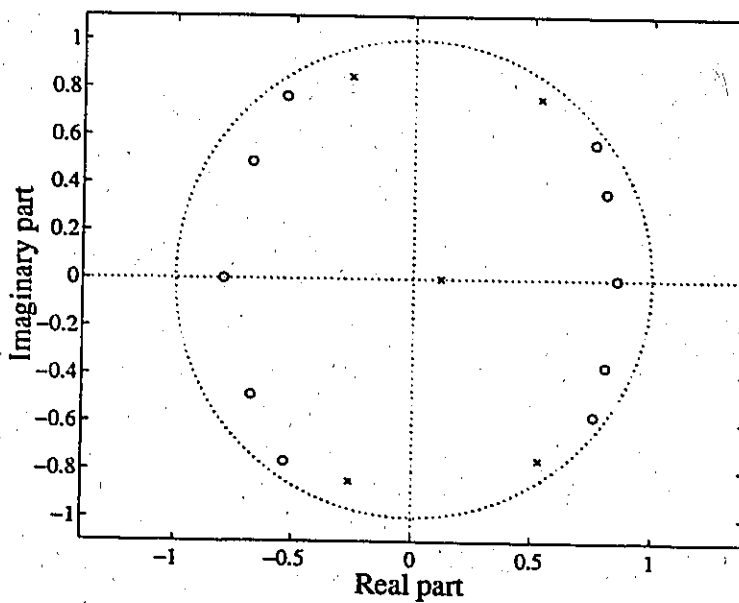


Figure 3.4: Example 6, o zero, x pole

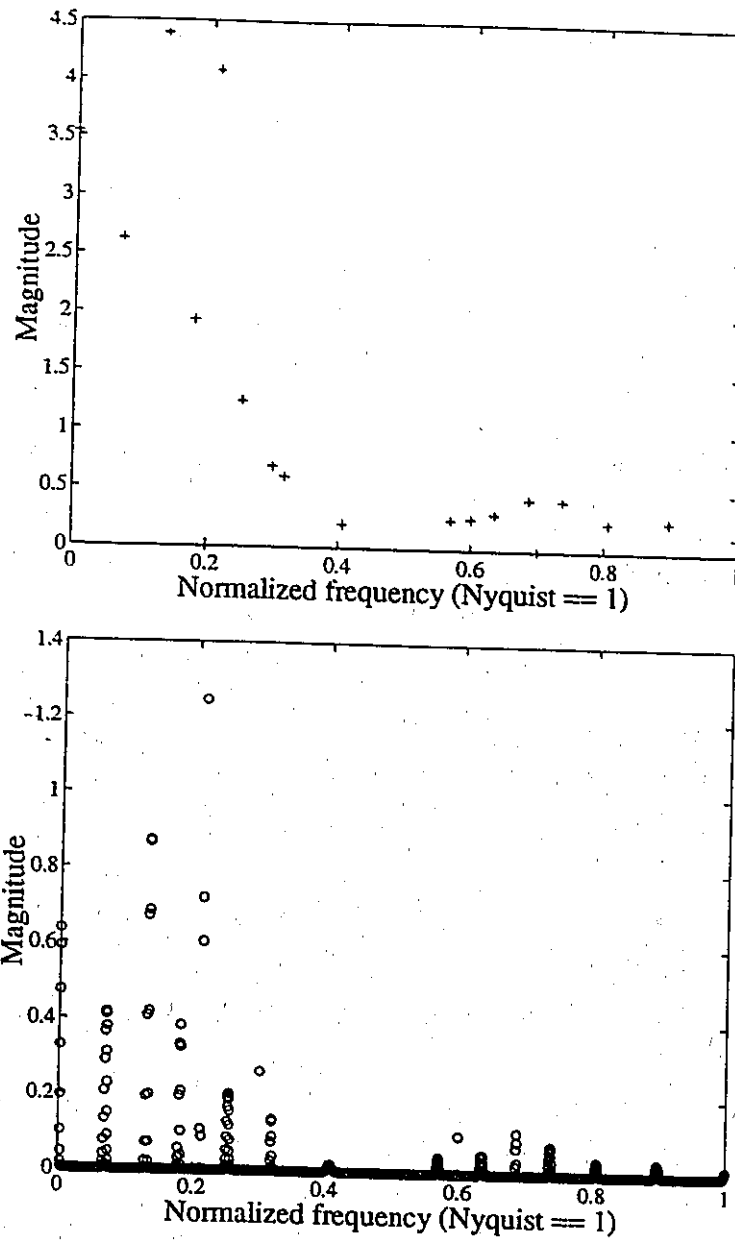


Figure 3.5: Example 6, weighting function  $L_{500}(e^{j\omega n})$ , x Proposed algorithm, o Kobayashi's method

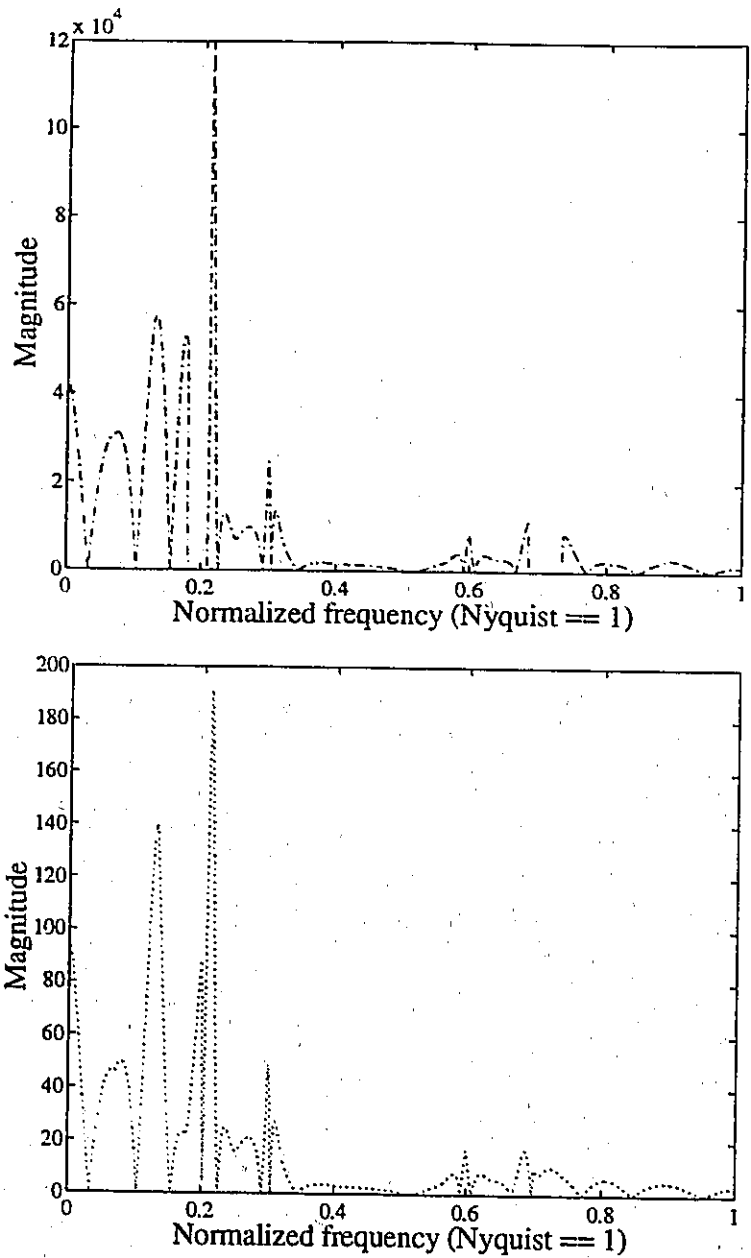


Figure 3.6: Example 6, weighting function  $L_{500}(e^{j\omega_n})$ ,  $\cdots$  Lim's method with rejection of extra extremals,  $-\cdots-$  original Lim's method

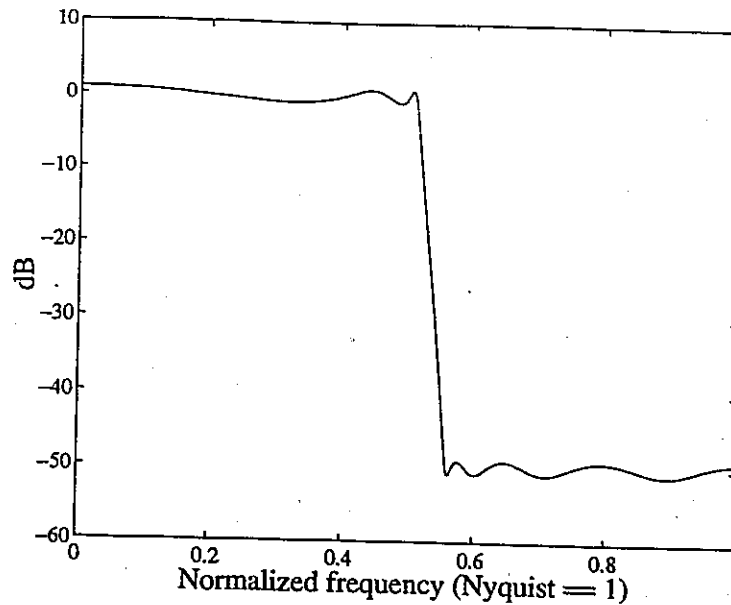


Figure 3.7: Example 7, IIR filter frequency response

The filter frequency response and log magnitude error obtained are plotted in Fig. 3.7 and Fig. 3.8. The log magnitude error has  $M + N + 1 = 15$  alternated extremals and the maximum error value is  $e_{\infty} = .9226844dB$ . Since the number of alternated extremals is less than  $M + N + 2$  the IIR filter obtained is not an optimal nondegenerate Chebyshev approximation.

The poles and zeros are plotted in Fig. 3.10. We can see that the zero at  $z = .11$  is very close to the pole at  $z = .12$ . Hence there is almost a pole-zero cancelation, which means that the filter obtained is almost degenerate.

The factor  $R(t_i)$  for the respective design algorithms is plotted in Fig. 3.9. The proposed Remez-type method is fast and accurate compared to the traditional IRLS methods. Note that since there are less than  $M + N + 2$  extremals, the rejection scheme fails to accelerate the design and the corresponding convergence factor is not shown. The frequency response of the filter obtained is plotted in Fig. 3.7.

Since the filter obtained is almost degenerate, it make sense to reduce the number of zeros and poles by 1 each, as shown in the next section.

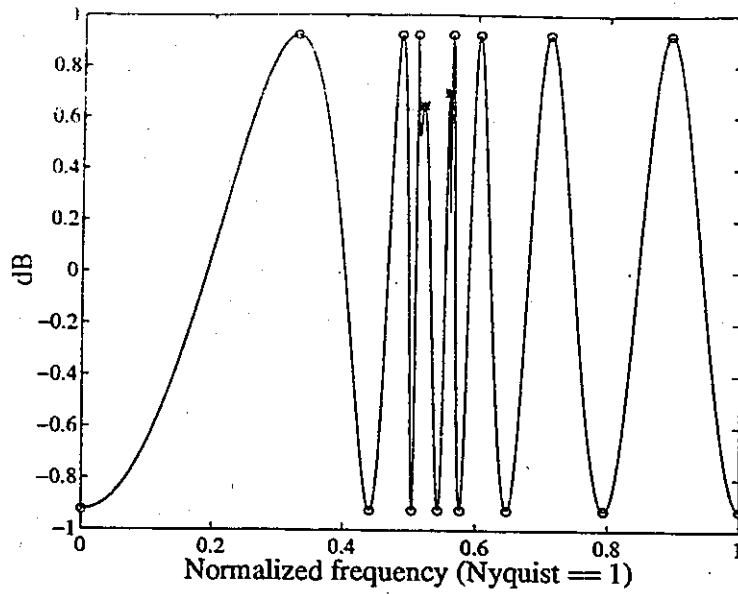


Figure 3.8: Example 7, — log magnitude approximation error, o extremal,\* extra ripple

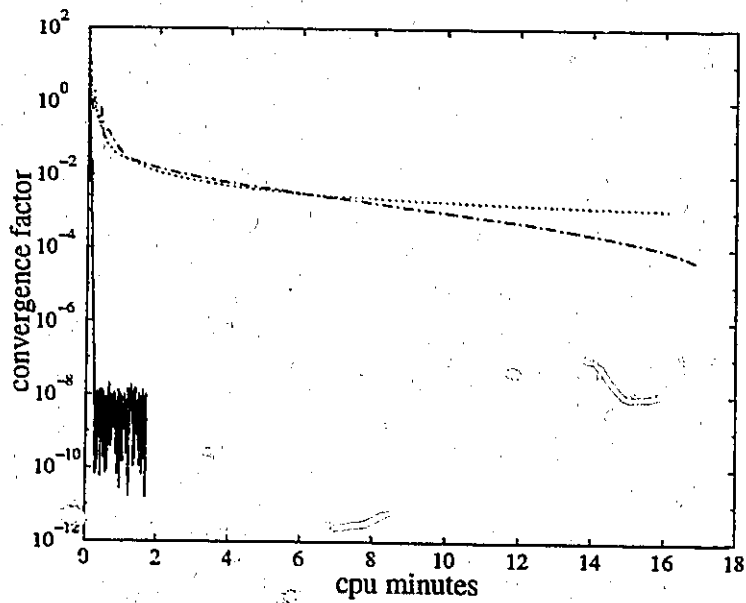


Figure 3.9: Example 7,  $R(t_i)$  for  $1 \leq i \leq 500$ , ... Kobayashi's method, - · - · - Lim's method, - - - Lim's method with rejection scheme, — proposed Remez-type algorithm

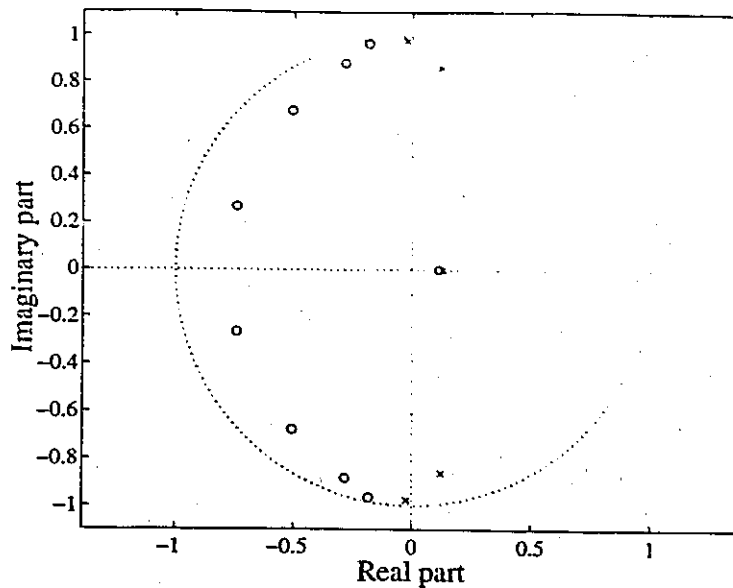


Figure 3.10: Example 7, o zero, x pole

**Example 8: bandpass filters  $M = 8$ ,  $N = 4$**

We have redesigned the filter of example 7 with  $M = 8$  zeros and  $N = 4$  poles. The log magnitude approximation error, shown in Fig. 3.11, appears to be the same as in example 2. Moreover the distribution of the zeros and the poles shown in Fig. 3.13 is similar to example 7 except for the cancelled pair.

If the filter of example 7 was strictly degenerate, the filter obtained here would be exactly the same. However since the filter was not strictly degenerate, the filters are slightly different: the maximum approximation error is a bit greater, i.e.  $e_{\infty} = .9363dB$  as opposed to  $.9226dB$ . Moreover the ripple at  $\omega = 0$  is not an extremal and has a magnitude  $.80dB < e_{\infty}$ .

The convergence factors are plotted in Fig. 3.12. We can see that Lim's method with the rejection of the smallest extra ripples fails to accelerate the convergence. This is probably due to the relatively large amplitude of the extra ripples.

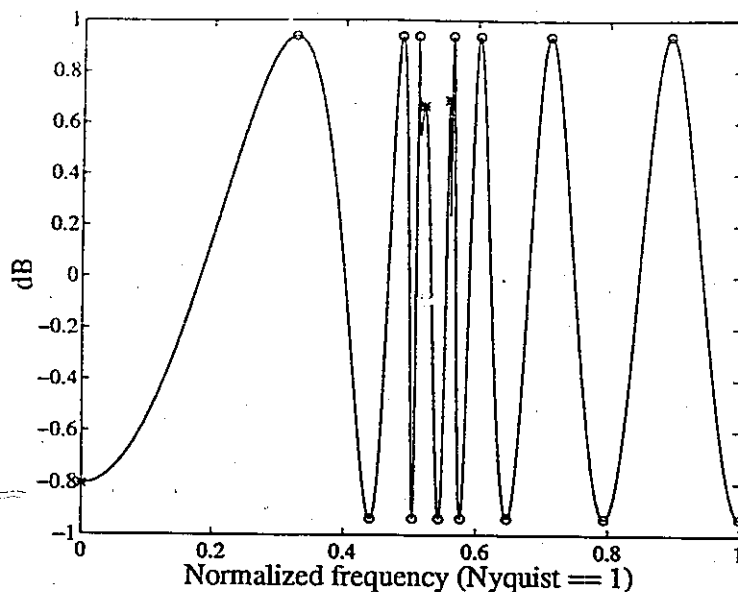


Figure 3.11: Example 8,  $-\log$  magnitude approximation error, o extremal,\* extra ripple

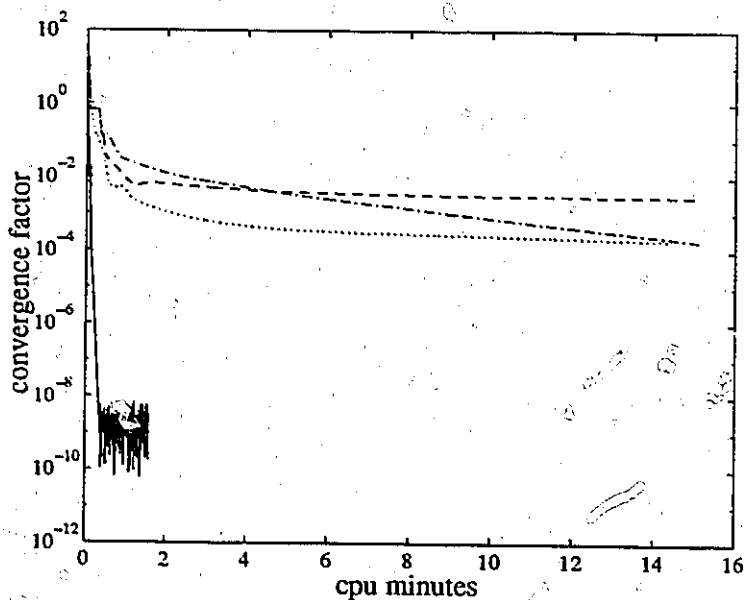


Figure 3.12: Example 8,  $R(t_i)$  for  $1 \leq i \leq 500$ ,  $\dots$  Kobayashi's method,  $-\cdot-\cdot-$  Lim's method,  $- - -$  Lim's method with rejection scheme,  $-$  proposed Remez-type algorithm

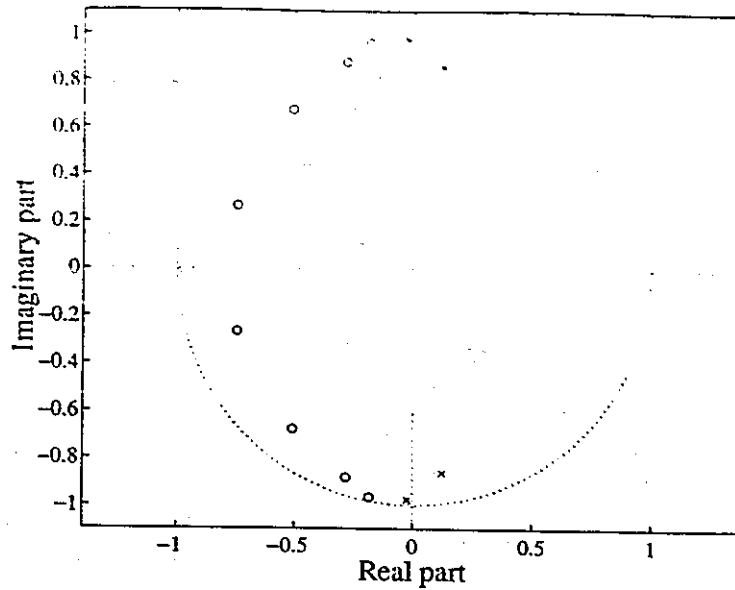


Figure 3.13: Example 8, o zero, x pole

**Example 9: unconventional specifications  $M = 11$ ,  $N = 9$**

This example illustrates the design of an IIR filter with unconventional log magnitude specifications. It also shows that when the extra ripples have relatively large amplitudes Lim's method with the rejection technique fails to speed up the design convergence.

The IIR filter designed has 11 zeros and 9 poles and approximates the following log magnitude function

$$20 \log |D(\omega)| = \begin{cases} 0dB & 0 \leq \omega \leq 0.2\pi \\ 50dB & \omega = .3\pi \\ 20dB & \omega = .4\pi \\ 50dB & \omega = .5\pi \\ 0dB & 0.6\pi \leq \omega \leq \pi \end{cases}$$

The filter frequency response is plotted in Fig. 3.14. As shown on Fig. 3.15, the approximation error has  $M + N + 2 = 22$  alternated extremals. Hence the filter obtained is the best Chebyshev approximation. The maximum error value is  $e_{\infty} = .7996898dB$ . The convergence factors are plotted in Fig. 3.16. The proposed

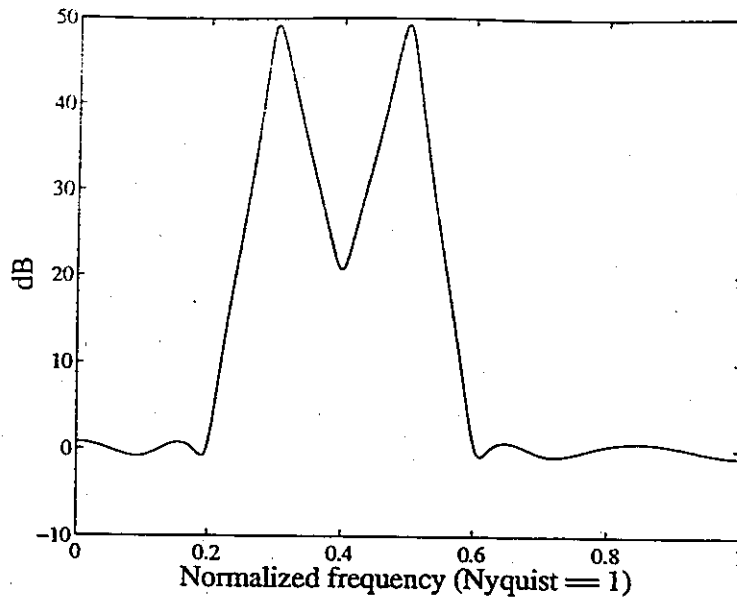


Figure 3.14: Example 9, IIR filter frequency response

method is fast and accurate. Lim's method with the rejection scheme result in a biased convergence probably because of the relatively large amplitude of the extra ripples. The zeros and poles of the filter obtained are plotted in Fig. 3.17.

### 3.8 Conslusions

In this chapter we have presented a Remez-type IRLS algorithm to design Chebyshev log IIR filters. This new method improves significantly the convergence speed of Kobayashi's and Lim's IRLS methods. Moreover it is simpler and more flexible than the traditional rational remez algorithm.

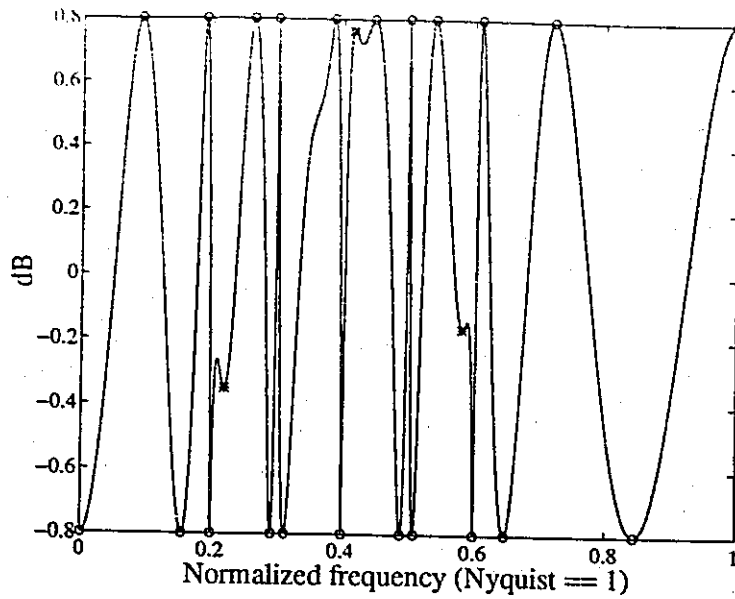


Figure 3.15: Example 9,  $-\log$  magnitude approximation error, o extremal, \* extra ripple

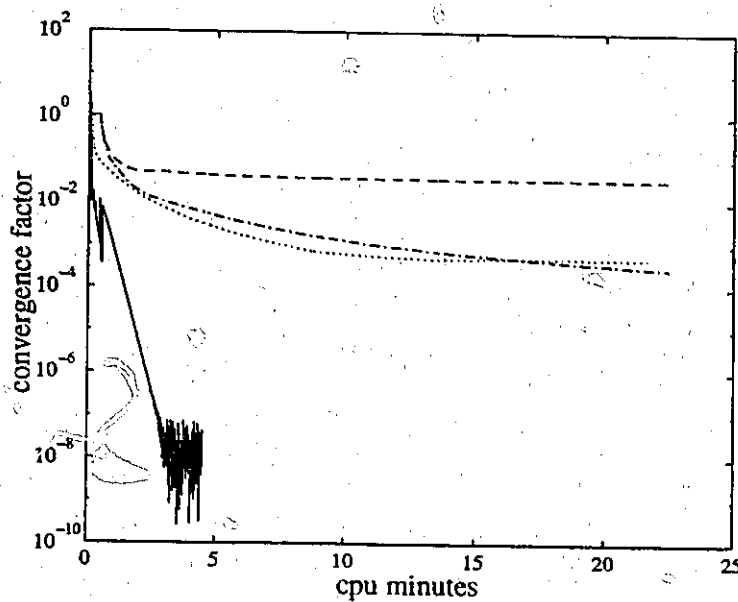


Figure 3.16: Example 9,  $R(t_i)$ ,  $\dots$  Kobayashi's method,  $-\cdot-\cdot-$  Lim's method,  $---$  Lim's method with rejection scheme,  $—$  proposed Remez-type algorithm

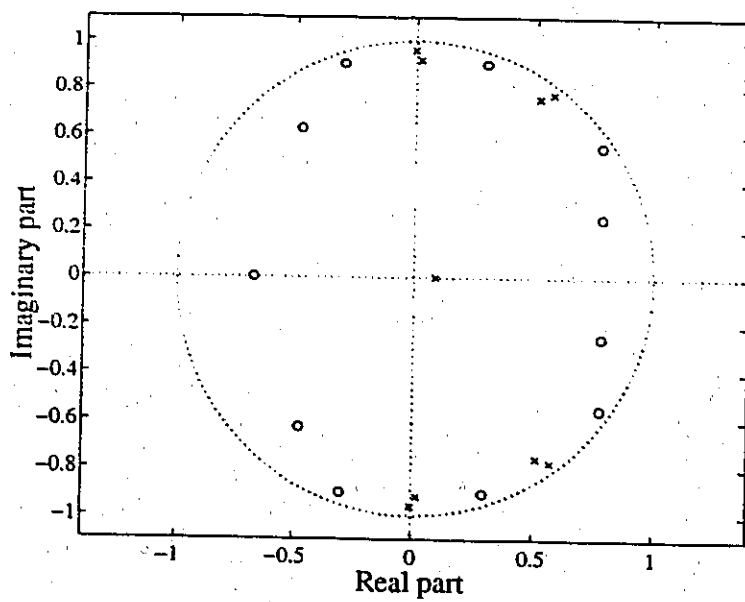


Figure 3.17: Example 9, o zero, x pole

## Chapter 4

# ILS Design of Uniform Cosine Modulated Filter Banks

Filter banks are used in a number of applications such as speech and image encoding [54], adaptive filtering [56]-[57], transmultiplexing [55] and estimation [58]. The distortions and the conditions for Perfect Reconstruction in uniform filter banks have been studied extensively in the past fifteen years [59]-[73]. The design of filter banks is generally performed by nonlinear optimization methods [61]-[73]. These optimization procedures are computationally very intensive, their convergences towards the optimum filter banks are slow and uncertain since the cost functions have many local minima in general. As noted in [61] and [65], the starting points are critical and significant human intervention is necessary to obtain acceptable filters. To improve, simplify and speed up the design of filter banks we have investigated ways to use the Iterative Least Squares (ILS) approach.

The use of the ILS approach to design filter banks has been proposed in [16] and [17]. However these methods are restricted to the design of 2-band QMF banks. Nayebi [18]-[19] proposed an ILS algorithm for M-band filter bank design. His design method is very general and can be used to design low delay filter banks, however his ILS method is associated with a complicated gradient based optimization method.

In this chapter we extend Jain's and Chen's ILS methods [16]-[17] to the design

of M-band Pseudo QMF banks, NPR Pseudo QMF banks and PR Filter banks. The algorithms presented are computationally efficient, simple to implement and flexible. For the design of Pseudo QMF banks and NPR Pseudo QMF banks the convergence have been observed to be independent of the starting point in simulations. An iteratively calculated weighting function can be used to shape the prototype stopband and/or the filter bank magnitude transfer function and perform the minimax or the gain constrained least squares approximation.

In section 4.1 we review the sources of distortion and the conditions for perfect reconstruction of QMF banks. Then in section 4.2, 4.3 and 4.4 the three algorithms, their respective design examples and MATLAB implementations are presented. The conclusions are given in section 4.5.

## 4.1 Filter banks design problem

Fig. 4.1 represents a classic uniform M-band filter bank where  $H_k(z)$  are the analysis filters and  $F_k(z)$  are the synthesis filters.

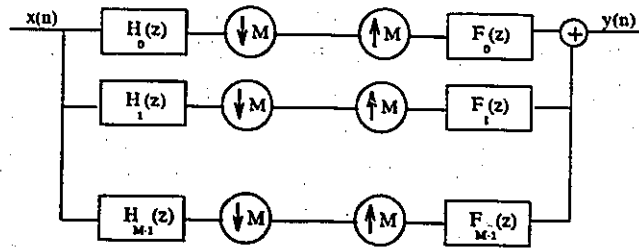


Figure 4.1: Uniform M-band filter bank

The expression of the output signal can be shown to be

$$Y(z) = \sum_{r=0}^{M-1} A_r(z) X(zW_M^r) \quad (4.1)$$

where

$$A_r(z) = \frac{1}{M} \sum_{k=0}^{M-1} F_k(z) H_k(zW_M^r) \quad (4.2)$$

and  $W_M = e^{-j\frac{2\pi}{M}}$ .

The Perfect Reconstruction property is satisfied if the output signal is a delayed version of the input signal, i.e.  $Y(z) = z^{-n_0} X(z)$ , for some number  $n_0$ . The conditions on the transfer functions  $\{A_r(z)\}$  for Perfect Reconstruction are as follows

$$A_0(z) = z^{-n_0} \quad (4.3)$$

$$A_r(z) = 0 \quad 1 \leq r \leq M - 1 \quad (4.4)$$

Three sources of distortion affecting the output signal can be identified from the expressions (4.1)-(4.4). Aliasing distortion is present when the condition (4.4) is not satisfied. There is phase distortion when  $A_0(z)$  does not have a linear phase, and magnitude distortion occurs when  $|A_0(z)|$  is not strictly flat.

In this chapter we consider the design of cosine modulated filter banks. The cosine modulation [62] has two main attractive properties: the design is facilitated since only one filter, the prototype filter, has to be optimized and there exists a fast implementation using the discrete cosine transform. The prototype filter,  $H(z)$ , is a linear phase lowpass FIR filter with a stopband frequency greater than  $\frac{\pi}{2M}$ . The analysis and synthesis filters are derived from  $H(z)$  as follows

$$\begin{cases} H_k(z) = \alpha_k H(zW_{2M}^{k+.5}) + \alpha_k^* H(zW_{2M}^{-(k+.5)}) \\ F_k(z) = z^{-N} H_k(z^{-1}) \end{cases} \quad (4.5)$$

for  $0 \leq k \leq M - 1$ , where  $N$  is the order of the prototype filter,  $\alpha_k$  is a phase factor equal to  $e^{j(-1)^k \frac{\pi}{4} W_{2M}^{(k+.5)\frac{N}{2}}}$  and  $\alpha_k^*$  is the complex conjugate of  $\alpha_k$ . Equivalently, in the time domain the cosine modulation can be written as

$$\begin{cases} h_k(n) = 2h(n) \cos\left((2k + 1)\frac{\pi}{2M}\left(n - \frac{N}{2} + (-1)^k \frac{\pi}{4}\right)\right) \\ f_k(n) = h_k(N - n) \end{cases} \quad (4.6)$$

for  $0 \leq k \leq M - 1$  and  $0 \leq n \leq N$ .

An other interesting property of the cosine modulation [62] is that the aliasing between adjacent bands, i.e.  $A_1(z)$ , is eliminated thanks to the appropriate phase factor  $\alpha_k$ .

Injecting the second equality of (4.5) into (4.2), we obtain the following expression of the filter bank overall transfer function

$$A_0(e^{j\omega}) = \frac{e^{-jN\omega}}{M} \sum_{k=0}^{M-1} |H_k(e^{j\omega})|^2 \quad (4.7)$$

We can see that the cosine modulation guarantees the cancellation of the phase distortion, that the delay introduced by the filter bank,  $n_0$ , is equal to the order of the prototype filter,  $N$ . Note that each analysis and synthesis filter is required to have a gain of  $\sqrt{M}$  in the passband for the filter bank to have an overall gain of 1.

As shown in [71], the transfer function  $A_0(z)$  can be expressed in terms of the shifted versions of the prototype frequency response as follows

$$A_0(z) = \frac{z^{-N}}{M} \sum_{k=0}^{2M-1} H(zW_{2M}^{k+.5})H(z^{-1}W_{2M}^{-(k+.5)}) \quad (4.8)$$

which leads to the following expression (see appendix for the details)

$$A_0(z) = 2z^{-N} \sum_{k=-E[\frac{N}{2M}]}^{E[\frac{N}{2M}]} (-1)^k \sum_{r=0}^{N-2M|k|} h(r)h(2M|k|+r)z^{-2Mk} \quad (4.9)$$

where  $E[x]$  is the integer part of  $x$ . Note that  $z^N A_0(z)$  is a function of  $z^{-2M}$ , which means that  $|A_0(e^{j\omega})|$  is periodical with a period  $\frac{\pi}{M}$ . From the expression (4.9), it is obvious that the magnitude distortion is canceled if and only if

$$\sum_{r=0}^{N-2Mk} h(r)h(2Mk+r) = \frac{1}{2}\delta(k) \quad 0 \leq k \leq E[\frac{N}{2M}] \quad (4.10)$$

where  $\delta(k)$  is the Kronecker symbol, i.e.  $\delta(0) = 1$  and  $\delta(k) = 0$  for  $k \neq 0$ .

As shown in [69], the perfect reconstruction is possible when the length of the prototype filter is  $N+1 = 2mM$ , for some integer  $m$ , and when for  $n = 0, \dots, E[\frac{M+1}{2}] - 1$  the following condition is satisfied

$$\sum_{r=0}^{2m-2k-1} h(n+rM)h(n+rM+2kM) = \frac{\delta(k)}{2M} \quad 0 \leq k \leq m-1 \quad (4.11)$$

Thanks to the symmetry of the prototype filter impulse response, i.e.  $h(2mM-1-n) = \mp h(n)$  for  $n = 0, \dots, 2mM-1$ , if (4.11) is satisfied for  $n = 0, \dots, E[\frac{M+1}{2}] - 1$ ,

it is also satisfied for  $n = E[\frac{M+1}{2}], \dots, M-1$ . Moreover it is easy to verify that the summation of the condition (4.11) for  $n = 0, \dots, M-1$  implies (4.10).

In this chapter, for the sake of simplicity we assume that the length of the prototype filter,  $N+1$ , is even and that the impulse response,  $h(n)$  for  $n = 0, 1, \dots, N$ , shows an even symmetry. For the design of Pseudo QMF and NPR Pseudo QMF banks, the algorithm can address the case of an odd length with minor modifications. Exploiting the even symmetry, the prototype filter frequency response can be expressed as

$$H(e^{j\omega}) = e^{-j\omega\frac{N}{2}} \sum_{n=0}^{\frac{N-1}{2}} h(\frac{N+1}{2} + n) 2 \cos(\omega(n + .5)) \quad (4.12)$$

The evaluation of the amplitude of the frequency response of the prototype filter, i.e.  $A(e^{j\omega}) = e^{j\omega\frac{N}{2}} H(e^{j\omega})$ , over an  $L$ -point frequency grid  $\Omega = \{\omega_0, \omega_1, \dots, \omega_{L-1}\}$  can be written in a vector matrix form as

$$[A(e^{j\omega_0}), \dots, A(e^{j\omega_{L-1}})]^t = Cp \quad (4.13)$$

where  $p = [h(\frac{N+1}{2}) \dots h(N)]^t$  and  $C$  is a  $L \times \frac{N+1}{2}$  matrix containing the cosine coefficients  $C_{r,n} = 2 \cos(\omega_r(n + .5))$  for  $0 \leq n \leq L-1$  and  $0 \leq r \leq \frac{N-1}{2}$ .

## 4.2 ILS design of Pseudo QMF banks

In this section we present the ILS method to design  $M$ -band Pseudo QMF banks. The unweighted design is first introduced. Then we present the Iterative Reweighted Least Squares (IRLS) method used to perform the minimax or the gain constrained least squares approximation of the prototype stopband and/or the filter bank magnitude transfer function. Design examples and the MATLAB program implementing the proposed algorithm are included.

### 4.2.1 Unweighted Pseudo QMF bank ILS design algorithm

As defined in [62], the design of  $M$ -band Pseudo QMF banks is the direct extension of the 2-band QMF bank design method of Johnston [61]. It consists of minimizing

the energy related to the magnitude reconstruction error of the filter bank,  $e_m$ , as well as the stopband ripple energy of the prototype filter,  $e_s$ , as follows

$$\min(e_s + \gamma e_m) \quad (4.14)$$

with

$$e_s = \frac{1}{\pi - \omega_s} \int_{\omega_s}^{\pi} |H(e^{j\omega})|^2 d\omega \quad (4.15)$$

$$e_m = \frac{1}{\pi} \int_0^{\pi} (|A_0(e^{j\omega})| - 1)^2 d\omega \quad (4.16)$$

where  $\omega_s$  is the stopband frequency edge of the prototype filter and  $\gamma$  is a positive number corresponding to a relative weight factor associated with the minimization of  $e_m$ . The larger  $\gamma$  is, the smaller the residual magnitude distortion is. For  $M > 2$  there is aliasing distortion between non adjacent bands. As pointed out in [71], the maximum level of the aliasing transfer functions,  $A_r(e^{j\omega})$  for  $r = 1, \dots, M - 1$ , is of the order of the stopband attenuation of the prototype filter. Hence the aliasing distortion can be kept small when the attenuation is sufficiently large for  $\omega \geq \frac{\pi}{M}$ .

To introduce the ILS approach, we wish to formulate the objective function (4.14) as a quadratic function of the vector of coefficients  $p$ . The stopband energy,  $e_s$ , is obviously quadratic. The discretization of the integral of (4.15) on  $\Omega = \{\omega_0, \dots, \omega_{L-1}\}$ , a dense and uniform frequency grid of  $[\omega_s, \pi]$  with  $L \gg N$ , leads to the following matrix expression

$$e_s \approx \frac{1}{L} \sum_{n=0}^{L-1} |H(e^{j\omega_n})|^2 = \frac{1}{L} p^t C^t C p \quad (4.17)$$

The other term of the objective function (4.14), i.e.  $e_m$ , is not quadratic. In fact, using the Parseval relation and the expression (4.9),  $e_m$  can be converted in the time domain, resulting in the alternative expression

$$e_m = \sum_{k=-E[\frac{N}{2M}]}^{E[\frac{N}{2M}]} (2(-1)^k \sum_{r=0}^{N-2M|k|} h(r)h(2M|k|+r) - \delta(k))^2 \quad (4.18)$$

Hence the least squares approximation can not be done in one shot. The method proposed here is iterative: the quantity  $e_m$  is approximated at each iteration  $i$  by a

quadratic term using the coefficients  $h_{i-1}(r)$  found in the previous iteration as follows

$$\hat{e}_m(i) = \sum_{k=-E[\frac{N}{2M}]}^{E[\frac{N}{2M}]} (2(-1)^k \sum_{r=0}^{N-2M|k|} h_i(r)h_{i-1}(2M|k|+r) - \delta(k))^2 \quad (4.19)$$

A matrix form of  $\hat{e}_m(i)$  can be obtained as follows

$$\hat{e}_m(i) = (G_i p_i - d)^t (G_i p_i - d) \quad (4.20)$$

where  $p_i$  is the coefficient vector at the iteration  $i$ ,  $[h_i(\frac{N+1}{2}), \dots, h_i(N)]^t$ ,  $d$  is the vector  $[1, 0, \dots, 0]^t$  and  $G_i$  is a size  $(E[\frac{N}{2M}] + 1) \times \frac{N+1}{2}$  matrix which contains the coefficients  $h_{i-1}(r)$  as follows

$$\begin{cases} G_i(1, r) = 4h_{i-1}(\frac{N+1}{2} + r - 1) & 1 \leq r \leq \frac{N+1}{2} \\ G_i(k, r) = 0 & 1 \leq r \leq M(k-1) \\ G_i(k, r) = 4\sqrt{2}(-1)^{k-1}h_{i-1}(\frac{N+1}{2} + r - 1 - 2M(k-1)) & M(k-1) + 1 \leq r \leq \frac{N+1}{2} \end{cases} \quad (4.21)$$

for  $2 \leq k \leq E[\frac{N}{2M}] + 1$ .

The proposed ILS algorithm consists of finding the prototype filter which minimizes the nonlinear objective function (4.14) by solving iteratively the following quadratic minimization problem

$$\min(e_s(i) + \gamma \hat{e}_m(i)) \quad (4.22)$$

At each iteration  $i$ , the minimization of (4.22) consists of solving the following overdetermined system of linear equations in the least squares sense

$$\begin{bmatrix} G_i \\ \frac{1}{\sqrt{L\gamma}} C \end{bmatrix} p_i = \begin{bmatrix} d \\ 0 \end{bmatrix} \quad (4.23)$$

The solution can be obtained using the pseudo-inverse matrix of  $[G_i^t \quad \frac{1}{\sqrt{L\gamma}} C^t]^t$  as follows

$$p_i = ([G_i^t \quad \frac{1}{\sqrt{L\gamma}} C^t] \begin{bmatrix} G_i \\ \frac{1}{\sqrt{L\gamma}} C \end{bmatrix})^{-1} [G_i^t \quad \frac{1}{\sqrt{L\gamma}} C^t] \begin{bmatrix} d \\ 0 \end{bmatrix} \quad (4.24)$$

The expression of the solution can be shown to be

$$p_i = 4[G_i^t G_i + \frac{1}{L\gamma} C^t C]^{-1} p_{i-1} \quad (4.25)$$

The matrix multiplication  $C^t C$  can be avoided since there exists an analytical formula for the limit  $S = \lim_{L \rightarrow +\infty} \frac{1}{L} C^t C$ . The coefficients of  $S$  are for  $1 \leq i \leq \frac{N+1}{2}$  and  $1 \leq j \leq \frac{N+1}{2}$  defined as

$$S(i, j) = \frac{4}{\pi - \omega_s} \int_{\omega_s}^{\pi} \cos(\omega(j-1) + .5) \cos(\omega(i-1) + .5) d\omega \quad (4.26)$$

It is easy to verify that for  $1 \leq k \leq \frac{N+1}{2}$  and  $2 \leq r < n \leq \frac{N+1}{2}$

$$\begin{cases} S(k, k) = \frac{-1}{\pi - \omega_s} \frac{\sin(\omega_s(2k-1))}{k-.5} + 2 \\ S(r, n) = S(n, r) = \frac{-2}{\pi - \omega_s} \frac{\sin(\omega_s(r+n-1))}{r+n-1} - \frac{2}{\pi - \omega_s} \frac{\sin(\omega_s(r-n))}{r-n} \end{cases} \quad (4.27)$$

To guarantee the mean of  $|A_0(e^{j\omega})|$  to be equal to 1, we normalize the filter coefficients obtained from (4.25) as follows

$$h_i(n) \leftarrow \frac{h_i(n)}{\sqrt{2 \sum_{r=0}^N h_i(r)^2}} \quad (4.28)$$

As for most of the ILS methods used in filter design applications, the convergence of our algorithm is not theoretically proven. However, from the experimentation we have found that it does converge very fast, and that the designed filter does not depend on the initial coefficients  $p_0$ . The termination criterion can simply consist of a tolerance on the maximum variation of the filters coefficient  $p_i$ . The algorithm can be summarized into the following steps

- *Step 1*, choose  $M$ ,  $N$ ,  $\omega_s$  and  $\gamma$ ,
- *Step 2*,  $i \leftarrow 0$ , initialize  $p_0$  with random coefficients,
- *Step 3*,  $i \leftarrow i + 1$ , build the matrix  $G_i$  with  $p_{i-1}$  using (4.21),
- *Step 4*, find  $p_i$  using (4.25),
- *Step 5*, normalize  $p_i$  using (4.28),
- *Step 6*, go to step 3 unless  $\max |p_i - p_{i-1}| \leq \epsilon$ , where  $\epsilon$  is a small number.

## 4.2.2 Pseudo QMF bank IRLS design algorithm

The ILS design of Pseudo QMF banks can be easily be coupled with an Iterative Reweighted Least Squares algorithm [20]-[22]. In this case the quantity  $e_s$  or/and  $\hat{e}_m$  are weighted in the frequency domain and the minimax or the gain constrained least squares approximation can be achieved.

The minimax approximation of the prototype stopband is of interest since it guarantees the same attenuation in all rejected bands. The gain constrained least squares approximation offers a trade off between the least squares and the minimax criteria. The weighted stopband energy considered is the following

$$\tilde{e}_s(i) = \sum_{n=0}^{L-1} |w_i(\omega_n)H(e^{j\omega_n})|^2 = p_i^t C^t W_i^t W_i C p_i \quad (4.29)$$

where  $w_i(\omega_n)$  is the weighting function at the iteration  $i$  defined on the frequency grid  $\Omega = \{\omega_0, \dots, \omega_{L-1}\}$  and  $W_i$  is the diagonal matrix  $\text{diag}([w_i(\omega_0), \dots, w_i(\omega_{L-1})])$ . As in (4.23), the weighted least squares problem leads to an overdetermined system of linear equations, i.e.

$$\begin{bmatrix} G_i \\ \frac{1}{\sqrt{\gamma}} W_i C \end{bmatrix} p_i = \begin{bmatrix} d \\ 0 \end{bmatrix} \quad (4.30)$$

which can be solved in the least squares sense with the pseudo-inverse method as follows

$$p_i = 4[G_i^t G_i + \frac{1}{\gamma} C^t W_i^t W_i C]^{-1} p_i \quad (4.31)$$

This least squares minimization can be done very efficiently using a QR least squares algorithm which avoids the explicit computation of the pseudo inverse matrix and directly considers the overdetermined system. An implementation of this algorithm is provided with the MATLAB package [9].

The weights are all initialized with the value  $\frac{1}{\sqrt{L}}$  which corresponds to the least squares design. The weights remain unchanged until the least squares design has converged. Then for the minimax design the weights are updated using Lim's method as follows

$$w_{i+1}(\omega_n) = w_i(\omega_n) (\text{env}(|H_i(e^{j\omega_n})|)) \frac{\theta}{2} \quad \text{for } \omega_n \in \Omega \quad (4.32)$$

where  $\theta$  is a number greater than zero (typically equal to 1) and  $env(|H_i(e^{j\omega_n})|)$  is the envelope of  $|H_i(e^{j\omega})|$ , i.e. the function that connects its maxima with straight lines. For the gain constrained least squares design, the weights are updated on a subset  $\hat{\Omega}_i$  of  $\Omega$  where  $env(|H_i(e^{j\omega})|)$  is greater than the prescribed maximum gain  $g_{max}$  as follows

$$\begin{cases} w_{i+1}(\omega_n) = w_i(\omega_n) (env(|H_i(e^{j\omega_n})|) / g_{max})^{\frac{\theta}{2}} & \text{for } \omega_n \in \hat{\Omega}_i \\ w_{i+1}(\omega_n) = w_i(\omega_n) & \text{for } \omega_n \in \Omega - \hat{\Omega}_i \end{cases} \quad (4.33)$$

Note that when  $g_{max}$  is small, i.e. less than the Chebyshev norm of the corresponding minimax filter, the two weight update procedures (4.32) and (4.33) are equivalent whereas when  $g_{max}$  is large, the weights remain unchanged and a least squares filter is designed. For both designs, the weights are normalized after each update, (4.32)-(4.33), such that the relative weight  $\gamma$  can remain the same at each iteration

$$w_{i+1}(\omega_n) \leftarrow \frac{w_{i+1}(\omega_n)}{\sqrt{\sum_{n=0}^{L-1} w_{i+1}(\omega_n)^2}} \quad (4.34)$$

The approximation error of the magnitude transfer function,  $|A_0(e^{j\omega}) - e^{-jN\omega}|$ , can also be weighted. The IRLS method can be used to reduce the peak values of  $|A_0(e^{j\omega}) - e^{-jN\omega}|$  and obtain a minimax approximation error on  $[0, \pi]$ . In this case, at each iteration  $i$ , the amplitude of  $A_0(e^{j\omega})$  is approximated by  $T_i(e^{j\omega})$  as follows

$$T_i(e^{j\omega}) = \sum_{k=-E[\frac{N}{2M}]}^{E[\frac{N}{2M}]} 2(-1)^k \sum_{r=0}^{N-2M|k|} h_i(r) h_{i-1}(2M|k| + r) e^{-j2Mk\omega} \quad (4.35)$$

Since  $T_i(e^{j\omega})$  is periodical of period  $\frac{\pi}{M}$ , the approximation error of the magnitude transfer function  $|T_i(e^{j\omega}) - 1|$  is weighted on the frequency band  $[0, \frac{\pi}{M}]$ . Let us consider  $\Phi = \{\varphi_0, \dots, \varphi_{L_m-1}\}$ , a dense and uniform frequency grid of  $[0, \frac{\pi}{M}]$ . Since the impulse response of  $T_i(z)$  shows an even symmetry and can be obtained from the coefficients  $G_i p_i$ , the evaluation of  $T_i(e^{j\omega})$  on  $\Phi$  can be expressed in a matrix form as

$$[T_i(e^{j\varphi_0}), \dots, T_i(e^{j\varphi_{L_m-1}})]^t = C_2 G_i p_i \quad (4.36)$$

where  $C_2$  is a size  $(E[\frac{N}{2M}] + 1) \times L_m$  matrix containing the cosine coefficients defined by  $c_2(n, 1) = 1$  and  $c_2(n, r) = \sqrt{2} \cos(2M(r-1)\varphi_{n+1})$  for  $r \geq 2$ . Let  $\tilde{w}_i(\varphi_n)$  be the

weighting function associated with the approximation error  $|T_i(e^{j\omega_n}) - 1|$ . At each iteration  $i$ , the integrated weighted squared approximation error can be expressed as

$$\tilde{e}_m(i) = (C_2 G_i p_i - u)^t \tilde{W}_i^t \tilde{W}_i (C_2 G_i p_i - u) \quad (4.37)$$

where  $u$  is the vector  $[1, \dots, 1]^t$  and  $\tilde{W}_i$  is the diagonal matrix,  $\text{diag}([\tilde{w}_i(\varphi_0), \dots, \tilde{w}_i(\varphi_{L_m-1})])$ . The minimization of  $(e_s(i) + \gamma \tilde{e}_m(i))$  leads to the following overdetermined system which can be solved in the least squares sense using either the pseudo inverse method or the QR least squares algorithm.

$$\begin{bmatrix} \tilde{W}_i C_2 G_i \\ \frac{1}{\sqrt{L_i}} C \end{bmatrix} p_i = \begin{bmatrix} \tilde{W}_i u \\ 0 \end{bmatrix} \quad (4.38)$$

In a similar way as in (4.32)-(4.34), the weights are initialized with the value  $\frac{1}{\sqrt{L_m}}$  and updated according to the approximation error  $|T_i(e^{j\omega}) - 1|$ .

Note that the iterative reweighted method can be applied simultaneously on the magnitude distortion and on the prototype stopband. In this case the overdetermined system of equation to be solved at each iteration is the following one

$$\begin{bmatrix} \tilde{W}_i C_2 G_i \\ \frac{1}{\sqrt{\gamma}} W_i C \end{bmatrix} p_i = \begin{bmatrix} \tilde{W}_i u \\ 0 \end{bmatrix} \quad (4.39)$$

### 4.2.3 Pseudo QMF bank design examples

In this section, we present four design examples. These examples show the fast convergence of the ILS method compared to the traditional nonlinear optimization method and the efficiency of the iterative reweighted design techniques.

#### Example 10: Comparison between the ILS and Johnston's methods

When  $M = 1$ , the objective function (4.14) is equivalent to that of Johnston's design method. Remember that Johnston's QMF banks are not cosine modulated, hence the prototype filter obtained with  $M = 1$  corresponds to the lowpass filter of a 2-band QMF bank. We have found that the ILS algorithm can design any of the filters tabulated by Johnston in [61] in very few iterations. For instance the design of Johnston's

filter 32D required no more than 5 iterations, i.e. 0.2 cpu seconds. To compare the convergence speed of the ILS method with the conventional nonlinear optimization method, we have performed the design with Johnston's method using a quasi Newton minimization algorithm (the function *fminu* of MATLAB optimization toolbox). With a proper starting point obtained with the Remez algorithm, Johnston's method converged in 17 cpu seconds requiring 350 evaluations of the objective function.

#### Example 11: 8-band Pseudo QMF bank

Let  $M = 8$ ,  $N + 1 = 140$ ,  $\omega_s = \frac{\pi}{M}$  and  $\gamma = 10^4$ . The algorithm converged in 15 iterations, requiring 4.2 cpu seconds. The normalized analysis filter bank,  $H_k(e^{j\omega})/\sqrt{M}$  for  $k = 0, \dots, 7$ , is plotted in Fig. 4.2. The filter bank magnitude transfer function,  $|A_0(e^{j\omega})|$ , is shown in Fig. 4.3. The maximum value of  $|A_0(e^{j\omega})|$  is  $6E^{-7}dB$ . The aliasing transfer functions,  $|A_r(e^{j\omega})|$  for  $r = 1, \dots, 7$ , are plotted in Fig. 4.4. The maximum aliasing level is  $-103dB$  which is of the same order as the prototype stopband attenuation. The aliasing transfer function at  $-300dB$  corresponds to  $|A_1(e^{j\omega})|$  which is entirely canceled by the cosine modulation. The gain of  $H(e^{j\omega})/\sqrt{M}$  is  $-83dB$  at  $\omega_s$ . Using the IRLS method, we have re-designed the prototype filter with the gain constraint  $|H(e^{j\omega})|/\sqrt{M} \leq -95dB$  in the stopband. The IRLS algorithm converged in 40 iterations with  $\theta = 1$ . The normalized prototype filter,  $H(e^{j\omega})/\sqrt{M}$ , is shown in fig. 4.5. The magnitude transfer function of the filter bank obtained is roughly the same as with the least squares design, with peak values at  $6E^{-7}dB$ . The maximum level of aliasing is  $-96dB$ .

#### Example 12: 4-band Pseudo QMF banks with least squares and equiripple magnitude transfer function

Let  $M = 4$ ,  $N + 1 = 32$ ,  $\omega_s = \frac{\pi}{M}$  and  $\gamma = 1.5$ . The unweighted and IRLS algorithms have been used to design two filter banks with a least squares and a minimax magnitude transfer function respectively. The IRLS algorithm converged in 20 iterations with  $\theta = 1$ . The prototype filters obtained have roughly the same stopband:

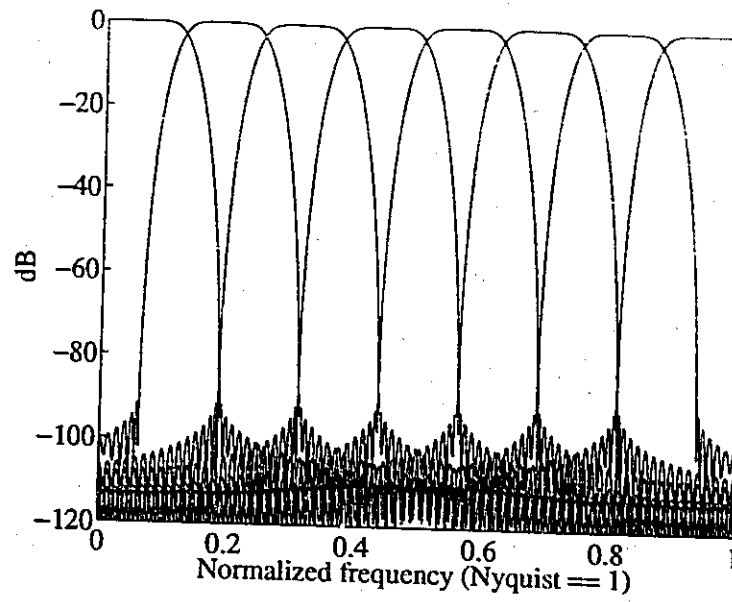


Figure 4.2: Example 11, 8-band Pseudo QMF analysis filter bank

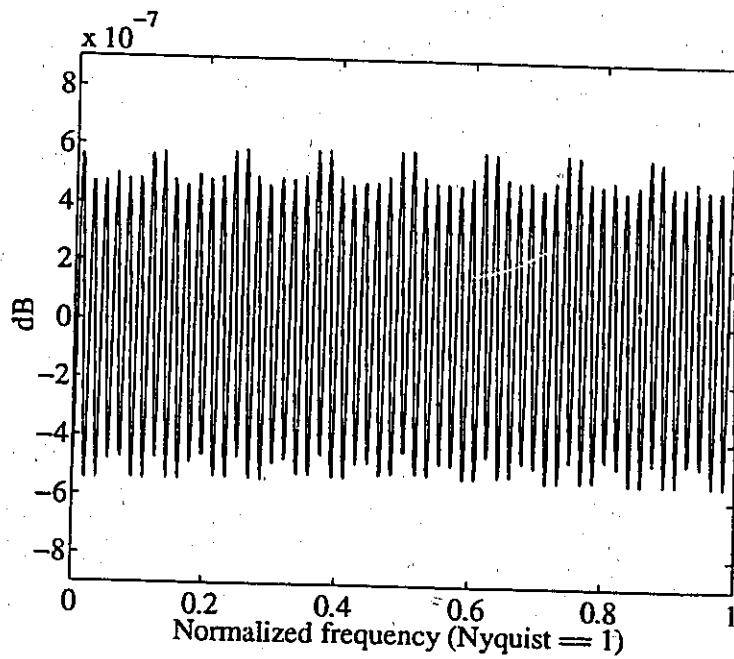


Figure 4.3: Example 11, filter bank magnitude transfer function,  $|A_0(e^{j\omega})|$

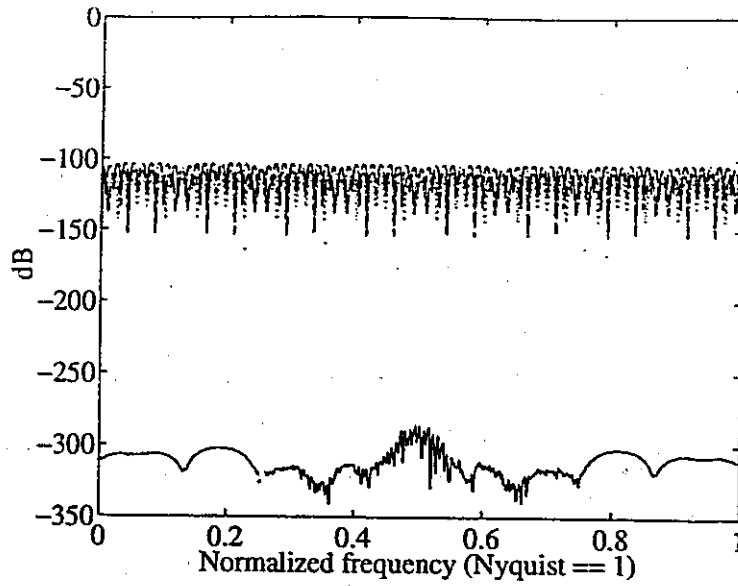


Figure 4.4: Example 11, aliasing transfer functions,  $|A_r(e^{j\omega})|$  for  $r = 1, \dots, 7$

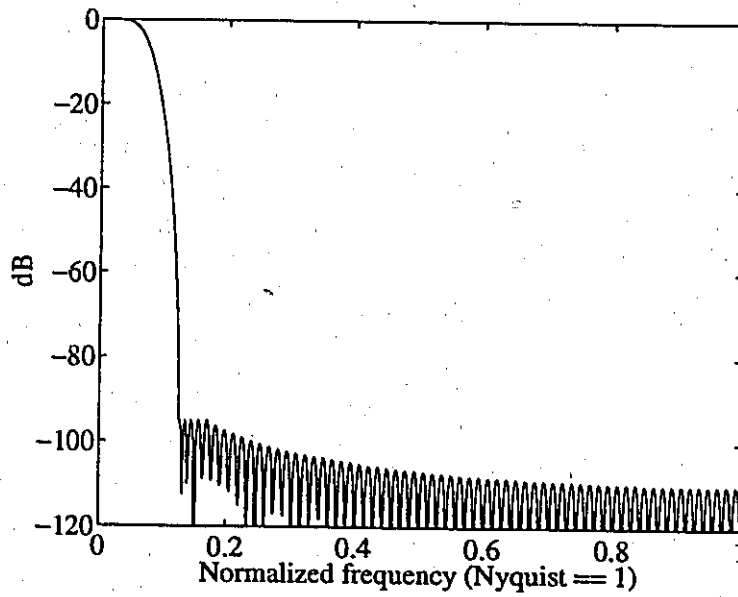


Figure 4.5: Example 11, 8-band Pseudo QMF prototype filter with a gain constrained least squares stopband

they have the same attenuation,  $45dB$ , at  $\omega_s$  and the same maximum level of aliasing,  $-55dB$ . The overall magnitude transfer functions are shown in Fig. 4.6. We can see that the minimax approximation results in an equiripple magnitude transfer function. The maximum value of the magnitude reconstruction error function for the least squares design,  $9.5E^{-3}dB$ , is larger than for the equiripple design,  $6E^{-7}dB$ .

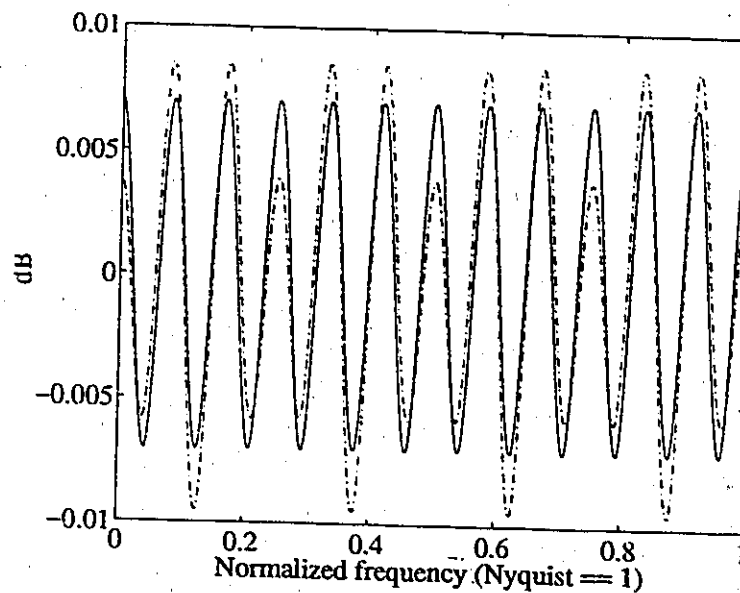


Figure 4.6: Example 12, 4-band Pseudo QMF bank magnitude transfer function,  $|A_0(e^{j\omega})|$ , - - - least squares design, — equiripple design

#### 4.2.4 MATLAB program for the ILS design of Pseudo QMF banks

The following MATLAB function, PQMF.m, implements the unweighted design of Pseudo QMF banks. The function plot\_QMF.m cosine modulates the prototype filter and plots the analysis filter bank, the overall magnitude transfer function and the aliasing transfer functions.

```
function h=PQMF(M,Lh,f,gamma)
% Pseudo QMF ILS design
% h: prototype filter, Lh length of h, M: number of bands,
% f stopband freq. in [1/2M 1/M], gamma: weight associated with em
```

```

% example: h=PQMF(8,140,1/8,10^-4);
% Author: Michel Rossi, University of Ottawa, 1996
%
epsilon=1E-8;to=cputime;R=Lh/2;p=rand(R,1);
d=-sin((2*[1:R]-1)*pi*f)/pi/(1-f)/4./([1:R]-.5)+.5;
for k1=1:R for k2=k1+1:R %Compute the matrix S
    S(k1,k2)=-[sin((k1+k2-1)*f*pi)/(k1+k2-1)+sin((k2-k1)*f*pi)/(k2-k1)]/2/pi/(1-f);
end;end;
S=[S;zeros(1,R)];S=4*(S'+S+diag(d));disp('i es em gamma max(delta(p))');
for i=1:40 pold=p;G=□;
    % build G
    for k=1:M:R
        G=[G;4*sqrt(2)*[zeros(1,k-1),p(k-1:-1:max(1,1-(R-2*(k-1))))],p(1:R-2*(k-1))]];
    end;G(1,:)=G(1,+)/sqrt(2);
    % Find the L2 solution
    p=4*(S/gamma+G'*G)\p;p=p/sqrt(4*sum(p.^2));
    es(i)=p'*S*p;mdeltap=max(abs(pold-p));ek(i)=sum((G(2:floor(Lh/(2*M)),:)*p).^2);
    disp([num2str(i),' ',num2str(es(i)),' ',num2str(ek(i)),' ',num2str(mdeltap)]);
    if mdeltap<epsilon break;end;
end;
disp([num2str(cputime-to),' cpu seconds']);h=[flipud(p);p];plot_QMF(h,M);

```

```

function plot_QMF(h,M);
% Plot the analysis filter bank, the magnitude and aliasing frequency responses
% h: prototype filter, M: number of band
% Author: Michel Rossi, University of Ottawa, 1996
%
clg;Lfg=1024;N=floor(Lfg/M);fg=0:2*pi/M/N:2*pi;fg=fg(1:length(fg)-1);
Lfg=length(fg);%frequency grid
h=h/sqrt(sum(h.^2)*2);L=length(h);%prototype normalization
% Cosine modulation
hi=2*ones(M,1)*h'.*cos(pi/2*(1/M*(2*(0:M-1))+1)*(...
(1:L)-(L+1)/2)+(-1).^(0:M-1)*ones(1,L)/2));
% Plot analysis filter bank
subplot(211);
for i=1:M
    H(i,:)=freqz(hi(i,:),1,fg); %analysis filters
    F(i,:)=conj(H(i,:)).*exp(-sqrt(-1)*(L-1)*fg); %synthesis filters
    plot(fg(1:Lfg/2)/pi,20*log10(abs(H(i,1:Lfg/2))));hold on;end;hold off;
% plot the filter bank magnitude transfer function
subplot(212);
plot((0:length(H(1,:))-1)/length(H(1,:)),20*log10(sum((abs(H)).^2)/M));
title('Magnitude transfer function');
xlabel('Normalized frequency');ylabel('dB');
% Plot the aliasing frequency responses
A=zeros(M,length(fg));
for l=0:M-1 for i=1:M
    Hl=[H(i,(Lfg-N*l+1):Lfg),H(i,1:(Lfg-N*l+1))];
    A(l+1,:)=A(l+1,:)+Hl.*F(i,:);
end;end;figure;plot(fg(1:Lfg/2)/pi,20*log10(abs(A(1:M,1:Lfg/2)/M)));
title('Aliasing components');ylabel('dB');
xlabel('Normalized frequency (Nyquist == 1)')

```

With the unconstrained design formulation (4.14), for large values of  $\gamma$ , the peak values of the magnitude transfer function are very small and take values of the order of  $10^{-7}dB$  as in example 11 or even less, down to  $10^{-9}dB$ . Experimentally we have found that when  $\gamma$  is further increased, the algorithm is unable to converge, probably because of the finite precision of the calculations. To address the case  $\gamma$  where tends towards infinity, i.e. where the magnitude distortion has to be entirely canceled, we have developed a Constrained ILS algorithm presented in the next section.

### 4.3 ILS design of Near Perfect Reconstruction Pseudo QMF banks

In this section we present an ILS algorithm for the design of Near Perfect Reconstruction Pseudo QMF banks. Design examples and a MATLAB implementing the ILS design algorithm are included.

#### 4.3.1 NPR Pseudo QMF bank ILS design algorithm

The distinction between Pseudo QMF banks and NPR Pseudo QMF banks is that in the latest the magnitude distortion is entirely canceled. NPR Pseudo QMF bank are designed using a constrained minimization approach [71]–[72] as follows

$$\min(e_s) \text{ subject to } e_m = 0 \quad (4.40)$$

As for general Pseudo QMF banks, there is some aliasing distortion in the output signal which can be kept small when the stopband attenuation of the prototype filter is sufficiently large.

As in section 4.2, at each iteration  $i$  we approximate  $e_m$  with the quadratic quantity  $\hat{e}_m(i)$ . The nonlinear constrained minimization problem (4.40) is simplified into an ILS approximation with linear constraints defined at each iteration  $i$  as follows

$$\min(p_i C^t C p_i) \text{ subject to } G_i p_i = d \quad (4.41)$$

This linear constrained least squares minimization problem can be solved using the Lagrangian multiplier method. Let  $L(p_i, \mu_i)$  be the Lagrangian corresponding to the optimization problem (4.41) defined as

$$L(p_i, \mu_i) = p_i^t C^t C p_i + \mu_i^t (G_i p_i - d) \quad (4.42)$$

where  $\mu_i$  is the vector containing the Lagrangian multipliers,  $[\mu_i(0), \dots, \mu_i(E[\frac{N}{2M}])]^t$ , associated with the linear constraints  $G_i p_i \leftarrow 0$ . The solution is obtained by setting to zero the derivative of  $L(p_i, \mu_i)$  with respect to the coefficients of  $p_i$  and  $\mu_i$ . This yields the following system of linear equations

$$\begin{bmatrix} C^t C & G_i^t \\ G_i & 0 \end{bmatrix} \begin{bmatrix} p_i \\ \mu_i \end{bmatrix} = \begin{bmatrix} 0 \\ d \end{bmatrix} \quad (4.43)$$

It is then easy to verify that

$$p_i = (C^t C)^{-1} G_i^t (G_i (C^t C)^{-1} G_i^t)^{-1} d \quad (4.44)$$

This algorithm requires only the inversion of a size  $E[\frac{N}{2M}] + 1$  matrix at each iteration. We have observed that the convergence speed of the algorithm depends directly on the number of constraints, i.e.  $E[\frac{N}{2M}] + 1$ . The fewer constraints, the faster the convergence is. To speed up the convergence the constraint in (4.41) for  $k = 0$  can be performed by the normalization of the coefficients as in (4.28). In this case the first coefficient,  $h(\frac{N+1}{2})$ , can be set to 1 to avoid the trivial zero solution. For the cases where the number of constraints is larger than 5, we recommend the use of the QR least squares algorithm to solve (4.43) rather than the direct formula (4.44). In fact thanks to the robustness of the QR algorithm, ill conditioned situations that may occur in (4.44) are avoided. The convergence of this algorithm has been experimentally found to be fast and independent of the starting point. The order of the peak values of the magnitude transfer function obtained are between  $10^{-12} dB$  and  $10^{-14} dB$ , which is comparable to that obtained in [71] and better than what can be obtained with the algorithm of section 4.2 for large values of  $\gamma$ . The algorithm can be summarized into the following steps

- *Step 1*, choose  $M$ ,  $N$  and  $\omega_s$ ,
- *Step 2*,  $i \leftarrow 0$ , initialize  $p_0(n)$  with random numbers.
- *Step 3*,  $i \leftarrow i + 1$ , build the matrix  $G_i$  with  $p_{i-1}$  using (4.21),
- *Step 4*, find  $p_i$  by solving (4.43) or (4.44);
- *Step 5*, go to step 3 unless  $\max |p_i - p_{i-1}| \leq \epsilon$ , where  $\epsilon$  is a prescribed small number.

To shape the stopband of the prototype filter, the IRLS methods of section 4.2 can be used. As shown in the design examples presented in the next section, prototype filters of NPR Pseudo QMF banks with minimax or gain constrained least squares stopbands can be designed.

### 4.3.2 NPR Pseudo QMF bank design examples

The following two examples illustrate the efficiency and fast convergence of the proposed algorithm.

#### Example 13: 16-band NPR Pseudo QMF bank design

Let the number of bands be  $M = 16$ , the length of the filter be  $N + 1 = 256$ , the stopband frequency edge  $\omega_s = \frac{\pi}{M}$ . With  $\epsilon = 1E^{-15}$  the algorithm converged in 33 iterations requiring 21 cpu seconds. The normalized analysis filter bank,  $|H_k(e^{j\omega})|/\sqrt{M}$ , is plotted in Fig. 4.7. The overall magnitude transfer function is shown in Fig. 4.8. We can see that the peak values of  $|A_0(e^{j\omega})|$  are of the order of  $2E^{-13}dB$ . The maximum level of aliasing is  $-80dB$ . The normalized prototype filter,  $|H(e^{j\omega})|/\sqrt{M}$ , has an attenuation of  $66dB$  at  $\omega_s$ .

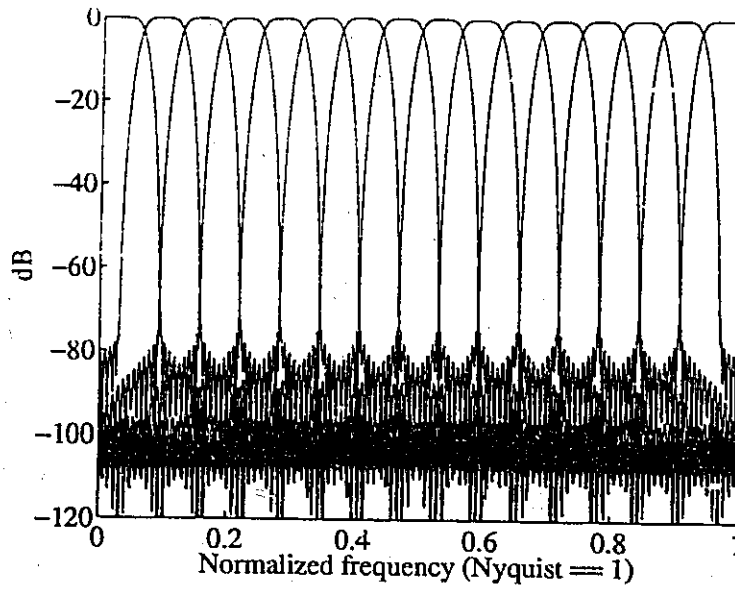


Figure 4.7: Example 13, 16-band NPR Pseudo QMF analysis filter bank

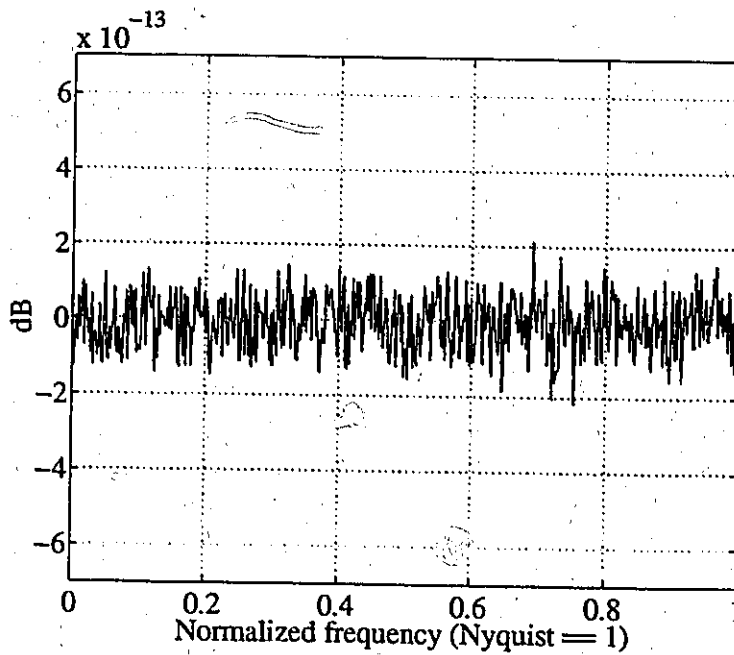


Figure 4.8: Example 13, filter bank magnitude transfer function,  $|A_0(e^{j\omega})|$

**Example 14: 16-band NPR Pseudo QMF bank with a minimax prototype filter**

With the same specification as in example 13, we have designed a prototype filter with a minimax stopband error. The normalized prototype filter obtained,  $|H(e^{j\omega})|/\sqrt{M}$ , has a minimum attenuation of  $79dB$  in the stopband  $[\omega_s, \pi]$ . Its frequency response is plotted in Fig. 4.9. The maximum value of  $|A_0(e^{j\omega})|$  and the maximum level of aliasing are the same as in example 13.

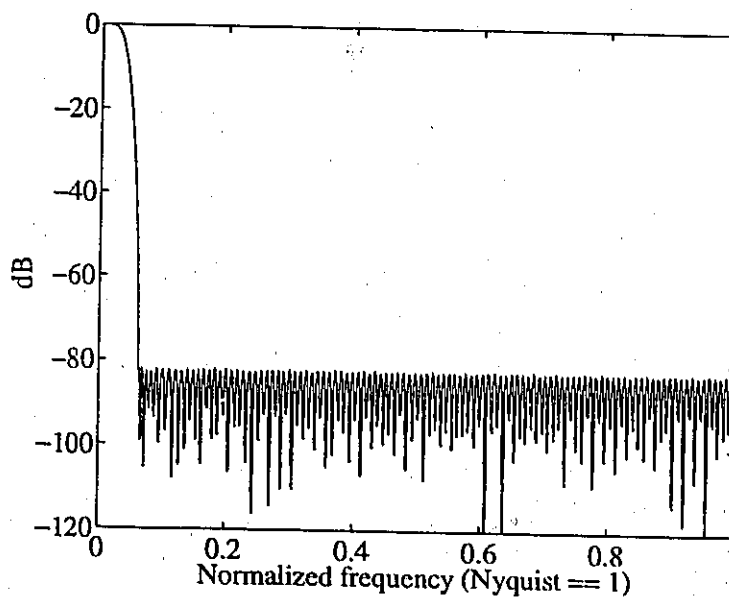


Figure 4.9: Example 14, equiripple prototype filter of a 16-band NPR Pseudo QMF bank

**Example 15: 16-band NPR Pseudo QMF bank with a gain constrained least squares prototype filter**

With the same specification as in example 13, we have designed a prototype filter with the least squares approximation and with the constraint  $|H(e^{j\omega})|/\sqrt{M} \leq -75dB$  in the stopband  $[\omega_s, \pi]$ . The normalized prototype filter obtained,  $|H(e^{j\omega})|/\sqrt{M}$ , is shown in Fig. 4.10. The maximum value of  $|A_0(e^{j\omega})|$  and the maximum level of aliasing are the same as in example 13.

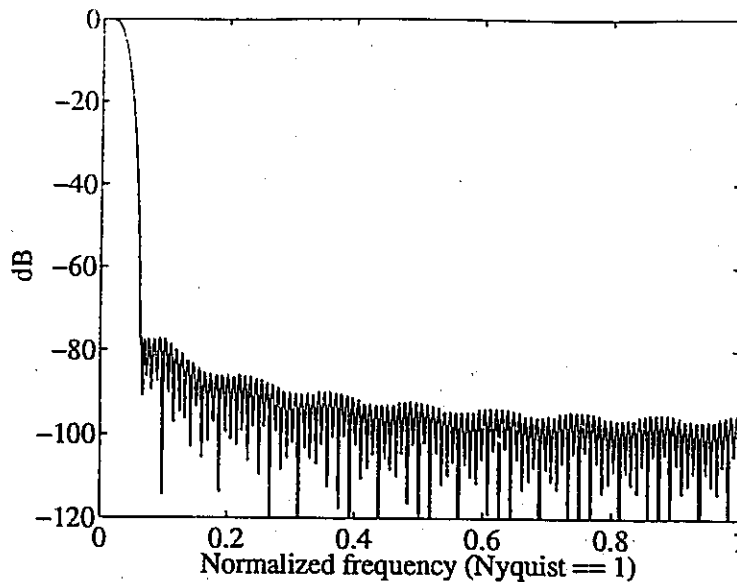


Figure 4.10: Example 15, gain constrained least squares prototype filter of a 16-band NPR Pseudo QMF bank

### 4.3.3 MATLAB program for the ILS design of NPR Pseudo QMF banks

The MATLAB function NPRQMF.m presented here implements the unweighted design algorithm of NPR Pseudo QMF Banks. The function plot\_QMF.m presented in section 4.2.4 is used by NPRQMF.m to plot the designed filter bank.

```
function h=NPRQMF(M,Lh,f)
% NPR Pseudo QMF ILS design
% h: prototype filter, Lh length of h, M: number of bands,
% f stopband frequency in [1/2M 1/M]
% example: h=NPRQMF(16,256,1/16);
% Author: Michel Rossi, University of Ottawa, 1996
%
epsilon=1E-15;to=cputime;R=Lh/2;p=rand(R,1);
d=-sin((2*[1:R]-1)*pi*f)/pi/(1-f)/4./([1:R]-.5)+.5;
for k1=1:R for k2=k1+1:R %Compute So
    So(k1,k2)=-[sin((k1+k2-1)*f*pi)/(k1+k2-1)+sin((k2-k1)*f*pi)/(k2-k1)]/2/pi/(1-f);
end;end;So=[So;zeros(1,R)];So=4*(So'+So+diag(d));
v1=So(2:R,1);S=So(2:R,2:R);disp('i es em max(delta(p))');
for i=1:40 pold=p;Go=[];
% build Go
for k=1+M:M:R
    Go=[Go;[zeros(1,k-1),p(k-1:-1:max(1,1-(R-2*(k-1))))',p(1:R-2*(k-1))']];
```

```

end;v2=Go(:,1);K=length(v2);G=Go(:,2:R);
% Find the Constrained L2 solution
solp=-[[S,G'];[G,zeros(K,K)]]\[v1;v2];p=[1:solp(1:R-1)];p=p/sqrt(4*sum(p.^2));
es(i)=p'*So*p;em(i)=32*sum((Go*p).^2);mdeltap=max(abs(pold-p));
disp([num2str(i),' ',num2str(es(i)),' ',num2str(em(i)),' ',num2str(mdeltap)]);
if mdeltap<epsilon break;end;
end;
h=[flipud(p(1:R));p];disp([num2str(cputime-to),' cpu seconds']);plot_QMF(h,M);

```

In this section and the previous one, we have seen that Pseudo QMF banks and NPR Pseudo QMF banks can be designed very efficiently using the ILS approach. In such filter banks only the magnitude distortion minimization is considered. The aliasing distortion can be kept small when the prototype filter stopband attenuation is sufficiently large. The ILS algorithm, presented in the next section, minimizes the magnitude and aliasing distortions and can design PR filter banks.

## 4.4 ILS design of Perfect Reconstruction filter banks

In this section we present the ILS algorithm for the design of M-band Perfect Reconstruction filter banks. Design examples and a MATLAB program are included.

### 4.4.1 PR filter banks ILS design algorithm

Let us assume that the length of the prototype filter  $N+1$  is  $2mM$ , for some integer  $m$ , and that  $M$  is even. As proposed in [73], the design of filter banks can be formulated as an unconstrained least squares optimization problem defined as

$$\min(e_s + \gamma e_d) \quad (4.45)$$

where  $e_d$  is the approximation error in satisfying the condition (4.11), i.e.

$$e_d = \sum_{k=0}^{m-1} \sum_{n=0}^{M/2-1} \left( \sum_{r=0}^{2m-2k-1} h(n+rM)h(n+rM+2kM) - \frac{\delta(k)}{2M} \right)^2 \quad (4.46)$$

The minimization of  $e_d$  guarantees the minimization of the magnitude distortion and the aliasing between non adjacent bands. In this case it is not necessary to use a prototype filter with a large stopband attenuation to guarantee the minimization of the aliasing distortion as with Pseudo QMF banks. Thus relatively low order filter banks can be designed provided that  $N + 1 = 2mM$ . The level of distortion depends on the constant  $\gamma$ . The larger  $\gamma$  is, the smaller the residual distortion is. When  $\gamma$  is sufficiently large, the filter banks obtained satisfy the perfect reconstruction property.

As in section 4.2, the proposed ILS algorithm relies on the approximation of the nonquadratic term,  $e_d$ , by a quadratic quantity,  $\hat{e}_d(i)$  defined at the iteration  $i$  by

$$\hat{e}_d(i) = \frac{1}{2} \sum_{k=0}^{m-1} \sum_{n=0}^{M-1} \left( \sum_{r=0}^{2m-2k-1} h_i(n + rM) h_{i-1}(n + rM + 2kM) - \frac{d(k)}{2M} \right)^2 \quad (4.47)$$

Note that to achieve a good approximation of (4.46), the summation goes from  $n = 0$  to  $n = M - 1$  and a factor  $\frac{1}{2}$  is used. A matrix form of  $\hat{e}_d(i)$  can be obtained as

$$\hat{e}_d(i) = \frac{1}{2} (Q_i p_i - v)^t (Q_i p_i - v) \quad (4.48)$$

where  $v$  is the vector  $[\frac{1}{2M}, \dots, \frac{1}{2M}, 0, \dots, 0]^t$  in which the first  $M$  coefficients are equal to  $\frac{1}{2M}$  and  $Q_i$  is a size  $mM$  square matrix containing the coefficients  $h_{i-1}(r)$  as follows

$$\begin{aligned} Q_i(km + n + 1, r + 1) &= h_{i-1}(n + mM + r + 2kM) \delta(r \bmod M) \\ &+ h_{i-1}(n + mM - 1 - r + 2kM) \delta((r + 1) \bmod M) \end{aligned} \quad (4.49)$$

for  $0 \leq k \leq m-1$ ,  $0 \leq n \leq M-1$ ,  $0 \leq r \leq mM-1$  where  $r \bmod M$  is the remainder of the integer division  $r/M$  and  $h_i(r) = 0$  for  $r > N$  and  $r < 0$ .

One can note the similarity between the design of Pseudo QMF banks and the problem formulation (4.45) and consider applying the ILS algorithm of section 4.2 to design PR filter banks by simply replacing the matrix  $G_i$  by  $Q_i/\sqrt{2}$  and  $d$  by  $v/\sqrt{2}$ . This means that at each iteration  $i$ ,  $p_i$  is found by solving the following overdetermined system of linear equation in the least squares sense

$$\begin{bmatrix} Q_i \\ \sqrt{\frac{2}{L\gamma}} C \end{bmatrix} p_i = \begin{bmatrix} v \\ 0 \end{bmatrix} \quad (4.50)$$

However, we have found from the experimentation that the resulting algorithm oscillates and does not converge. To guarantee the convergence of algorithm, we average the coefficients obtained after each least squares approximation, as follows

$$p_i \leftarrow \frac{p_i + p_{i-1}}{2} \quad (4.51)$$

This simple modification allows the algorithm to converge, however we have observed that the designed prototype filter is dependent on the initial filter as opposed to with the algorithms of section 4.2 and 4.3. When the initial filter is not a lowpass filter, the algorithm fails to design a “good” lowpass prototype filter. Experimentally we have found that the algorithm designs filter banks with small stopband-energy when  $p_0$  is initialized with the coefficients of the filter that minimizes the stopband energy  $e_s$ . This filter can be obtained by setting  $\gamma$  to zero at the first iteration. Moreover the stopband attenuation of the design filter can be improved when  $\gamma$  is gradually increased to its final value denoted by  $\gamma_\infty$ . In the implementation of the algorithm, the set  $\{\gamma_i\}$  is defined as:  $\gamma_0 = 0$ ,  $\gamma_1 = 1$  and  $\gamma_{i+1} = \min(K * \gamma_i, \gamma_\infty)$  for  $i \geq 1$ . In addition we have noticed that the stopband attenuation of the prototype filters obtained depends on the variation speed of  $\gamma$ , i.e. on the number  $K$ . The slower the variation of  $\gamma$  is, the better the stopband attenuation of the filter obtained is. The algorithm can be summarized into the following steps

- *Step 1*, choose  $M$ ,  $N$ ,  $\omega_s$ ,  $\gamma_\infty$  and  $K$ ,
- *Step 2*,  $i \leftarrow 0$ , initialize  $p_0(n)$  by minimizing  $e_s$ , set  $\gamma_1 = 1$ .
- *Step 3*,  $i \leftarrow i + 1$ ,
- *Step 4*, build the matrix  $Q_i$  with  $h_{i-1}(n)$  as in (4.49),
- *Step 5*, solve least squares problem using (4.50),
- *Step 6*,  $\gamma_{i+1} = \min(K * \gamma_i, \gamma_\infty)$ ,
- *Step 7*,  $p_i \leftarrow \frac{p_i + p_{i-1}}{2}$ ,

- Step 8. go to step 3 unless  $\max |p_i - p_{i-1}| \leq \epsilon$ , where  $\epsilon$  is a prescribed small number.

#### 4.4.2 PR filter bank design examples

The following two design examples illustrate the fast convergence of the ILS algorithm, and the perfect reconstruction of the filter bank obtained with  $\gamma_\infty$  sufficiently large.

##### Example 16: 8-band filter bank

Let the number of bands be  $M = 8$ , the length of the prototype filter be  $N + 1 = 80$ , the stopband frequency edge be  $\omega_s = 1.5\pi/M$  and  $\gamma_\infty = 10^6$ . With  $K \hat{=} 5$  and  $\epsilon = 5E^{-5}$  the algorithm converged in 12 iterations requiring 3.9 cpu seconds. The normalized analysis filters,  $H_k(e^{j\omega})/\sqrt{M}$ , are plotted in Fig 4.11. As shown in Fig. 4.12 the peak values of the magnitude transfer function,  $|A_0(e^{j\omega})|$ , are of the order of  $2E^{-5}dB$ . The aliasing transfer functions,  $|A_l(e^{j\omega})|$  for  $l = 1, \dots, 7$  are plotted in Fig. 4.13, their maximum level is  $-116dB$ .

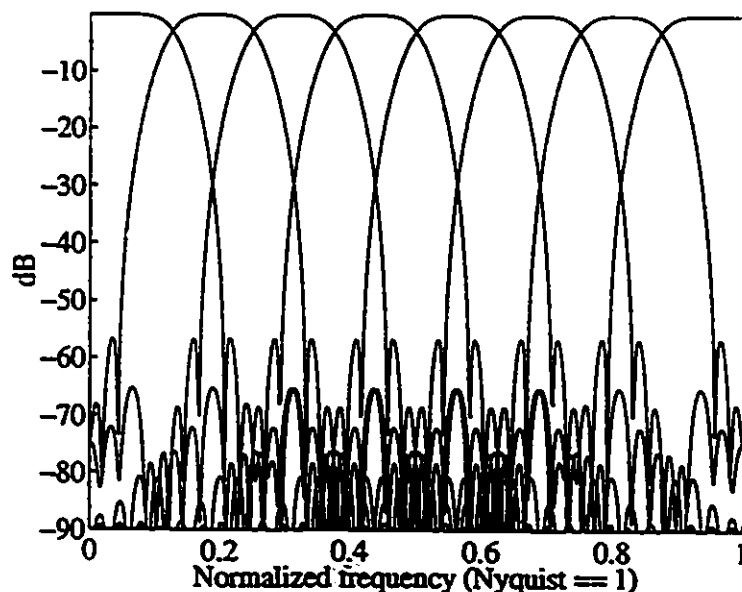


Figure 4.11: Example 16, 8-band analysis filter bank

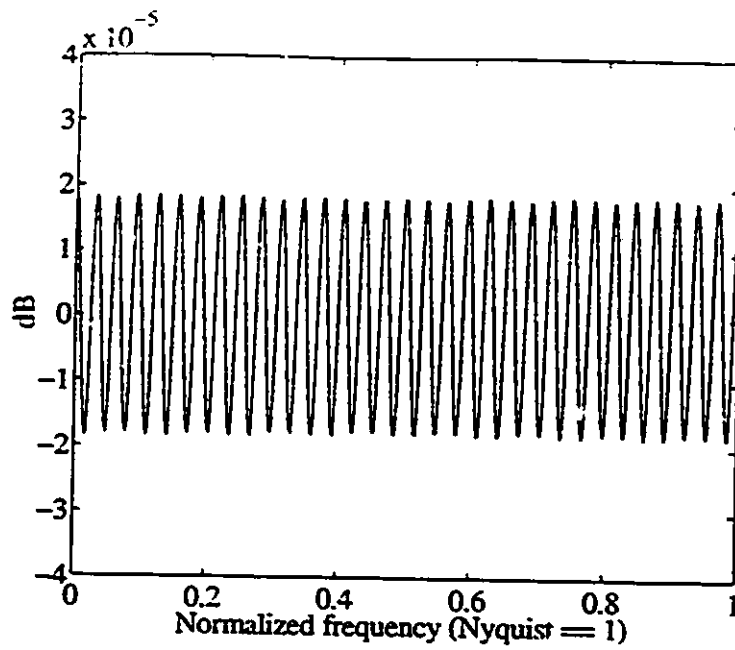


Figure 4.12: Example 16, filter bank magnitude transfer function,  $|A_0(e^{j\omega})|$

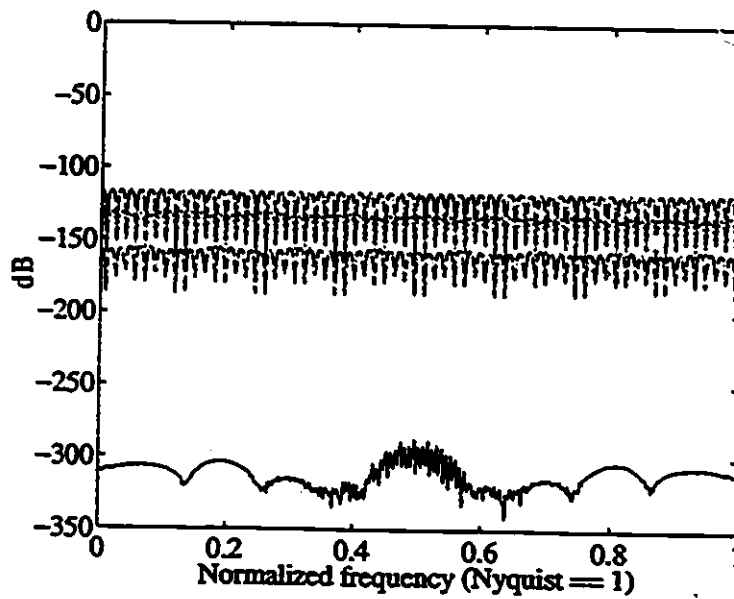


Figure 4.13: Example 16, aliasing transfer functions,  $|A_r(e^{j\omega})|$  for  $r = 1, \dots, 7$

### Example 17: 8-band PR filter bank

In this example we use the same specifications as in the example 16 except for  $\gamma_\infty = 10^{22}$ . With  $K = 3.5$ , the algorithm converged in 41 iterations requiring 26 cpu seconds. The normalized analysis filters obtained,  $H_k(e^{j\omega})/\sqrt{M}$ , are plotted in Fig 4.14. As shown in Fig. 15 the peak values of magnitude transfer function are of the order of  $5E^{-14}dB$ . The aliasing transfer function are plotted in Fig. 16. The maximum level of the aliasing is  $-287dB$ . Hence we can see that when  $\gamma_\infty$  is sufficiently large, the resulting filter bank can be considered as a PR filter bank.

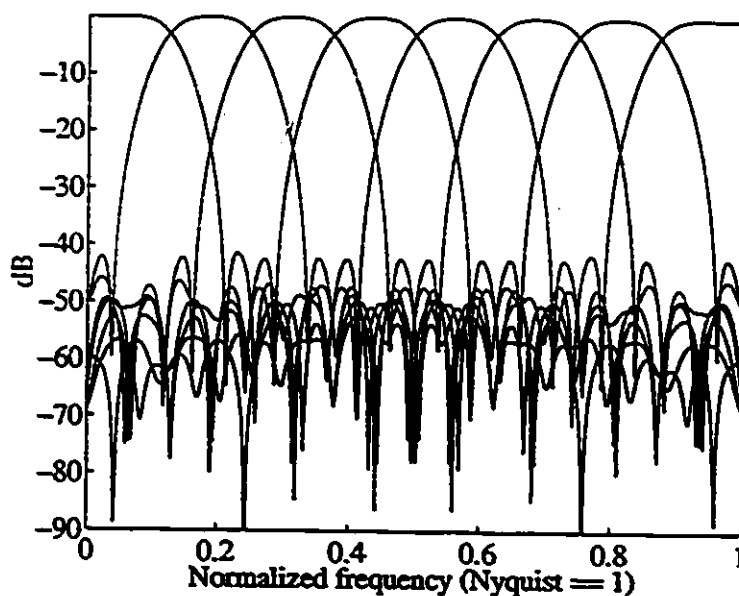


Figure 4.14: Example 17, 8-band PR analysis filter bank

#### 4.4.3 MATLAB program for the ILS design of PR Filter banks

The MATLAB function PRQMF.m implements the ILS algorithm for the design of PR Filter Banks. The function plot\_QMF.m presented in section 4.2.4 is used by PRQMF.m to plot the filter banks obtained.

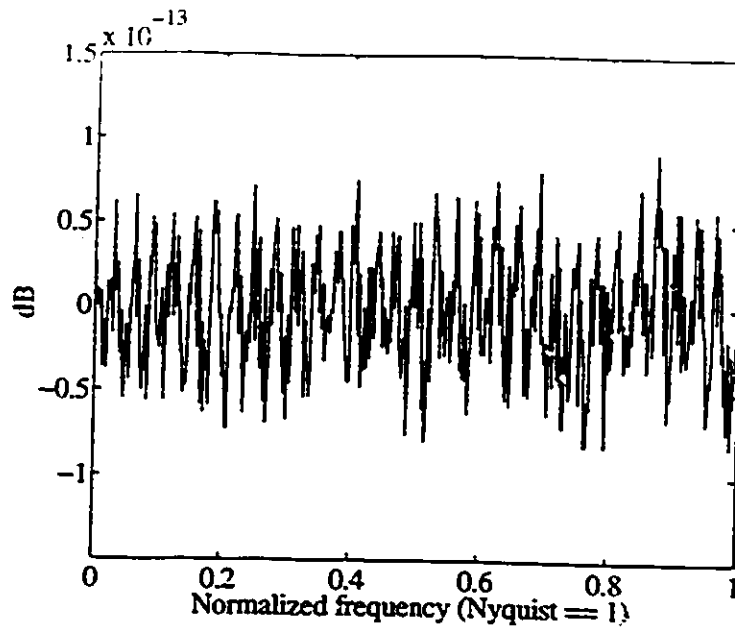


Figure 4.15: Example 17, filter bank magnitude transfer function,  $|A_0(e^{j\omega})|$

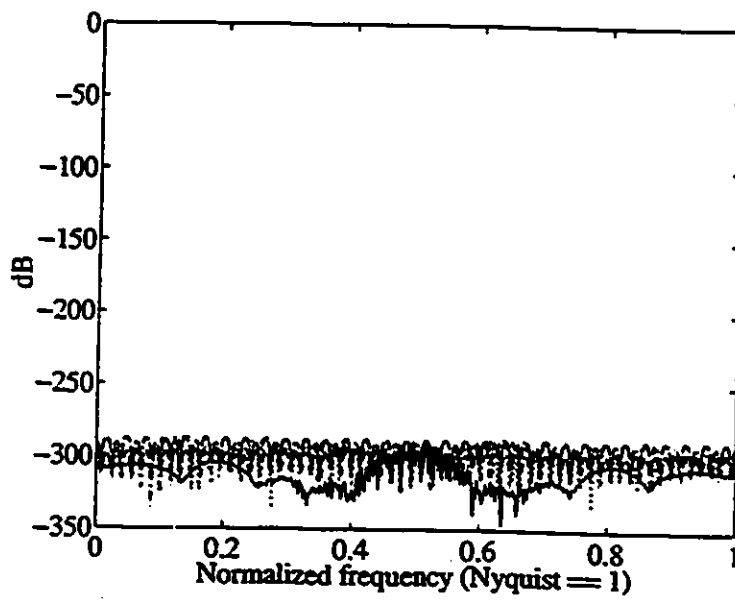


Figure 4.16: Example 17, aliasing transfer functions,  $|A_r(e^{j\omega})|$  for  $r = 1, \dots, 7$

```

function h=PRQMF(M,Lh,fs,gammaf,K):
% PR Cosine Modulated Filter Bank ILS design
% h: prototype filter, M: nb of bands (even),
% Lh: filter length (2Mm);fs stop band edge >1/M.
% gammaf: final gamma, K: variation cste of gamma
% example: h=PRQMF(8,80,1.5/8.1E6,5);
% example: h=PRQMF(8,80,1.5/8.1E22,3.5);
% Author: Michel Rossi, University of Ottawa, 1996
%
epsilon=5E-6;gamma=1;to=cputime;L=4*Lh;f=[(fs*(1-fs)/(L-1):1)'];
Ad=zeros(L,1);R=Lh/2;C=2*cos(pi*(f*([1:R]-0.5)));S=C'*C/L;
disp('i es em gamma max(delta(p))');p=[1;-S(2:R,2:R)\S(2:R,1)];
h=[flipud(p);p]; %starting point
for i=1:100
    gamma=min(gamma*K,gammaf);Qi=[];pold=p;
    %Build the matrix Qi with h
    for n=0:M-1 tmp=h'.*(rem((0:Lh-1)-n,M)==0);
        for k=0:2*M:Lh-1
            if k==0 Qi=[[zeros(1,k),tmp(1:length(tmp)-k)];Qi];
            else Qi=[Qi;[zeros(1,k),tmp(1:length(tmp)-k)]];
        end;end;end; Lg=length(Qi(:,1));Qi=(Qi(:,R+1:Lh)+fliplr(Qi(:,1:R)));
    %Least squares solution (prefer the second formula, it is more robust)
    %newp=(2*S/gamma+Qi'*Qi)\sum([zeros(R);Qi(1:M,:)])/M/2;
    newp=[C/sqrt(gamma/2);Qi]\[Ad;ones(M,1)/2/M;zeros(Lg-M,1)];
    p=(p+newp)/2;h=[flipud(p);p];es(i)=p'*S*p;
    em(i)=sum(abs(Qi*p-[ones(M,1);zeros(Lg-M,1)]/2/M).^2);
    disp([num2str(i), ' ',num2str(es(i)), ' ',num2str(em(i)),...
        ' ',num2str(gamma), ' ',num2str(max(abs(p-pold)))]);
    if max(abs(p-pold))<epsilon&gamma==gammaf break;end;
end;
disp([num2str(cputime-to), ' cpu seconds']);
plot_QMF(h,M);

```

## 4.5 Conclusions

In this chapter we have presented three algorithms for the design of uniform cosine modulated filter banks based on the ILS approach. The main advantages of this approach compared to traditional nonlinear optimization methods are its computational efficiency, simplicity and flexibility. For the design of Pseudo QMF banks and NPR Pseudo QMF banks, the convergences of the proposed algorithms have been observed to be independent of the starting point in simulations. Moreover iteratively calculated weighting functions can be used to shape the stopband of the prototype filter and/or the magnitude reconstruction error and perform the minimax or the gain constrained

least squares approximation. We have also shown that the ILS approach allows the design of PR filter banks in a very efficient and simple manner.

# Chapter 5

## Conclusions

### 5.1 Thesis summary

In this thesis we have considered the use of the Iterative Least Squares approach to improve and simplify the design of M-band cosine modulated filter banks and IIR digital filters.

In chapter 2, we have reviewed and compared the Iterative Reweighted Least Squares methods used to design Chebyshev and  $L_p$  linear phase FIR filters. We have explained the slow convergence of Lawson's algorithms compared to Lim's and Kahng's methods and shown its relations with the Remez algorithm.

In chapter 3, we have considered the Chebyshev approximation of log IIR filters. To speed up Kobayashi's IRLS method and simplify the traditional rational Remez algorithm, we have proposed to merge these two methods into a Remez-type IRLS algorithm. This novel approach converges significantly faster than Kobayashi's algorithm and is simpler and more robust than the traditional Remez algorithm.

In chapter 4, we have considered the design of M-band filter banks. To obtain alternatives to traditional design methods, based on complicated and computationally intensive nonlinear optimizations, we have developed three new ILS algorithms for the design of Pseudo QMF banks, NPR Pseudo QMF banks and PR Filter banks. These algorithms are computationally efficient, simple to implement and flexible. For

the design of Pseudo QMF banks and NPR Pseudo QMF banks the convergence have been observed to be independent of the starting point and a weighting function can be used to shape the stopband attenuation and the magnitude reconstruction error and perform the Chebyshev approximation. Short MATLAB program implementing the proposed methods have been presented.

## 5.2 Suggestions for further research

We believe that the Remez-type ILS algorithm presented in chapter 2 can be extended to the design of IIR filters in the magnitude square domain. This extension needs to be evaluated and compared to the classical rational remez algorithm.

We have seen that Lawson's algorithm is an interesting way to perform the interpolation step of the Remez algorithm because it does not require the rejection of the extra ripples. In the design of multiband filters [33], the more transition bands, the more extra ripples and the less reliable the Parks McClellan algorithm is. Hence Lawson's algorithm is probably a solution to the problematic rejection of the extra ripples. This statement need to be verified and evaluated through comparative tests.

The proposed ILS algorithms for the design of filter banks are simple and flexible. Linear constraints can be imposed using the Lagrangian multiplier as for the design of NPR Pseudo QMF banks. This allows the design of filter banks with vanishing moments suitable for image processing application. In addition, the ILS algorithms can also be coupled with a search algorithm to perform the optimal quantization of the coefficients [79] necessary for ASIC implementation. Prospective research can be done in these directions.

# Appendix A

## Filter Bank Transfer Function

From the expression (4.8) we have

$$A_0(z) = \frac{z^{-N} 2^{M-1}}{M} \sum_{s=0}^{2M-1} G(zW_{2M}^s) \quad (\text{A.1})$$

where

$$\begin{aligned} G(z) &= H(zW_{2M}^{.5})H(z^{-1}W_{2M}^{-.5}) \\ &= \sum_{k=-N}^N g(k)z^{-k} \end{aligned} \quad (\text{A.2})$$

and

$$g(k) = \sum_{r=0}^{N-|k|} h(r)h(|k|+r)W_{2M}^{\frac{kr}{2}} \quad (\text{A.3})$$

Injecting (A.2) and (A.3) into (A.1) we obtain

$$\begin{aligned} A_0(z) &= \frac{z^{-N} 2^{M-1}}{M} \sum_{s=0}^{2M-1} \sum_{k=-N}^N g(k)z^{-k}W_{2M}^{-ks} \\ &= \frac{z^{-N}}{M} \sum_{k=-N}^N g(k)z^{-k} \sum_{s=0}^{2M-1} W_{2M}^{-ks} \\ &= \frac{z^{-N}}{M} \sum_{k=-E[\frac{N}{2M}]}^{E[\frac{N}{2M}]} g(2Mk)z^{-2Mk} 2M \\ &= 2z^{-N} \sum_{k=-E[\frac{N}{2M}]}^{E[\frac{N}{2M}]} \sum_{r=0}^{N-2M|k|} h(r)h(2M|k|+r)(-1)^k z^{-2Mk} \end{aligned} \quad (\text{A.4})$$

# Bibliography

- [1] R. Liu, *Digital Filters and the Fast Fourier Transform*, John Wiley and Sons, 1975.
- [2] D. Childers, A. Durling, *Digital Filtering and Signal Processing*, West Publishing Company, 1975.
- [3] R.E. Bogner, A. G. Constantinides, *Introduction to Digital Filtering*, John Wiley and Sons, 1975.
- [4] V. Cappelini, A. G. Constantinides, P. Emiliani, *Digital Filters and their Applications*, Academic Press, 1978.
- [5] Lim, Oppenheim, *Advanced Topics in Signal Processing*, Englewood Cliffs, NJ: Pentice Hall, 1988.
- [6] A. V. Oppenheim, R.W. Schafer, *Digital Signal Processing*, Englewood Cliffs, NJ: Pentice Hall, 1989.
- [7] A. Antonious, *Digital Filters, analysis, design and applications*, McGraw-Hill, 1993.
- [8] S. K. Mitra, J. F. Kaiser *Digital Signal Processing*, John Wiley and Sons, 1993.
- [9] C. Moeler, J. Little and S. Bangert, *Matlab User's guide*, South Natick, MA: The Math Works Inc., 1989
- [10] Signal Processing Work-systems.

- [11] A. G. Decszky "Synthesis of Recursive Digital Filters Using the Minimum  $P$  Error Criterion." IEEE trans. Audio, Electroacoustics, VOL 20, pp. 257-263, Oct. 1972.
- [12] Digital Signal Processing Committee. "Programs for Digital Signal Processing." IEEE Press., New-York 1979.
- [13] V. R. Algazi, M. Suk, C. S. Rim. "Design of almost minimax FIR filters in one and two dimensions by IRLS techniques." IEEE trans. Circuits and Syst., VOL CAS-33, pp. 590-596, Jun. 1986.
- [14] C. H. Hsieh, Y. L. Han, C. M. Kuo, Y. D. Jou, "A new WLS method for the design of two dimensional FIR digital filters," in Proc. ICASSP'94.
- [15] T. Kobayashi, S. Imai, "Design of IIR digital filters with arbitrary log magnitude function by IRLS techniques." IEEE Trans. Signal Processing, vol 38, pp. 247-252, Feb 1990.
- [16] Vijay K. Jain, "Quadrature Mirror Filter Design in the Time Domain," IEEE trans. Signal Processing, VOL. 32, NO. 2, pp. 353-361, Apr. 1984.
- [17] C.-K. Chen, J.-H. Lee, "Design of Quadrature Mirror Filters with Linear Phase in the Frequency domain," IEEE trans. Circuits and Systems-II, VOL. 39, NO 9, pp. 593-605 Sept 1992.
- [18] K. Nayebi, T. P. Barnwell, Mark J. T. Smith "General time domain analysis and design framework for exact reconstruction FIR analysis synthesis filter banks" in Proc. Int. Symp. Circuits Syst., pp. 2022-2025, May 1990.
- [19] K. Nayebi, T. P. Barnwell, M. J. T. Smith "Time-Domain Filter Banks Analysis: A new Design Theory," IEEE trans. Signal Processing, VOL. 42, NO. 1, pp. 24-31, Jan. 1994.

- [20] Y.C. Lim, J.-H. Lee, C. K. Chen, R. H. Yang. "A Weighted Least Squares Algorithm for Quasi-Equiripple FIR and IIR Digital Filter Design," IEEE trans. Signal Processing, VOL. 40, NO. 3, pp. 551-558, March 1992.
- [21] S. Sunder and V. Ramachandran, "Design of Equiripple Nonrecursive Digital Differentiators and Hilbert Transformers using a Weighted Least-Squares Technique," IEEE Trans. Signal Processing, vol 42, pp. 2504-2509, Sept. 1994.
- [22] C. Sidney Burrus, J. A. Barreto, I. W. Selesnick, "Iterative Reweighted Least-Squares Design of FIR filters," IEEE Trans. Signal Processing, vol 42, pp. 2926-2936, Nov 1994.
- [23] M. Lang, T. I. Laasko, "Simple and Robust Method for the Design of Allpass Filters Using Least-Squares Phase Error Criterion," IEEE trans. CAS-II, VOL 41, NO. 1, Jan. 1994.
- [24] T. Q. Nguyen, T. I. Laasko, R. D. Koipillai, "Eigenfilter Approach for the Design of Allpass Filters Approximating a Given Phase Response," IEEE trans. Signal Processing, VOL 42, NO. 9, Sept. 1994.
- [25] C.-Y. Tseng, "A Generalized Remez Multiple Exchange Algorithm for Complex FIR Filter Design," in Proc. ICASSP'94.
- [26] S. C. Pei, J. J. Shyu, "Design of Arbitrary Complex Coefficient FIR Digital Filters by Complex Weighted Least Squares Approximation," IEEE trans. Circuits and Syst. II, VOL 41, NO 12, pp. 817-820, Dec. 1994.
- [27] C.-Y. Tseng, "An efficient Implementation of Lawson's algorithm with application to Complex Chebyshev FIR filter Design," IEEE trans. Circuits and Syst. I, VOL 42, pp. 245-260, Apr. 1995.
- [28] S. Sunder, Kidambi, R. P. Ramachandran, "Design of Nonrecursive Filters Satisfying Arbitrary Magnitude and Phase Specifications Using a Least Square Approach," IEEE trans. Circuits and Syst. II, VOL 42, pp. 711-716, Nov. 1995.

- [29] B. A. Weisburn, T. W. Parks and R. G. Shenoy, "Error criteria for filter design" in Proc. ICASSP'90.
- [30] J. W. Adams, "FIR filters with least squares stopbands subject to peak gain constraints," in IEEE Trans. on Circuits and Syst., VOL 39, NO 4pp. 376-388, April 1991.
- [31] I. W. Selesnick, M. Lang, C. S. Burrus, "Constrained Least Square Design of FIR Filters Without Specified Transition Bands," in Proc. ICASSP '95.
- [32] J. H. McClellan, T. W. Parks "A computer program for designing optimum FIR linear phase digital filters," IEEE trans. Audio Electroacoust., VOL 21, pp. 506-526, Dec 1973.
- [33] D. J. Shipar, A. Antoniou, "A Generalized Remez Method for the Design of FIR Digital Filters," IEEE trans. Circuits Syst., VOL 37, pp. 161-174, Feb. 1990.
- [34] I. W. Selesnick, C. S. Burrus, "Exchange Algorithms that Complement the Parks-McCellan Algorithm for Linear Phase Filter Design," submitted to IEEE in 1994.
- [35] C. L. Lawson, "Contributions to the theory of linear least maximum approximations," Ph. D. dissertation, U.C.L.A. 1961
- [36] J. R. Rice and K. H. Usow, "The Lawson algorithm and extensions," Math. Comput., VOL 22, pp. 118-127, 1968
- [37] J. R. Rice, "The approximation of functions, Vol III" Addison-Wesley, Reading, Mass., 1969
- [38] A.K. Cline, "Rate of convergence of Lawson's algorithm and extensions" Math. Comput., VOL 26, pp. 118-127, 1968
- [39] S. W. Kahng, "Best  $L_p$  approximation," Math. Comput., VOL 26, NO. 118, pp. 505-508, 1972

- [40] E. W. Cheney, *"Introduction to Approximation Theory."* New York: McGraw-Hill, 1966.
- [41] T. J. Rivlin, *"An Introduction to the Approximation of Functions."* Blaisdell, Waltham, Mass., 1969.
- [42] G. A. Watson, *"Approximation Theory and Numerical Methods."* John Wiley and sons, 1980.
- [43] G. C. Maenhout and W. Steenaart, "A direct approximation technique for digital filters and equalizers," *IEEE Trans. Circuit Theory*, Vol CT-20, pp. 548-555, Sept. 1973.
- [44] S. Imai, T. Kitamura, H. Takeya, "A direct approximation technique of log magnitude response for digital filters." *IEEE Acoustic. Speech Sig. Process.* Vol 25, pp. 127-133. Apr. 1977.
- [45] B. Yengnarayana, "Design of ARMA digital filters by pole-zero decomposition." *IEEE trans. Acoust. Speech Signal Processing*, vol ASSP-25, pp. 127-133, Apr. 1977.
- [46] C. E. Schmid, "Design of IIR/FIR filters using a frequency domain bootstrapping technique and LPC method," *IEEE trans. Acoust. Speech Signal Processing*, vol ASSP-31, pp. 999-1006, Aug 1983.
- [47] S.C. Pei and J.-J. Shyu. "Design of arbitrary FIR log Filters by weighted least squares techniques," *IEEE Trans. Signal Processing*, vol 42, pp. 2495-2499, 1994.
- [48] C. M. Lee, F. D. K. Roberts "A Comparison of Algorithms for Rational  $L_\infty$  Approximation," *Math. Comput.* VOL 27, pp. 111-120, 1973.
- [49] A. G. Decszky "Equiripple and Minimax (Chebyshev) Approximations for Recursive Digital Filters," *IEEE trans. Acoust. Speech Signal Process.*, VOL 22, NO 2, pp. 98-111, April 1974.

- [50] H. G. Martinez, T. W. Parks "Design of recursive digital filters with optimum magnitude and attenuation poles on the unit circle." IEEE trans. Acoust. Speech Signal Process., VOL 26, NO 2, pp. 150-156, 1978.
- [51] T. Samaraki. "Design of optimum recursive digital filters with zeros on the unit circle." IEEE trans. Acoust. Speech Signal Process., VOL 31, pp. 450-458, April 1983.
- [52] L. B. Jackson. "An improved Martinez/Parks Algorithm for IIR Design with Unequal Numbers of Poles and Zeros." IEEE trans. Signal Process., VOL 42, NO 5, pp. 1234-1238, May 1994.
- [53] I. W. Selesnick, M. Lang, C. S. Burrus, "Magnitude Squared Design of Recursive Filters with the Chebyshev Norm using a Constrained Rational Remez algorithm," IEEE trans. Signal Process., VOL 42, NO 5, pp. 1234-1238, May 1994.
- [54] J. W. Woods. "Subband Image Coding," Boston, MA: Kluwer Academic, 1991.
- [55] R. D. Koipillai, T. Q. Nguyen, P.P. Vaidyanathan, "New results in theory of crosstalk-free transmultiplexer," IEEE trans. Signal Processing, pp. 2174-2183, Oct. 1991.
- [56] A. Gilloire, M. Vetterli, "Adaptive Filtering in Subbands with Critical Sampling: Analysis, Experiments and Application to Acoustic Echo Cancellation," IEEE trans. on Signal Processing, VOL. 40, No. 8, pp. 1862-1875, Aug. 1992.
- [57] B. E. Usevitch, M. T. Orchard, "Adaptive Filtering Using Filter Banks," IEEE trans. Circuits and Syst. II, VOL. 43, No. 3, pp. 255-265, March 1996.
- [58] F. Sattar, G. Salamonson, "Nonparametric Waveform Estimation Using Filter Banks," IEEE trans. Circuits and Syst. II, VOL. 44, No. 2, pp. 239-247, Feb. 1996.
- [59] P.P Vaidyanathan, "Multirate Systems and Filter Banks," Englewood Cliffs, NJ: Prentice-Hall, 1992.

- [60] H. S. Malvar. *"Signal Processing with Lapped Transforms."* Norwood, MA, Artech House, 1992.
- [61] J. D. Johnston, "A filter family designed for use in quadrature mirror filter banks," in Proc. ICASSP'80, Denver, CO, pp. 291-294.
- [62] Joseph H. Rothweiler, "Polyphase quadrature filters - a new subband coding technique," in Proc. ICASSP '83.
- [63] G. Pirani, V. Zingarelli, "An analytical formula for the design of QMF," IEEE trans. Signal Processing, VOL. 32, NO. 3, pp. 645-648, June 1984.
- [64] Peter L. Chu, "Quadrature Mirror Filter Design for an Arbitrary Number of Equal Bandwidth Channels," IEEE trans. Signal Processing, VOL. 33, NO. 1, pp. 203-217, Feb. 1985.
- [65] Richard V. Cox, "The design of uniformly and nonuniformly spaced pseudo quadrature mirror filters," IEEE trans. Acoustics Speech Signal Processing, VOL. 34, NO. 5, pp. 1090-1096, Oct 1986.
- [66] P. P. Vaidyanathan, "Theory and Design of M-channel Maximally Decimated Quadrature Mirror Filters with Arbitrary M, Having the Perfect Reconstruction," IEEE trans. Acoustics Speech Signal Processing, VOL. 35, NO. 4, pp. 476-492, April 1987.
- [67] T. Q. Nguyen, P. P. Vaidyanathan "Two channel Perfect Reconstruction FIR QMF Structures Which Yield Linear Phase Analysis and Synthesis Filters," IEEE trans. Acoustics Speech Signal Processing, VOL. 37, NO. 5, pp. 676-690, May 1989.
- [68] T. Q. Nguyen, "Structures for M-channel Perfect Reconstruction FIR QMF Banks Which Yield Linear Phase Analysis Filters," IEEE trans. Acoustics Speech Signal Processing, VOL. 38, NO. 3, pp. 433-446, March 1990.

- [69] H. S. Malvar, "Modulated QMF filter banks with perfect reconstruction." *Electron. Lett.* VOL. 26, pp. 906-907, June 1990.
- [70] R.D. Koilpillai and P.P Vaidyanathan, "Cosine modulated FIR filter banks satisfying perfect reconstruction." *IEEE trans. Signal Processing.* VOL. 40, NO. 4, pp. 770-783, Jul. 1992.
- [71] T. Q. Nguyen, "Near-Perfect-Reconstruction Pseudo-QMF Banks." *IEEE trans. Signal Processing*, VOL. 42, NO. 1, pp. 65-75, Jan. 1994.
- [72] T. Q. Nguyen, "Digital Filter Bank Design Quadratic-Constrained Formulation," *IEEE trans. Signal Processing*, VOL. 43, NO. 9, pp. 2103-2108, Sept: 1995.
- [73] John Princen, "The design of Nonuniform Modulated Filter banks," *IEEE trans. Signal Processing*, VOL. 43, NO. 11, pp. 2550-2560. Nov. 1995.
- [74] C. D. Creusere, S. K. Mitra "A Simple Method for Designing High-Quality Prototype Filters for M-Band Pseudo QMF Banks," *IEEE trans. Signal Processing*, VOL. 43, NO. 4, pp. 1005-1007, April. 1995.
- [75] M. Rossi, J. Y. Zhang, W. Steenaart, "Two fast convergent algorithms for the design of minimax IIR and FIR filters in the Log Magnitude sense," in *Proc. ISCAS '96*, May 1996.
- [76] M. Rossi, J. Y. Zhang, W. Steenaart, "A New Algorithm for Designing Prototype Filters for M-band Pseudo QMF banks," in *Proc. EUSIPCO'96*, Sept 1996.
- [77] M. Rossi, J. Y. Zhang, W. Steenaart, "Iterative Least Squares Design of Near Perfect Reconstruction Pseudo QMF Banks," in *Proc. CCECE'96*, Canadian Conference on Electrical and Computer Engineering, May 1996
- [78] M. Rossi, J. Y. Zhang, W. Steenaart, "Iterative Least Squares Design of Perfect Reconstruction QMF Banks," in *Proc. CCECE'96*, Canadian Conference on Electrical and Computer Engineering, May 1996

- [79] Y. C. Lim, S. R. Parker, "*Discrete Coefficient FIR Digital Filter Design Based Upon an LMS Criteria.*" IEEE trans. Circuits and Syst., vol 30, NO 10, pp. 723-739, March 1993.